University of Natural Resources and Life Sciences, Vienna

Department of Agrobiotechnology, IFA-Tulln
Institute of Environmental Biotechnology

Master Thesis

To obtain the academic degree of Dipl.-Ing.

at the university of Natural Resources and Life Sciences, Vienna

Expression of Polyamide-hydrolyzing Enzyme

Submitted by:

B.Sc. Raditya Subagia

Vienna, September 2016

Supervisor:

Univ. Prof. DI Dr. Georg Gübitz, Institute of Environmental Biotechnology

MSc. Antonino Biundo

ABSTRACT

Found in nature as plant cuticle-degrading enzymes, cutinases have been described as versatile enzymes, hydrolyzing a wide variety of industrial important esters. Being esterolytic enzyme, cutinases share interestingly the same α/β-hydrolase fold and the Ser/His/Asp catalytic triad with prolyl oligopeptidases. By introduction of hydrogen acceptor to *Humicola insolens* cutinase (HiC) upon mutation, mimicking the spatial arrangement of hydrogen bond formed with the reacting nitrogen of the amide substrate, which facilitates the prerequisite nitrogen inversion in amide bond hydrolysis, we explored the possibility of increasing amide bond hydrolyzing capability by combining mutation investigated in the work by Syrén et al. (2012).

Genes of the *Hi*C WT, SM (I167Q), DM (L64H - I167Q) were subcloned into pET-26b(+), preserving the pelB leader sequence for periplasmic expression of soluble proteins and His-tag sequence for affinity-based purification method. Transformation into the expression host BL21-Gold(DE3) permitted the expression of enzyme after induction. An early harvest of shaker flask fermentation at the 8^{th} hour was attempted to optimize the yield against product loss into the medium caused by lysis of the cells, yet no significant gain of soluble protein was achieved. Large scale production in bioreactor yielded a moderate amount of product per biomass of the WT, SM, and DM as follows: 0.83 mg g^{-1}, 1.20 mg g^{-1}, 1.75 mg g^{-1}.

The water contact angle of treated PA 6.6 film by the SM and DM at 37 °C as well as 50 °C did not show any decrease of its hydrophobicity compared to the WT, which is supported by the GC/MS result, that there is no significant amount of released hydrolysis product at the corresponding temperature detected. Further hydrolysis investigation at higher temperature (60 °C), which still lies below the T_m of *Hi*C and near the T_g of PA 6.6 representing conducive working temperature for hydrolysis, may unlock the full capability of the variant enzymes.

ZUSAMMENFASSUNG

Cutinasen katalysieren in der Natur den Abbau von Cutin, dem polyesterartigen Hauptbestandteil der Cuticula von Pflanzen, und werden industriell für die Hydrolyse wichtiger Ester eingesetzt. Cutinasen weisen die gleiche α/β-Hydrolase-Faltung und die Ser/His/Asp katalytische Triade wie Prolyl oligopeptidasen auf. Durch Einführung von Wasserstoff-Akzeptoren in die *Humicola insolens* Cutinase (HiC) via Mutation, die die räumliche Anordnung der Wasserstoffbindung mit dem reagierenden Stickstoff des Amidsubstrats nachahmt, wird die voraussetzende Stickstoffinversion für die Hydrolyse von Amidbindungen ermöglicht. Basierend auf der Arbeit von Syrén et al. (2012) wurde die Möglichkeit der weiteren Erhöhung der Amidbindung hydrolysierende Fähigkeit durch das Kombinieren der Mutationen evaluiert.

Das Wildtyp HiC Gene, sowie die Singlemutante SM (I167Q) und Doppelmutante DM (L64H - I167Q) wurden in den Vektor pET-26b(+) subkloniert, unter Erhaltung der pelB-Leader-Sequenz für eine periplasmatische Expression und der His-Tag Sequenz für eine anschliessende Affinitäts-Reinigung. Die Transformation in den *E.coli* BL21-Gold-(DE3) erlaubt die Expression des Enzyms via Induktion. Eine frühe Ernte des Enzyms nach achtstündiger Induktion in der Schüttelkultur wurde durchgeführt, um den Produktverlust durch Lyse der Zellen zu verhindern. Jedoch wurde keine hohe Ausbeute an löslichem Protein erzielt. Die Enzymproduktion im Bioreaktor ergab einen moderaten Ertrag an Produkt pro Biomasse von WT, SM und DM wie folgt: 0.83 mg g^{-1}, 1.20 mg g^{-1}, 1.75 mg g^{-1}.

Der Wasserkontaktwinkel der mit SM und DM bei 37 °C sowie bei 50 °C behandelten PA 6.6 Filme zeigte keine Abnahme ihrer Hydrophobizität im Vergleich zu dem WT. Keine signifikante Menge an freigesetztem Hydrolyseprodukt wurde entsprechend durch GC/MS erkannt. Weitere Hydrolyse Versuche bei höheren Temperatur (60 °C), die noch unter der Tm von HiC und nah an der Tg von PA 6.6 liegt, sollte das volle Potenzial der mutierten Enzyme erschließen.

PREFACE

Cutinases have been described as versatile enzyme, which find use in many application in industrial products and processes. As the class of the serine α/β hydrolase superfamily showing member with low molecular weight, cutinases show capability of hydrolyzing a wide variety of industrial important esters, including water-soluble short acyl chain esters which could be recognized by esterases, insoluble long-chain triglycerides which are specifically hydrolyzed by lipases, as well as synthetic fibers such as poly(ethylene terephthalate) (PET) and poly(ε-Caprolactone) (PCL). Being an intermediate between lipase and esterase, cutinase has been also reported to hydrolyze triacylglycerol without the presence of calcium, displaying benefit upon commercial lipases used in laundry and dishwashing detergents. Cutinase from *Humicola insolens* (*Hi*C) has been compared with other cutinases including the most studied *Fusarium solani* cutinase in the mentioned regards, showing superior quality in terms of thermostability, pH stability, and residual activity, displaying potential of new applications and improvements of its usability.

The fact that cutinases share the same α/β-hydrolase fold as well as the Ser/His/Asp catalytic triad with serine protease, such as prolyl oligopeptidase, but show very low to undetectable activity on amide bonds, has been a particular interest from mechanistic point of view of how different these enzyme are. The hydrogen bond donated by the scissile NH-group has been demonstrated as a general feature of amidases, where the hydrogen bond acceptor can be either on the substrate or on the enzyme, facilitating the prerequisite nitrogen inversion important in hydrolysis of amide bonds.

In the work by Syrén et al., (2012), a substrate assisted hydrogen bond in prolyl oligopeptidase was used as a template in its transition state to introduce feasible mutation resembling an enzyme assisted hydrogen bond in *Hi*C, resulting in significant increase of relative reaction specificity on amide to ester substrate in all mutants having amino acid residue, which potentially accept the hydrogen donated by the reacting nitrogen of amide substrate. In the scope of this work, we explore the possibility of increasing the amidase activity by combining point mutations into one mutant enzyme (L64H, I167Q). The single mutant I167Q (SM), and the native *Hi*C (WT) were expressed in parallel to the double mutant (DM) in order to make a comparison of amidase activity.

ACKNOWLEDGEMENT

Foremost, I would like to express my gratitude to my supervisors, Univ. Prof. DI Dr. Georg Gübitz from University of Natural Resources and Life Sciences in Vienna for giving me the opportunity to work on this thesis under his guidance. Furthermore, my sincere thanks also go to co-supervisor in the field, MSc. Antonino Biundo for guiding and helping me with every aspect of my thesis, for his time, patience and exceptional supervision. Warm gratitude also to people around me in the laboratory, Johanna, Nadine, Katrin G., Barbara Z., Caro, Lucia, Orti, Robert, who always provide a conducive working atmosphere, support me in every way, and treat me as one of the big family of IFA Tulln.

I would like to express my gratitude to FH-Prof. DI Dr. Michael Maurer from FH Campus Wien for the collaboration in expressing the enzyme in bioreactor scale, assuring the our work with enzyme in quality and quantity. Moreover, my sincere thanks to MSc. Frederik Hoppe for his time, patience and remarkable supervision during the enzyme expression.

I also want to thank my parent for believing in me, and for their support in every step of my life, also to my sister for being my role model.

The last but not least, I would like to thank Ling for being there.

TABLE OF CONTENTS

LIST OF FIGURES

Figure

LIST OF TABLES

Table

1. INTRODUCTION

1.1. Cutinase

1.1.1. Vast potential of *Humicola insolens* cutinase

Due to their versatility and noteworthy properties, cutinases have found uses in many applications in industrial products and processes. In laundry or dishwashing detergent composition, cutinases have been applied as lipolytic enzymes to remove fats (Flipsen, Appel, van der Hijden, & Verrips, 1998; Okkels et al., 1997; Unilever, 1994), displaying benefit in comparison to the commercial lipase (Lipolase™), showing the ability to hydrolyze triacylglycerols in a single wash process. Another potential use includes their application in the dairy industry to hydrolyze milk fat, in the oleochemistry industry i.e. transesterification of fats and oils or (stereo)selective esterification of alcohols and in the synthesis of structured triglycerides, polymers, and surfactants (Carvalho, Aires-Barros, & Cabral, 1999). Cutinases have also been reported to degrade insoluble polymer films such as poly(ethylene terephthalate) (PET) (Herrero Acero et al., 2011; Ronkvist, Lu, Feder, & Gross, 2009) and poly(ε-Caprolactone) (PCL) (Z. Liu et al., 2009; Murphy, Cameron, Huang, & Vinopal, 1996). The Cutinase derived from *Fusarium solani* (*Fs*C) has been the most studied in this regard (Araújo et al., 2007; Baptista et al., 2003; Carvalho et al., 1999; de Barros, Fonseca, Fernandes, Cabral, & Mojovic, 2009; Eberl et al., 2008; Murphy et al., 1996; Pio & Macedo, 2009; Vidinha et al., 2004, 2006)

In the study conducted by Baker et al. (2012), five cutinases have been examined and compared for their residual activities at a range of elevated temperatures at pH 8 for *p*-NPB hydrolysis. *Fs*C, *Humicola insolens* cutinase (*Hi*C), *Aspergillus oryzae* cutinase (*Ao*C), *Alternaria brassicicola* cutinase (*Ab*C), *Aspergillus fumigatus* cutinase (*Af*C), having sufficient sequence diversity between 45% and 65%. *Hi*C still maintained 50% of its residual activity after heated to 85 °C, whereas all the other cutinases displayed less than 10% of their initial activity under identical conditions for incubation time of 1 h. The residual activities of nearly all cutinases drop significantly after they have been heated above their T_m (melting temperature). *Ab*C exhibits the lowest residual activity across all temperatures owing to its T_m, being the lowest. Followed by *Af*C, exhibiting the similar trend like *Ab*C, despite its significantly high residual activity compared to *Fs*C, if the heat treatment does not exceed its T_m. Interestingly, *Ao*C and *Hi*C do not follow this trend; still displaying significant activity after being heated to temperatures above their T_m, thus suggesting a thermodynamically favorable refolding upon

cooling. In addition, *Hi*C retained a significant 81% and 52% of its overall structure at pH 5.0 and 3.0, respectively, owing to the residues that surround the active site, defined as the "crowning area", maintaining a more neutral charge. This feature facilitates PCL degradation by *Hi*C even under high acidic conditions (pH 3), at which pH all the ionizable side chains are protonated leading to a charge–charge repulsion and subsequently the loosening of side chain packing, resulting in exposure of hydrophobic residues to the solvent, thus loss of secondary structure is imminent (Shashidhara & Gaikwad, 2010).

Moreover *Hi*C exhibited enhanced thermostability with T_m values of 62.7 °C, 64.3 °C and 51 °C at pH 8.0, 5.0, and 3.0 respectively, displaying a T_m higher than 40 °C, the temperature at which the experiments for PCL degradation were conducted (Baker, Poultney, Liu, Gross, & Montclare, 2012). Further inspections of temperature-dependent *Hi*C-catalyzed low crystallinity PET (lcPET) hydrolysis showed that a dramatic increase of hydrolysis activity was observed at temperatures above 65 °C (Ronkvist, Xie, Lu, & Gross, 2009). Welzel's Ph.D. dissertation demonstrated that the mobility of amorphous phase influences polyester biodegradability. It has been shown that the degradation temperature should be close to the T_g (glass transition temperature) of the polymer itself. This could help the degradation of aromatic polyesters such as PET (Ronkvist, Xie, et al., 2009). However the degree of crystallinity of the polymer is an essential factor affecting biodegradability, due to the fact that enzymes mainly attack the molecules in the loosely packed amorphous region (paracrystalline) owing to its accessibility, rather than the more-ordered crystalline regions (Parvinzadeh, Assefipour, & Kiumarsi, 2009).

Synthetic polymers such as PET, polyamides (PAs), and polyacrylonitrile (PAN) made up about 90% of all synthetic fibers produced worldwide. They have unique properties such as high uniformity in comparison to naturally occurring fibers, and have mechanical strength or resistance against chemicals or abrasion. However their hydrophobic and inert nature leads to poor wettability, difficulties in applying finishing compounds and coloring agents, which are undesirable properties of synthetic materials (Battistel, Morra, & Marinetti, 2001; Kellis Jr, Poulose, & Yoon, 2001; Vertommen, Nierstrasz, Van der Veer, & Warmoeskerken, 2005; M.-Y. Yoon, Kellis, & Poulose, 2002). In the preparation of wide range of synthetic polymer materials, having surface properties that are different from the bulk ones, is often desirable for the coupling of different compounds (Silva, Matama, & Cavaco-Paulo, 2010). The use of enzymes is an interesting alternative for surface modification of polymer. The large size and incompatibility of enzymes with polymeric substrates restricts the hydrolysis only to material

surfaces, providing changes in surface functionality while preserving bulk properties (Fischer-Colbrie, Heumann, & Guebitz, 2006b; Vertommen et al., 2005).

In the scope of our work, we carried out the hydrolysis of Nylon (PA) 6.6 film by three different variants of *Hi*C enzymes. PA 6.6 is a semicrystalline polymer synthesized by the polycondensation of equal amounts of a diacid (adipic acid) and a diamine (hexamethylenediamine) (Palmer, 2002; Silva et al., 2010). It exhibits excellent mechanical and thermal properties, high relation strength/weight, good chemical resistance, excellent deformation recovery and high resistance to bending and low permeability to gases (Burkinshaw, 1995). The basic of the hydrolysis of PA is the breakage of the amide bond on the polymer surface yielding carboxylic and amino groups, which can be used to increase hydrogen binding, facilitating the chemical bonding between substrates and adhesives (Silva & Cavaco-Paulo, 2004; Silva et al., 2010). Several works about functionalization of PA fiber has been published, and are handled in the review by Silva et al. (2010) into some extent. Glass transition and melting points of standard plain weave nylon 6.6 has been observed at about 55 °C and 255 °C, respectively (Parvinzadeh et al., 2009). However a compromise has to be made between materials modification requiring selective hydrolysis at the surface of the polymer, yielding new functional groups, and the increasing material degradation by high level of hydrolysis products (Silva et al., 2010).

1.1.2. Cutinase in nature

The plant cuticle is an extracellular hydrophobic layer that covers the aerial epidermis of all land plants, providing protection against abiotic or biotic stress such as desiccation, temperature, extremes, gravity, and exposure to UV radiation (Leliaert, Verbruggen, & Zechman, 2011; Waters, 2003). The cuticle is structurally diverse among species but exhibits the organization of a composite material consisting of two major components, which are the covalently linked macromolecular scaffold of cutin and a variety of organic solvent-soluble long-chain fatty acids (C20–C40) as well as their derivatives that include alkanes, aldehydes, primary and secondary alcohols, ketones, esters, and depending on the species also secondary metabolites such as flavonoids and triterpenoids which are collectively termed as cuticular waxes (epicuticular and intracuticular waxes- Figure 1) (Samuels, Kunst, & Jetter, 2008).

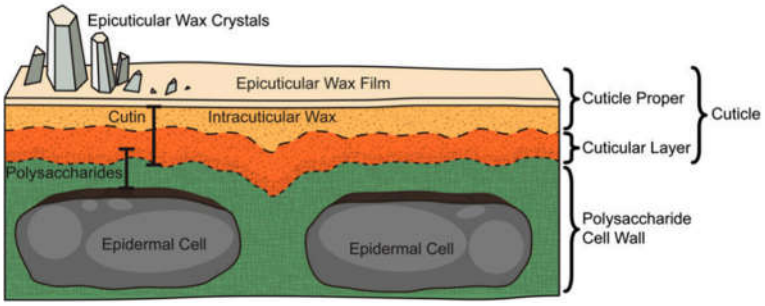

Figure 1. Plant cuticle structure. Schematic diagram depicting the structural features of the cuticle and underlying epidermal cell layer (not drawn to scale). The cuticular layer is referred to as the cutin-rich domain with incorporated polysaccharides, and the overlying layer with less abundant polysaccharides but enriched in waxes, referred to as the cuticle proper (Yeats & Rose, 2013).

The biopolyester, cutin, is typically made of esterified ω- and mid-chain hydroxy and epoxy C16 and C18 fatty acids (Heredia, 2003). Ester bonds predominate in cutin, although peroxide bridges and ether linkages have also been presented. Many phytopathogenic fungi have mechanisms to actively gain entry through the plant outer structural barriers, the cuticle and the epidermal cell wall, by generally secreting a cocktail of hydrolytic enzymes, including cutinases, cellulases, pectinases, and proteases (Knogge, 1996). In the review by Kolattukudy, P.E, (1985), the pivotal role of cutinase in enzymatic degradation of cutin in fungal penetration process has been documented into some details. For example, the inhibition of the enzyme by the use of different chemical inhibitors or cutinase-specific antibodies has been shown to prevent infection by *Fusarium solani f. pisi* of pea stem segments with intact cuticle but not of those with mechanically breached cuticle. Another support came from the observation of *Mycosphaerella sp*, a wound pathogen affecting papaya fruits, which was able to penetrate intact fruits only when transformed with the cutinase gene from *Fusarium solani f. pisi*. It has been also reported that several phytopathogenic fungi grow on cutin as the sole source of carbon (Hankin & Kolattukudy, 1971; Heinen & Vries, 1966; Purdy & Kolattukudy, 1973; Shishiyama, Araki, & Akai, 1970).

1.1.3. Cutinase structure

Cutinases are the smallest members of the serine α/β hydrolase superfamily and have been shown to have capability of hydrolyzing a wide variety of industrially important esters, including soluble synthetic esters (Egmond & de Vlieg, 2000; Koschorreck, Liu, Kazenwadel, Schmid, & Hauer, 2010; Z. Liu et al., 2009; Maeda et al., 2005; Purdy & Kolattukudy, 1975) and insoluble long-chain triglycerides (triolein and tricaprylin) (Gonçalves, Cabral, & Aires-Barros, 1996; Melo, Airesbarros, & Cabral, 1995). They have been found to have good hydrolytic activity on synthetic fibers such as poly(ethylene terephthalate) (PET) (Ronkvist, Lu, et al., 2009) and poly(ε-Caprolactone) (PCL).

Until recently there has been three dimensional (3D) structure reported for three cutinases, *Fs*C (Longhi et al., 1997), being the most studied cutinase, *Glomerella cingulate* cutinase (*Gc*C) (Nyon et al., 2008, 2009), and *Ao*C (Z. Liu et al., 2009), while *Hi*C has yet to be structurally characterized (Baker et al., 2012).

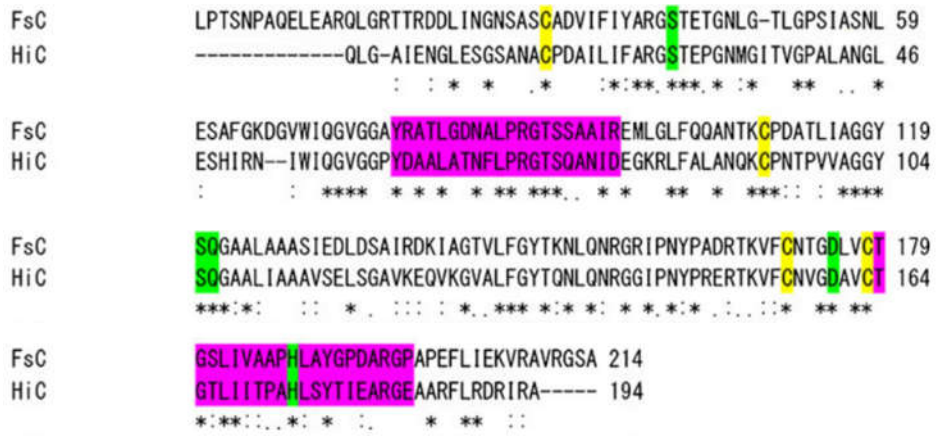

Figure 2. Multiple sequence alignment of cutinase sequences (adapted from Baker et al. 2012). The homology of HiC (accession number ABC06408.1) to FsC (Longhi et al. 1997) is 55.3%. The regions in the "crowning area" of the cutinase active site are labeled in purple. Cysteines involved in disulfide bonds are labeled in yellow and conserved residues of the catalytic triad as well as the oxyanion hole are labeled in green. Asterisk indicates conserved residues, colon indicates a conserved substitution, and full stop indicates a semi-conserved substitution

Cutinases are proteins with a monomeric structure and have molecular weight of around 22–26 kDa for fungal origin (Koller & Parker, 1989). X-ray crystallography studies of *Fs*C (accession number K02640) revealed an α/β-hydrolase fold comprising a central β-sheet of five parallel strands surrounded by α-helices on either side of the sheet, which is very similar to those of *Hi*C described in the structural investigation by Kold et al., (2014). Four cysteines forming two disulfide bridges, and highly conserved stretch Gly-Tyr-Ser-Gln-Gly consisting the active site Ser 120 (in HiC Ser 105 - Figure 2) has a strong homology with the consensus

sequence Gly-(Tyr or His)-Ser-X-Gly commonly presents in lipases (Jelsch, Longhi, & Cambillau, 1998). The catalytic triad of *Hi*C (Ser 105, His173, Asp160) superimpose closely on those of *Fs*C (Figure 3C), and the differences has been described to be restricted to small variation in the surface loops and the chain termini (Kold et al., 2014).

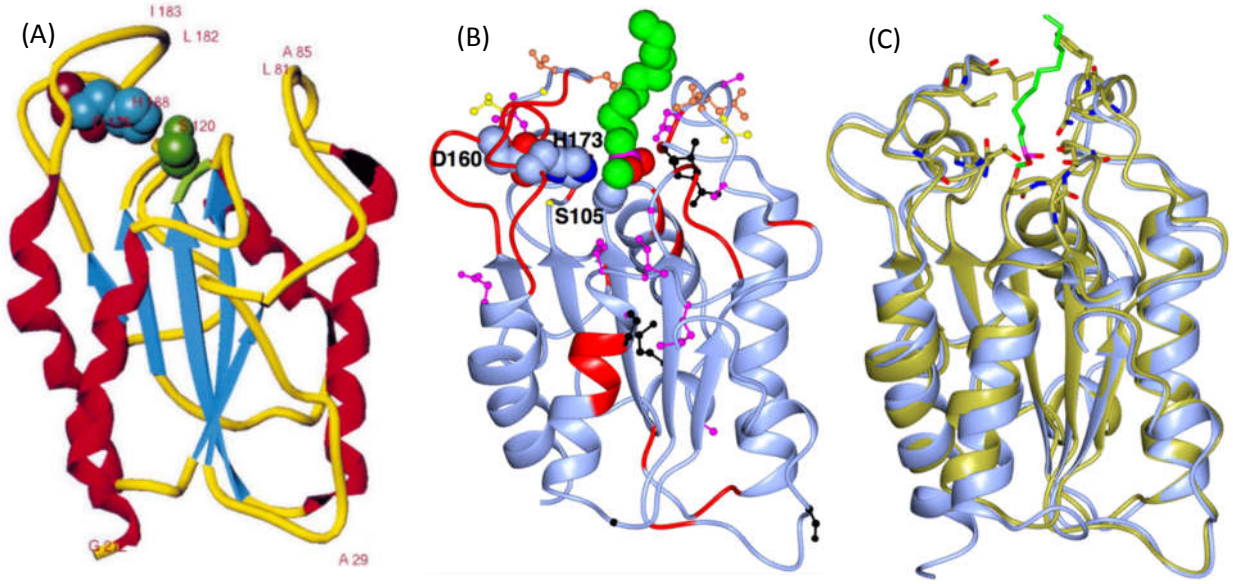

Figure 3. Ribbon representation of FsC and HiC. (A) ribbon representation of FsC. α-Helices (red), βstrands (blue) and coils (yellow) are shown. The residues of the catalytic triad (Ser120, green; Asp175, red; His188, blue) are represented. Residues of the loops (residues 80-88 and 180-188) circumvent the catalytic crevice of FsC.(Longhi, S. & Cambillau, C., 1999). (B) HiC-DEP with active-site (amino acids 105, 160 and 173) shown as spheres and the unassigned non-proline residues in red. (C) PDB structure 1XZM25 of FsC (backbone in pale blue) with O-methyl-undecylphosphonate esterified to active site serine, superimposed with HiC in gold, with the side chains close to the FsC ligand shown as sticks (Kold et at. 2014). DEP (diethyl-phosphate) depicted as green sphere in (B) and green stick in (C) is inhibitor used in the corresponding conformational study of FsC and HiC (Kold et at. 2014).

The absence of surface loops resembling a lid, masking the active-site as in the case of lipases, make the catalytic triad of cutinases, which located at one extremity of the protein ellipsoid at the bottom of a crevice circumvented by the loops 80-87 and 180-188 (in *Fs*C - Figure 3A), accessible to solvent and substrate (Jelsch et al., 1998; Martinez, De Geus, Lauwereys, Matthyssens, & Cambillau, 1992; Martinez, de Geus, Stanssens, Lauwereys, & Cambillau, 1993). The binding of cutinase to non-hydrolysable analogue seems not to require a main-chain rearrangement representing feature unique to cutinases (Longhi et al., 1997; Martinez et al., 1992). The presence of a small pocket provides a structural explanation for the substrate preference of cutinases for short chains (C4) triglyceride (Mannesse et al., 1995).

Interestingly, the active site, consisting of the catalytic triad Ser, Asp and His, is the mirror image of the reminiscent of active site found in serine proteases (Longhi & Cambillau, 1999). Analogous to the serine proteases, cutinases contains an oxyanion hole for the stabilization of the tetrahedral intermediate.

1.2. Attempts to increase amidase activity on esterolytic enzymes: cutinase and lipase

As mentioned before esterases/lipases contains the highly homologous Ser/His/Asp catalytic triad found in the serine proteases (Brady et al., 1990; Ollis et al., 1992; Winkler, D'Arcy, & Hunziker, 1990). While serine proteases such as chymotrypsin and subtilisin hydrolyze both amides and esters (Abrahmsen et al., 1991, p. 30; Bonneau, Graycar, Estell, & Jones, 1991; Zerner, Bond, & Bender, 1964), it is surprising that typical esterolytic enzymes such as lipases have very low or undetectable amidase activity (Duarte, Castillo, Bárzana, & López-Munguía, 2000; Henke & Bornscheuer, 2003; Kazlauskas & Bornscheuer, 1998). Probably this is due to different structural features which allow substrate to enter the active site in different ways leading to different catalytic mechanisms.

The presence of a rather small pocket accommodating the substrate provides a structural explanation for the smaller substrate preference of cutinases, which would be responsible for the drop in the activity when longer ester chains are used (Longhi & Cambillau, 1999). In order to better fit a larger polymer chain, mutations of *Fs*C by site-directed mutagenesis has been attempted to modify residues near the active site (Araújo et al., 2007). Substitution of bulky side chain of L182 by a smaller residue such as alanine (the L182A mutant) enlarged the active site, which provides less restrain, hence creating more space to better fit a large chain, e.g. polymer, in the active site of the cutinase. The native *Fs*C used in the previous mentioned work (Araújo et al., 2007) has been also confirmed to have a very low ability to biodegrade polyamide aliphatic substrates such as PA 6.6. (Silva & Cavaco-Paulo, 2004). Although modeling studies led to stabilization of the tetrahedral intermediate, the most promising mutant L182A in this work did not give a significant improvement of activity. In addition to that, pre-adsorption of the enzyme on the solid substrate which is assumed to take place before the catalysis can proceed, was interestingly observed to be 3 times higher for PET than for PA 6.6 by the native and the mutant cutinase (Araújo et al., 2007).

Besides the catalytic machinery, the pre-organized oxyanion hole polarizing the carbonyl group by hydrogen bonding interactions as well as stabilizing the negative charge, which develops on the former carbonyl oxygen in the TS, plays a major role in an efficient catalysis (Syrén, 2013). By the fact that lipases have topologically similar active site to those found in serine proteases consisting Ser, His, Asp/Glu catalytic triad, as well as perform the same double displacement mechanism via an acyl enzyme intermediate in hydrolysis of esters as observed in serine proteases counterpart (Jaeger, Dijkstra, & Reetz, 1999), saturation mutagenesis of the oxyanion

hole has been performed on the Lipase from *Pseudomonas aeruginosa* (Nakagawa, Hasegawa, Hiratake, & Sakata, 2007). The saturation mutagenesis still preserved the presence of oxyanion hole by any amino acid substitutions, but a subtle difference in its geometries were expected by the mutations in the side chain. This should explore the possibilities of significant change on the catalytic activity. However, the attempt did not fall in accordance with the initial expectations of improved amidase activities (Nakagawa et al., 2007).

Regions on the surface outside the active site are essential for the interaction with the polymer and hydrolysis among polymer-hydrolases like cellulases or proteases (Gusakov, Sinitsyn, Berlin, Markov, & Ankudimova, 2000; Kellis, Estell, & Cascão-Pereira, 2012). In attempt to increase hydrolysis efficiency on esters, the cutinase from the closely related *Thermobifida cellulosilytica* has been compared. The dissimilarities in their electrostatic and hydrophobic surface properties in the vicinity to the active site found to be responsible for pronounced differences in polyester hydrolysis efficiencies for i.e. PET (Herrero Acero et al., 2011).

The minimal requirements for esterase activity have been also explored by computationally designed enzymes. Modification and incorporation of general base/acid as well as an oxyanion hole is adequate to achieve efficient ester bond hydrolysis (Richter et al., 2012). However, such arrangement is not sufficient to achieve efficient hydrolysis of amides. The variation of the order of the amino acids constituting the catalytic machinery in the primary sequence as well as in their spatial arrangement cannot provide any explanation for this phenomenon (Syrén, 2013). It has been of particular interest from both the mechanistic and practical points of view to understand why esterases/lipases are not able to demonstrate an efficient amidase activity, despite the structural similarities to serine proteases (Nakagawa et al., 2007).

1.3. General catalytic strategy in amide hydrolysis

The hydrolysis of amides is due to the resonance-stabilized nature of amides energetically more demanding than the hydrolysis of esters, and therefore it is not amenable for esterases/lipases to catalyze the reaction (Henke & Bornscheuer, 2003). The difference between amides and esters is that amides have partial C-N double bond and an extra hydrogen sitting on the amide nitrogen, which is not present in esters. Syrén & Hult (2011) suggested that the ability of an enzyme to utilize the interactions with this hydrogen in the transition state, which results in the reduction of the activation energy of hydrolysis would distinguish proteases/amidases from esterases/lipases.

Previously presented by Syrén (2013), the hypothesis of the histidine ring flip mechanism and low barrier hydrogen bond, which limited to serine protease and Ser/His/Asp catalytic triad, was described to understand the reaction mechanisms of enzyme catalyzed amide bond hydrolysis. Therefore general explanation of catalytic motif for an efficient amide bond hydrolysis is necessary to explain the amidase activity of a serine protease, prolyl oligopeptidase, which have the same catalytic machinery and the α/β-hydrolase fold found in esterases/lipases, but in contrary demonstrating poor catalytic ability in the hydrolysis and synthesis of amide bonds (Syrén, 2013).

An important mechanistic aspect of the nitrogen of the scissile amide bond has been discussed in the literature during the last few decades, in which the lone pair of the scissile nitrogen facing antiperiplanar due to stereoelectronic requirements resulting in non-productive conformation in the enzyme active site has to invert its configuration during amide bond hydrolysis in order to produce a catalytically competent tetrahedral intermediate (TI) (Bizzozero & Dutler, 1981; Hedstrom, 2002; B. Liu, Schofield, & Wilmouth, 2006).

In addition to the general interactions in the active site of amidases, which is sufficient to achieve efficient ester bond hydrolysis, comprising the incorporation of general base/acid catalysis and stabilization by the oxyanion hole (Henderson, 1970), the review by Syrén (2013) demonstrated two additional catalytic strategies facilitating amide bond hydrolysis/synthesis by favorably handling the stereoelectronic constrain during catalysis. The first strategy is an enzyme or substrate assisted hydrogen bond acceptor facilitating nitrogen inversion (referred herein to as the H-bond strategy), and the second catalytic strategy is the proton shuttle mechanism that avoids inversion and delivers a hydrogen to the lone pair (Syrén, 2013).

Molecular modeling suggested that the H-bond strategy can be generally implemented and expanded to include many amidases/proteases (Syrén, 2013). By analyzing the modeled tetrahedral intermediates as representations of transition states with molecular dynamics (MD) simulations, it has been demonstrated that the hydrogen bond donated by the scissile NH-group in sixteen analyzed amidases representing ten different reaction mechanisms and eleven folding families, is a general feature of amidases and is important for nitrogen inversion (Syrén & Hult, 2011).

The significance of the hydrogen bond in the transition state in relation to that in the enzyme–substrate (ES) complex, is that a fully developed hydrogen bond in the ES complex in the TS will be reflected in an increased specificity of the enzyme (i.e. an increased k_{cat}/K_M value for amide substrates), while on the other hand a stronger hydrogen bond in the TS would principally lead to an increase in k_{cat} (Syrén & Hult, 2011).

The hydrogen bond was found to be either enzyme assisted or substrate assisted. The hydrogen bond acceptor is typically a backbone carbonyl oxygen that can reside either in the enzyme (enzyme assisted catalysis) or in the substrate itself (substrate assisted catalysis) (Syrén & Hult, 2011). The absence of hydrogen-bond acceptor in the case of esterases, could be principally compensated by using substrate engineering to introduce a substrate assisted catalysis (Cammenberg, Hult, & Park, 2006).

1.4. Amide bond hydrolysis

The acylation step of amide bond hydrolysis is composed of following steps with concomitant TSs depicted in the Figure 4.

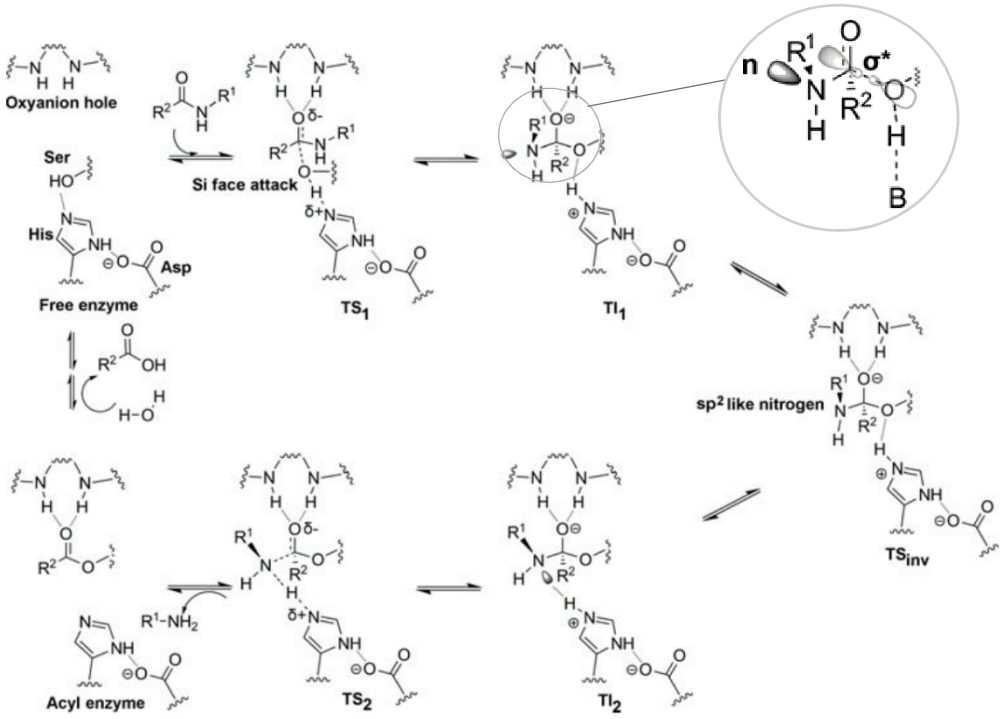

Figure 4. The acylation step of amide bond hydrolysis catalyzed by a serine hydrolase. The Ser/His/Asp catalytic triad is depicted together with two enzyme backbone amide groups forming the oxyanion hole. Three major steps in amide bond hydrolysis comprised 1. The nucleophile attack of the substrate carbonyl carbon by the catalytic serine, 2. Nitrogen inversion or rotation providing competent conformation for proton transfer and 3. Cleavage of the scissile CN bond. Bonds that are formed/broken are shown with dashed lines. The circle magnifies the substrate enzyme complex depicting the orbital interaction and stereoelectronic effect after Deslongchamp. B : catalytic base histidine.(Syrén, 2013)

In the first transition state (TS1) the catalytic nucleophile (Ser) attacks the carbonyl carbon of the amide substrate and donates its proton to the catalytic base (His). In accordance to Deslongchamps stereoelectronic effects, a favorable n–σ* interaction between the (developing) lone pair of the amide substrate and the antibonding orbital of the bond formed/ broken between the nucleophile serine and the carbonyl carbon in the transition state (TS) dictates the precise orientation of the lone pair of the scissile nitrogen (Deslongchamps, 1975; Gorenstein, 1987). Due to this stabilizing orbital overlapping, the lone pair will be situated antiperiplanar to the bond formed between the catalytic nucleophile and the former carbonyl carbon of the amide substrate in the formed tetrahedral intermediate (TI1). This spatial arrangement represents an unproductive conformation for proton abstraction from the catalytic base histidine. In order to proceed, inversion and/or rotation around the C–N bond assisted by hydrogen bond donated by the reacting nitrogen atom is required to produce the second tetrahedral intermediate (TI2),

which is a requirement for proton abstraction from the base by the reacting nitrogen atom (Bizzozero & Dutler, 1981; Hedstrom, 2002; B. Liu et al., 2006). In the second transition state (TS2) the proton is transferred from the base (His) to the reacting nitrogen atom and followed by the breakage of the bond between the former carbonyl carbon and the nitrogen, hence the release of the N-terminal part of the original amide substrate. During deacylation, water molecule attacks the acyl enzyme releasing the carboxylic group (Syrén, 2013). As mentioned before, esters are readily hydrolyzed by proteases/amidases (ester substrates alcoholysis), the proton from the general base can be accepted by the additional lone pair sitting on the ester oxygen without major structural rearrangements and the rate limiting step is often found to be the deacylation step (Fresht, 1999). For amide bond hydrolysis, it has been concluded by calculations on small, and larger model of a serine hydrolase, that nitrogen inversion is the rate limiting in TS (Syrén & Hult, 2011).

1.5. Introducing amidase-like property to *Humicola insolens* cutinase (*Hi*C)

The orientation of the lone pair of the nitrogen of the scissile amide bond is an important aspect for enzyme design purposes (Syrén, 2013). In the work described by Syrén, (2013), Prolyl oligopeptidase having the same catalytic machinery and the same α/β-hydrolase fold as found in cutinases and demonstrating a substrate-assisted hydrogen bond which is donated by the scissile NH group and accepted by the substrate P2 carbonyl oxygen (Fülöp, Szeltner, Renner, & Polgár, 2001; Syrén & Hult, 2011), was used as a template to find a viable enzyme assisted hydrogen bond acceptor in *Hi*C (Syrén et al., 2012). By overlapping the TS models of both enzymes with molecular modelling, identification of amino acids residues that could be mutated to be hydrogen bond acceptors was possible. The amino acid residues in *Hi*C that closely constituting the corresponding spatial arrangement of the substrate P2 carbonyl oxygen in amide bond hydrolysis by the prolyl oligopeptidase TS were depicted in Figure 5 (Syrén et al., 2012).

For *Hi*C, L64 and I167 were the closest residue which could be the potential amino acids mimicking the hydrogen-bond acceptor upon mutation. Molecular modelling of the *Hi*C mutant I167Q showed the relevant hydrogen bond could be formed with the hydrogen donated by the scissile NH group in the TS (Figure 5).

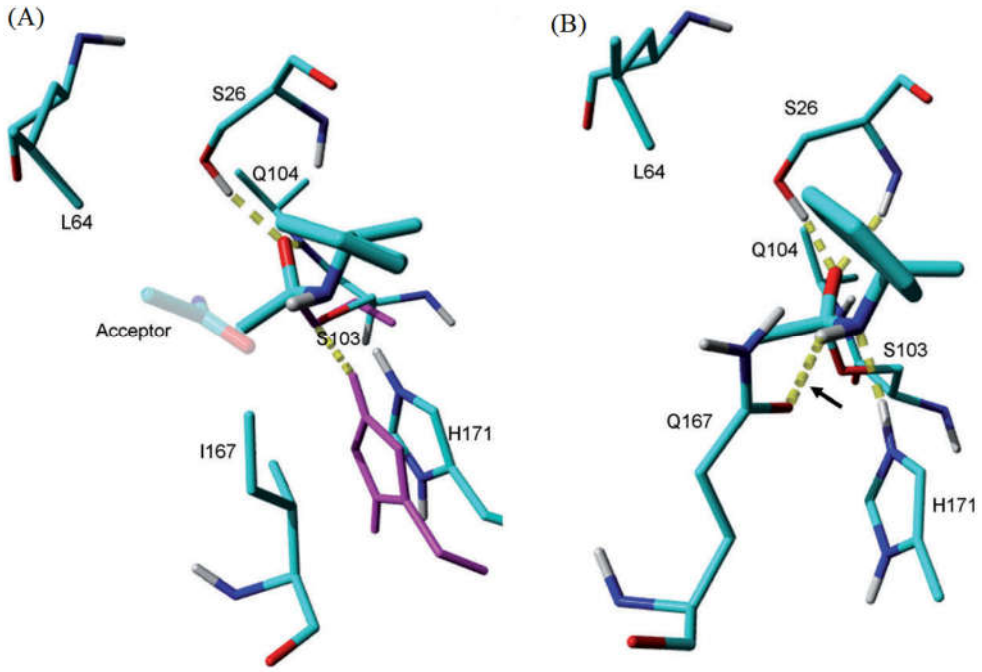

Figure 5. Introduction of a hydrogen-bond acceptor into H. insolens cutinase (HiC) by rational design to mimic substrate assisted catalysis of prolyl oligopeptidase. A) Superimposition of the TS model of HiC with the corresponding TS model for prolyl oligopeptidase in amide bond hydrolysis. Parts of the catalytic triad (S103, H171) and the oxyanion hole (S26, Q104) are shown for HiC and parts of the model substrate covalently bound to S103 ((R)-1-phenylbutyramide) are shown as enlarged sticks. The hydrogen-bond acceptor of the substrate P2 carbonyl group in the substrate assisted catalysis by prolyl oligopeptidase shown as shaded stick located between the two residues of HiC, L64 and I167, resembles the spatial arrangement of potential mutations of the corresponding amino residues for the introduction of enzyme assisted hydrogen bond acceptor. Atoms of the catalytic Ser and His residues shown in magenta are of prolyl oligopeptidase B) Snapshot from an MD simulation of the HiC I167Q mutant. The arrow indicates the hydrogen bond introduced into the TS Colour code: cyan—carbon, red—oxygen, blue—nitrogen. Not all atoms are shown for clarity (Syrén., 2012).

The results presented in the Table 1 provides valuable informations regarding the reaction mechanism of amide bond hydrolysis. By introducing the enzyme-assisted hydrogen bond in the TS, the reaction specificity for amide bond hydrolysis has increased up to fifty times in the case of *Hi*C and Lipase mutants (Syrén et al. 2012).

Table 1. Substrate specificities of wild type HiC and engineered variants for amide and ester (Syrén., 2012)

Variant	Relative reaction specificity (k_{cat}/K_M, amide)/(k_{cat}/K_M, ester)[b]	k_{cat}/K_M [$M^{-1}s^{-1}$] Amide	Ester
H. insolens cutinase			
wild-type	1	0.09	770000
L64H	5	0.24	42000
L64Q	16	0.24	120000
I167Q	47	0.69	120000

[a] Hydrolysis performed at 37 °C in potassium phosphate buffer (100 mM, pH 8) using *p*-nitrobutyranilide and *p*-nitrophenyl butyrate as amide and ester substrate, respectively. [b] Relative to wild-type.

The spatial arrangement for the hydrogen bond and the nitrogen inversion has proven to be the key interaction in amidases, as can be seen in the engineered *H. insolens* cutinase variants,

where higher amidase activity and increased reaction specificity displayed by all mutants that could potentially accept a hydrogen bond in the TS. The better positioned I167 for the introduction and to mimic the hydrogen bond acceptor found in the TS of amidases, showed the highest amidase activity among other investigated mutations at position 64. The work by Syrén et al. (2012) presented the lower limit for the contribution of the hydrogen bond donated by the scissile NH group in the TS to catalysis of amide bond hydrolysis, considering the large distance for the insertion of a hydrogen-bond acceptor to mimic the spatial arrangement found in substrate assisted amide hydrolysis by prolyl oligopeptidase. It has been shown that a perfect enzyme assisted hydrogen bond could not be introduced by performing a simple point mutations (Syrén, 2013) and therefore a further engineering of esterases fold is necessary to provide an optimal conformation for hydrogen-bond formation in conformity to the situation in amidases (Syrén et al., 2012).

In the scope of our work, we explored the possibility of amidase activity increase by combining these point mutations in one mutant enzyme. The point mutation L64H displaying the same degree of reaction specificity (k_{cat}/K_M) to amide but lower specificity to ester substrate -in comparison to the other mutation at the same position 64 (L64Q)-, was combined with the point mutation I167Q thus creating a double mutant enzyme. The single mutant I167Q, and the native *Hi*C were expressed in parallel in order to compare the amidase activity of the double mutant.

1.6. Heterologous protein expression

Theoretically, obtaining a recombinant protein follows a very straightforward set of steps: cloning of gene of interest in an expression vector, transformation into the host of choice, induction of the host to produce the protein, and then purification as well as characterization of the protein itself. However, in practice, there are a lot of factors that take influence in the expression of recombinant protein, such as poor growth of the host, formation of inclusion body (IB), protein inactivity, and in the worst case no recoverable protein upon purification (S. H. Yoon, Kim, & Kim, 2010).

The over-production of heterologous proteins in the *E.coli* often leads to the formation of insoluble intracellular aggregates (inclusion bodies) leading to their incorrect folding (Kane & Hartley, 1988). The formation of such aggregates has advantages that they are highly enriched in the protein of interest, and the purification is accomplished by simply collecting the IB and washing them, in which step detergents or denaturing agents are often required to solubilize the protein through refolding step, obtaining the protein with the correct secondary and tertiary

structure. However refolding of the protein results in loss of product due to the inefficiency of the folding process and leading to decreased yields in the production process. Furthermore disulfide bonds that help maintaining the tertiary structure is more likely to happen in the oxidative environment of the periplasm (Makrides, 1996). Another potential disadvantage of cytoplasmic protein production is an inefficient removal of the initiation methionine by endogenous enzyme. For these reasons, secretion systems that translocate the protein in a compartment where purification might be facilitated, and where the process to achieve a desired amino-terminal sequence, as well as the folding of polypeptide into its native conformation can occur, has been a growing interest for utilization of periplasmic expression (Hsiung & Becker, 1988). Moreover, targeting the protein of interest to the periplasmic space enables a simpler downstream processing at a reduced process cost.

However secretory production of heterologous proteins in *E. coli* remains problematic, despite many successful examples. In the review by Choi, J. H. & Lee, S. Y., (2004), there are some secretory obstacles described, including an incomplete processing of signal sequences, variable secretion efficiency depending on the characteristics of the proteins, low or undetectable amounts of recombinant protein secretion, formation of inclusion bodies in the cytosol and periplasm upon usage of strong promoters, and incorrect formation of disulfide bonds (Chung et al., 1998; Jeong & Lee, 2000; Lucic et al., 1998; Pritchard et al., 1997; Wong, Ali, & Ma, 2003). The first three problems could be solved by trial-and-error approach, such as using different promoters, signal sequences, host strains and variation of culture conditions (e.g. temperature). Experiments have been undertaken in the past to elucidate the role of mature protein sequences in secretion. The signal sequence is indeed necessary for protein export in *E.coli*, however it is concluded to be not sufficient for many proteins. The other important component is the secretion sequences, which lie within the mature protein directing the protein to its final destination, as well as the cellular export machinery itself, resulting in a secretion incompatibility or on the other hand conferring positive information allowing an optimal export of protein (Ferenci & Silhavy, 1987). The use of host strain deficient in periplasmic proteases could also be a solution in the case of the occurance of periplasmic proteolysis of the recombinant protein. The last two problems have been solved by manipulating periplasmic chaperones, or the use of other secretory systems, i.e TAT system, which offers a good alternative solution (J. H. Choi & Lee, 2004).

In the scope of our work, we used pelB signal sequence for periplasmic protein expression, pET-26b(+) as the expression vector, *E.coli* strain XL10 featuring the Hte phenotype making

this strain ideal for the transformation of large plasmids and ligated DNA for the consecutive screening of successful ligation by sequencing, and *E.coli* strain BL21-Gold(DE3) as the host to overexpress the protein of interest.

1.6.1. Host bacterial cells and plasmids

Being a workhorse organism owing to the wealth of knowledge about its physiology, *Escherichia coli* has been the most widely used organism for mass-production of recombinant proteins of pharmaceutical and industrial importance. Despite the lack of post-translational modification such as disulfide bonds and the existence of endotoxin, *E. coli* has numerous desirable characteristics as a production host such as fast cell growth with doubling time of about 20 min at given optimal physiological and environmental conditions (Sezonov, Joseleau-Petit, & D'Ari, 2007), reaching stationary phase with inoculation of 1/100 dilution of starter culture in just a few hours hence achieving high cell density cultivation (Rosano & Ceccarelli, 2014). Not to mention the easy manipulation, and its capacity to hold over 50% of foreign protein in total protein expression (Jong Hyun Choi, Keum, & Lee, 2006). However the expression of a recombinant protein may put strain on the metabolism of the microorganism, causing a considerable decrease in generation time (Bentley, Mirjalili, Andersen, Davis, & Kompala, 1990).

Plasmids are DNA molecule used as a vehicle to artificially carry foreign genetic material (in this case, DNA coding our protein of interest – *Hi*C) into the host cells. Plasmids contain replicons which are able to undergo replication as autonomous units. A suitable vector copy number residing in the replicon is an important parameter to consider (Del Solar & Espinosa, 2000).

Due to high-level expression, the BL21-Gold-derived expression strains are ideal for performing protein expression studies, which utilize the T7 RNA polymerase promoter such as in pET system. In the *E. coli* BL21(DE3) host strain with pET system, the T7 RNA polymerase gene is supplied by the host bacterium in form of λ-lysogen (DE3), whose expression is under the control of the IPTG-inducible lac UV5 promoter (Studier & Moffatt, 1986; Studier, Rosenberg, Dunn, & Dubendorff, 1990). Derived from parental *E. coli* strain B, these expression strain is deficient in the Lon protease, which degrades many foreign proteins (Gottesman, 1996). In addition to that, the gene encoding the outer membrane protease OmpT, which degrade extracellular proteins, was deleted from the genome of the ancestors of BL21. This could be problematic in the case extracellular expression or recovery of recombinant

proteins from the medium as it may be digested by the released OmpT due to the lysis of the cells (Grodberg & Dunn, 1988). Plasmid loss is further prevented owes to the *hsd*SB mutation resulting in disruption of DNA methylation and degradation.

1.6.2. Signal peptide and disulfide bonds formation

In comparison to cytoplasmic production, secretory production targeting a protein of interest to the periplasmic space has numerous desirable advantages: Isolation and purification of recombinant protein are much simpler due to reduced contamination of various cellular components thus preventing proteolytic degradation by intracellular proteases. Due to the presence of numerous reductases and reducing agents such as glutathione, the cytoplasm of wild-type *E. coli* does not permit the correct folding of eukaryotic proteins containing multiple disulfide bonds, thus it requires a set of cell envelope proteins, the Dsb system (where Dsb stands for disulfide bond), found in periplasm that form (oxidation), break (reduction) and shuffle (isomerization) the disulfide bonds within a polypeptide in vivo. Furthermore, secretory process allows the removal of the amino-terminal signal sequence by signal peptidase, yielding mature proteins with the naturally occurring sequences without N-terminal methionine (Francetic, Belin, Badaut, & Pugsley, 2000). These features make periplasm an ideal compartment for expression of certain therapeutic proteins enabling the accumulation of properly folded, soluble protein (Berkmen, 2012).

With the type II system of at least three different types of protein secretion systems described by Pugsley (1993) being the most widely used, the maturation of the protein involves a two-step process in which a premature protein synthesized in the cytoplasm, featuring a destining short (15–30) specific amino acid sequence, called signal sequence, is exported to the periplasmic space using the Sec pathway and processed into a mature protein.

Signal sequences that have been used displaying efficient secretory production of recombinant proteins in *E. coli*, include PelB, OmpA, PhoA, endoxylanase, and StII (J. H. Choi & Lee, 2004). Of particular interest for the expression of disulfide bonded proteins is the use of pET vectors containing the N-terminal pelB (pectatelyase B of *Erwinia carotovora* CE (Lei, Lin, Wang, Callaway, & Wilcox, 1987)) secretion signal (S. H. Yoon et al., 2010). Synthesis of high levels of cutinase have been reported, and owing to periplasmic localization of the recombinant cutinase, purification in large quantities are amendable (Lauwereys, De Geus, De Meutter, Stanssens, & Matthyssens, 1991). However the efficiency of protein secretion varies depending on the combination of the signal sequence, host strain, and the type of protein to be secreted.

An optimum signal peptide should be found by trial and error and there is no general rule to date that would guarantee a successful secretion of recombinant protein (J. H. Choi & Lee, 2004).

Disulfide bonds that exist in proteins have biologically significant functions, such as structural, signaling and catalytic function (Berkmen, 2012). Two consecutive disulfide bonds are present in *Fs*C (see comparison with *Hi*C in Figure 2). The first is between Cys31-Cys109, which links the N-terminal end with the L-turn contributing to the stabilization of the overall molecular folding. The second disulfide bridge is between Cys171- Cys178, which is assumed to have an important role participating in the stabilization of the two consecutive L-turns on which the catalytic Asp175 is located (Longhi & Cambillau, 1999). This structural function of disulfide bonds gives the protein its conformation and an increased thermostability (Zhang, Bertelsen, & Alber, 1994). The catalysis of disulfide bond formation in protein folding are carried out by a set of machinery composed of Dsb (disulfide-bond formation) proteins, DsbA and DsbB, which are oxidoreductases that allow the formation of disulfide bonds. DsbA rapidly and efficiently catalyzes disulfide bond formation as an unfolded protein is translocated into the periplasm (Kadokura, Tian, Zander, Bardwell, & Beckwith, 2004). However its tendency to oxidize cysteines in a consecutive manner (Berkmen, Boyd, & Beckwith, 2005; Kadokura et al., 2004), often cause misfolding of non-consecutive disulfide bonds, which normally degraded rapidly by DegP protease preventing accumulation of proteins with misfolded conformation. Disulfide-bond rearrangement is then catalyzed by two periplasmic disulfide bond isomerases, DsbC and DsbD.

1.6.3. Codon optimization

As discussed above, there are many factors to consider for a high level gene expression. One of the most important factors is to adapt the codon usage of the transcript gene to the typical codon usage of the host (Lithwick & Margalit, 2003). A codon usage bias occurs when the frequency of occurrence of synonymous codons in the foreign coding DNA is significantly different from that of the host. If a gene contains codons that are rarely used by the host, the tRNAs of low-abundance will deplete rapidly during overexpression of recombinant proteins. This deficiency will reflect in the low level of expression, and moreover may lead to amino acid misincorporation and/or truncation of the polypeptide, thus compromising the activity of expressed protein (Gustafsson, Govindarajan, & Minshull, 2004). This may be one of the limitations of heterologous protein expression (Gustafsson et al., 2004).

Codon usage optimization basically involves alteration of the rare codons in the target gene so that they more closely reflect the codon usage table of the host while preserving the amino acid sequence of the encoded protein, and is usually performed as one of the very first step in the design process of a nucleic acid sequence that will be introduced into a new host to express a certain protein in large amounts (Puigbò, Guzmán, Romeu, & Garcia-Vallvé, 2007).

1.6.4. Bioreactor

Bioreactor is a system specifically designed to influence metabolic pathways, in which organisms are cultivated in a controlled manner and/or biological conversion, such as materials conversion or transformation via specific reactions, is effected (Williams, 2002). Well designed bioreactor systems should provide a higher degree of control over process upsets, maintaining the desired biological activity and eliminating or minimizing undesired activities such as contaminations.

Change of viscosities of culture that may occur during growth and production phases, is to be taken into account as the medium often display a non-Newtonian property as the biomass progressed. Bacteria are relatively tolerant to high-shear environments, thus exhibiting robustness on mixing which is important for an efficient heat and mass transfer during the production phases. Major advantages of cultivation in bioreactor compared to lab scale shaker flasks production, are the control upon process parameters such as pH, temperature, substrate; water, salts, vitamins, and oxygen (in case of aerobic processes), as well as removal of product and by product (Williams, 2002).

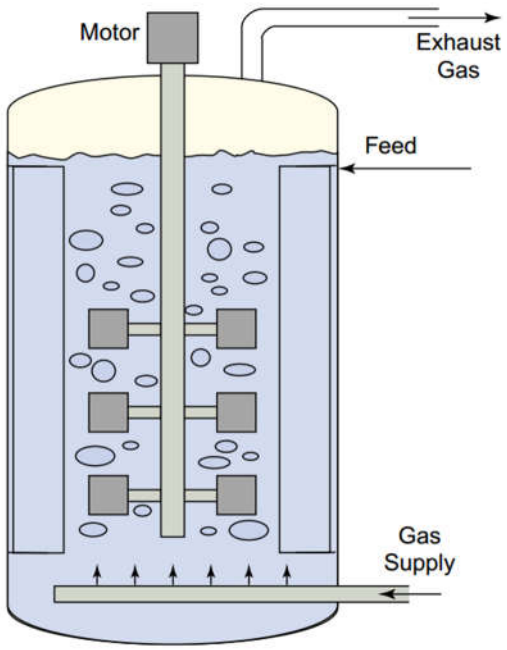

Figure 6. Schematic depiction of bioreactor. For optimal mixing, the tank features an agitator system as well as baffles, which help prevent a whirlpool effect that could hinder proper mixing. .(Williams, J.A. 2002)

In the scope of our work, we used semi-batch bioreactors, a hybrid of batch and continuous operations, to increase the quantity of the biomass significantly, which is restricted by the lesser degree of process control in lab scale shaker flask production. The first phase is the initiation of biomass in batch mode to yield high density culture. The biomass cultivation in batch operation follows the generic growth curve. The lag phase is described as the phase right after inoculation, in which the cell density remains almost constant for a while, requiring some time for the adjustment to the new environment before the growth begins. After the adaptation, the cells begin to grow rapidly, resembling an exponential increase of cell density, which marked the log phase. And as growth-limiting substrate has been consumed, growth stops and the organisms enter the stationary phase. Then in the second continuous phase, the substrate containing IPTG, is fed to the reactor as it steadily maintained the cell growth and induces the expression of the recombinant protein.

LB medium is the most commonly used medium for culturing *E. coli,* and has been used in our lab scale production of recombinant protein. It has rich nutrient contents and the osmolarity for optimal growth at early log phase. Despite having features that are adequate for protein production, cell growth stops at a relatively low density and it makes LB not the best option to achieve high cell density cultures, due to the scarce amounts of carbohydrates (and other utilizable carbon sources) and divalent cations (Sezonov et al., 2007). Adding glucose to the medium is a big help in this regard if control over process parameters, such as pH, are available, i.e. through automated base addition in bioreactor operation. Due to acid generation by glucose metabolism, the limited buffer capacity of LB (at least in shaker flasks) could be easily overwhelmed, and laborious at the same time (Scheidle et al., 2011; Weuster-Botz, Altenbach-Rehm, & Arnold, 2001). Divalent cation supplementation ($MgSO_4$ in the mM range) encouraging higher cell growth, and the addition of peptone or yeast extract resulting in higher cell densities (Studier, 2005), are also considered in composing growing medium.

2. MATERIAL

2.1. Heterologous expression

2.1.1. Subcloning

Codon optimized wild type, single mutant (I167Q) and double mutant (L64H, I167Q) gene of *Humicola insolens* cutinase were purchased from Life Technologies (USA). *Escherichia coli* strain XL10, ,strain BL21-Gold(DE3) (Agilent technology, USA), Expression vector pET-26b(+), agarose, sybersafe (ThermoFisher Scientific, USA), MiniPureYield TM Plasmid Miniprep System (PROMEGA, USA), restriction enzyme *Nco*I and *Xho*I (NEB, USA), CutSmart® buffer (NEB, USA), antarctic phosphatase (NEB, USA), antarctic phosphatase buffer (NEB, USA) T4 ligase (ThermoFisher Scientific, USA), QIAquick Gel extraction system, Cellytic B (Sigma-Aldrich, USA).

2.1.2. Nutrient agar

Recipe for 1000 mL: Nutrient agar 23 g (VWR International, USA), autoclaved for 20 min at 121 °C

2.1.3. Luria Bertani medium

Recipe for 1000 mL: Tryptone 10 g (Sigma-Aldrich, USA), Yeast Extract 5 g (Oxoid, UK), NaCl 5 g (Fluka, Switzerland), autoclaved for 20 min at 121 °C.

2.2. Bioreactor

2.2.1. Growing media

Potassium dihydrogen phosphate (KH_2PO_4) Magnesium sulfate heptahydrate ($MgSO_4 \cdot 7H_2O$)	(Roth, Germany)
Dipotassium phosphate (K_2HPO_4) Calcium chloride dehydrate ($CaCl_2 \cdot 2H_2O$)	(Merck, Germany)
Glucose monohydrate ($C_6H_{12}O_6 \cdot H_2O$) Yeast extract	(Agrana, Austria) (Sigma-Aldrich, Germany)
Sodium citrate dehydrate ($Na_3C_6H_5O_7 \cdot 2H_2O$) Ammonium chloride ($NH_4Cl$) Diammonium sulfate ($(NH_4)_2SO_4$)	(Neuber, Austria)

IPTG (Clontech, Japan).
Trace Element Solution

2.2.2. System

Minifors Bioreactor (Switzerland), Ammonium hydroxide (NH_4OH) (Sigma-Aldrich, Germany), Glanapon 2000 (Bussetti, Austria).

2.2.3. Kanamycin

Stock solution: 50 mg mL^{-1}. 0.5 g of kanamycin (Sigma-Aldrich, USA)is dissolved into a final volume of 10 mL H_2O, the solution is then filtered through a 0.22 μm syringe filter under laminar flow workbench, and aliquoted ready for storage at -20 °C for 1 year (or at 4 °C for 3 months). Working concentration is 40 μg mL^{-1}.

2.2.4. IPTG

Stock solution: 1 M. 2.38 g of IPTG (Isopropyl-β-D-1-thiogalactopiranoside) (Sigma-Aldrich, USA) is dissolved into a final volume of 10 mL MQ-H_2O, the solution is then filtered through a 0.22 μm syringe filter under laminar flow workbench, and aliquoted ready for storage at -20 °C for 1 year (or at 4 °C for 3 months). Working concentration is 0.05 mM

2.3. SDS PAGE

β-Mercaptoethanol (Merck, Germany), Coomassie Brillinat Blue R250 (Sigma-Aldrich, USA), Bromophenol blue (Sigma-Aldrich, USA), Glycerol, 10x Tris/Glycine/SDS Buffer (Bio-Rad, USA), ethanol (Sigma-Aldrich, USA), acetic acid (Merck, Germany) Protein Marker peqGOLD Protein Marker IV, 10 bands (PEQLAB, Germany)

2.4. Protein purification

NaH_2PO_4 (Sigma-Aldrich, USA), NaCl (Sigma-Aldrich, USA), imidazole (Sigma-Aldrich, USA)

Binding buffer (A) : 20 mM NaH_2PO_4, 500 mM NaCl, 10 mM imidazole pH 7.4

Elution buffer (B): 20 mM NaH_2PO_4, 500 mM NaCl, 500 mM imidazole pH 7.4

2.5. Determination of protein concentration

Bovine Serum Albumin (BSA) (Sigma-Aldrich, USA), Bio-Rad protein assay 5x Solution (Bio-Rad,USA), 96-well plate (Sarstedt, Germany).

2.6. Characterization of enzymes

KH_2PO_4 (Sigma-Aldrich, USA), *p*-NP-acetate (*p*-NPA) (Sigma-Aldrich, USA), *p*-N-acetaanilide (*p*-NAA) were purchased from Sigma-Aldrich, USA), Dimethyl sulfoxide (DMSO) was from Fluka (Switzerland).

2.7. Hydrolysis of PA 6.6

Nylon 6.6 film 0.5 mm (Goodfellow, UK), Triton-X 100 (Baker, USA), Na_2CO_3 (Sigma-Aldrich, USA), KH_2PO_4 (Sigma-Aldrich, USA), 96-well plate (Sarstedt, Germany) were used.

2.8. Gas Chromatography and Mass Spectrometry

Acetonitrile (Sigma-Aldrich, USA), Agilent GC column DB-17ms (Agilent Technologies, USA), Agilent Technologies 7890A GC system (Agilent Technologies, USA), Agilent Technologies 5975C VL MSD with triple-Axis detector (Agilent Technologies, USA).

2.9. Laboratory facilities

pH meter	(Microprocessor)
Balance	(Scaltec, Germany), AdventurerTM (Canada)
Pipettes	(Gilson, France)
Bench autoclave	(Certoclav Sterilizer, USA)
Flask 100 mL	(Duran Group, Germany)
Flask 500 mL	(Duran Group, Germany)
Laminar air HB 2472	(Heraeus Instrument, Germany)
Spectrophotometer DR 3900	(Hach Lange, Germany)
Centrifuge Berkman JU-MI	(BeckmanCoulter, USA)
Ultracentrifuge Sorvall Lynx 4000	(Thermo fisher scientific, USA)

Digital Sonifier 250	(Brandson Ultrasonic Corporation, USA)
0.2µm "Rotilobo Syringe filters, PES"	(Carl Roth, Germany)
ÄKTA Purifier	(Amersham pharmacia biotech, Sweden)
His trap FF 5 mL	(GE Healthcare, UK)
PD-10 desalting column	(GE Healthcare, UK)
Vivaspin® 20 ml (molecular weight cut-off: 10kDa)	(GE Healthcare, UK)
SDS chamber	(Bio-Rad, USA)
Chemidoc	(Bio-Rad, USA)
Plate Reader Tecan Infinite M200 Pro	(Tecan, Switzerland)
Semi-micro Cuvette	(Carl Roth, Germany)
Spectrophotometer HITACHI U 2900	(Metrom INULA, Austria)
Thermomixer comfort	(Eppendorf, Germany)
Incubator Infors HT Multitron	(Infors, Switzerland)
Freeze drier	(Lab Conco, USA)
Quartz microcuvette	(Carl Roth, Germany)
Drop Shape Analyzer - DSA100	(KRÜSS, Germany)
AvantiTM J-20xp	(Beckman coulter, USA)

3. METHODS

3.1. Microbial expression

In order to perform the overexpression of *Humicola insolens* cutinases, the genes encoding three different forms of the enzyme were codon optimized for the expression system *E. coli* BL21-Gold(DE3). The codon optimized genes were cloned into the expression vector pET-26b(+) under the leader sequence pelB for periplasmic expression. For the cloning of the genes into the expression vector, digestion with *Nco*I and *Xho*I were performed on both, the plasmid carrying the gene for excision of the gene and the vector pET-26b(+), forming compatible ends

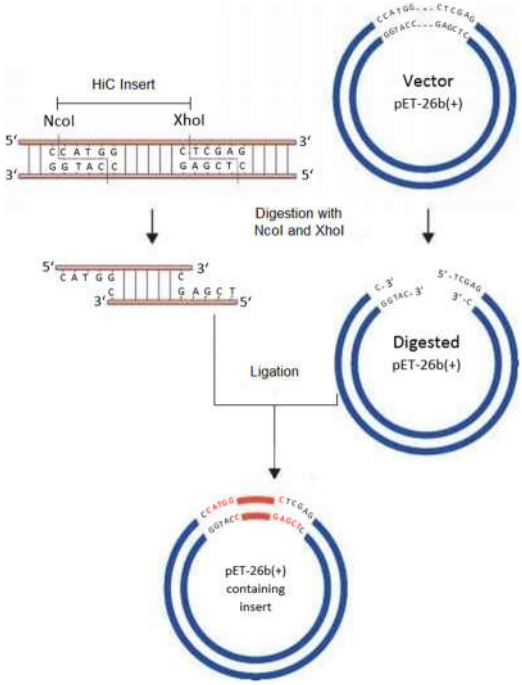

Figure 7. Scheme of Subloning of the HiC gene into the expression vector pET-26b(+). The digestion of the insert and the vector was performed by restriction enzymes NcoI and XhoI forming a compatible sticky ends on both side, and followed by ligation of both components by T4 ligase. The expression vector containing the gene of interest was transformed into the expression system BL21-Gold(DE3) and cultured under specified condition to obtain the desired biomass as well as for the subsequent expression of recombinant protein.

Upon ligation of both components, the expression vector containing the gene of interest was transformed into *E.coli* strain XL10 and subsequently cultivated. The plasmid of selected grown cells were sequenced to identify the colony containing the correct ligation product, that will rule out the self-ligated expression vector without the gene of interest, which could still be formed by an incomplete digestion of the vector. The confirmed plasmid was then transformed into the designated expression host *E.coli* strain BL21-Gold(DE3) and ready for the overexpression of *Hi*C.

3.1.1. Subcloning

The gene encoding the wild type (WT), single mutant (SM) and double mutant (DM) cutinase originating from *Humicola insolens* were codon optimized for the expression host *E.coli* and ordered from Life Technology, shipped as plasmids consisting the particular gene of interest. The subcloning of the three genes from the parent vector to a destination vector (pET-26b(+)) proceed after the same method as follows : the plasmid DNA of pET-26b(+) and the plasmid containing gene of interest were each introduced to *E.coli* strain XL10, which is artificially induced by treatment with calcium chloride for competency, by heat-shock transformation process. The transformed cells were plated on standard nutrient agar containing kanamycin as

selection factor and incubated overnight at 37 °C. The grown colonies showed a successful transformation of cells with kanamycin resistant gene encoded plasmid, which as well embodies the gene of interest. A colony was taken for liquid culture using LB medium. Plasmid minipreps were carried out and the concentration of DNA plasmid (in ng μL^{-1}) was subsequently determined by NanoDrop giving information for the calculation of needed volume used in the subsequent steps.

3.1.2. Digestion of the gene of interest and the expression vector

The plasmid DNA of *Hi*C WT, SM, DM, and pET-26b(+), were each digested separately. The digestion by the same restriction enzyme for both DNA material, the insert and the destination vector, provides compatible ends for the subsequent ligation of both components. In pET-26b(+), N-terminal pelB signal sequence and C-terminal His-Tag sequence were conserved for potential periplasmic localization and for purification based on affinity chromatography respectively.

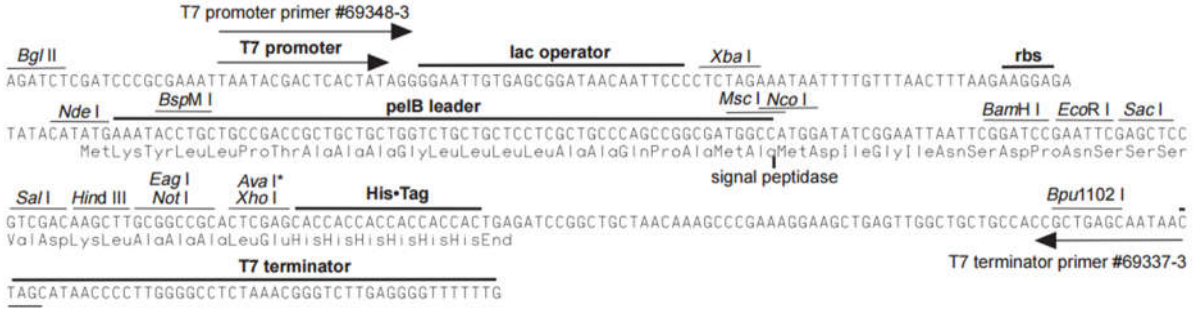

Figure 8. pET-26b(+) cloning/expression region. The DNA of interest originating from Humicola insolens in its wild type (WT) variant, and the variant with one (SM) and two point mutations (DM) are inserted into the multiple cloning site upon mutation after digestied by using NcoI and XhoI restriction enzyme, yielding intact pelB leader for periplasmic product localization and His-tag for purification based on affinity chromatography.

For the digestion mix, the volume of each plasmid DNA constituting an end-mass of 0.5-1 µg were calculated from predetermined concentration. Quantitative composition of each mix is shown in Table 3 in the result section. The mixture were subsequently incubated at 37 °C, for 2 h without mixing.

In order to purify the digested products, each mixture was run on 0.8% agarose gel revealing the digested fractions of *Hi*C genes and expression vector by SYBR safe under UV light. The fraction of interest were subsequently extracted through excision. Further purification of the DNA was carried out by QIAquick Gel extraction system. The concentration of purified DNA plasmid was then determined by NanoDrop for the later calculation of needed volume used in further process.

3.1.3. Dephosphorylation

The expression vector pET-26b(+), was subsequently dephosphorylated by *Antartic* phosphatase removing the 5' phosphate group required for ligation thus prohibits self-ligation of the digested plasmid DNA. The appropriate volume of 10x Phosphatase buffer and 5000 U *Antartic* phosphatase were calculated achieving working concentration of 1x and 5U for each component respectively. The incubation of the mix was carried out at 37 °C for 15 min and followed by inactivation of phosphatase at 70 °C for 20 min.

Table 2. Dephosphorylation composition

Component	Volume
pET-26b(+)	26 µL
Buffer	2.9 µL
Antartic phosphatase	1 µL
Total	29.9 µL

3.1.4. Ligation and sequencing

The required amount of both, vector and insert DNA, were calculated with a molecular weight calculator (http://sciencelauncher.com/MWcalc.html) with a maximum moles ratio of vector to insert DNA of 1 : 10 with approximately 25 fmol of vector DNA to its concentration dependent moles of insert DNA. In consideration of the size of the molecule (0.576 kbp), and molecule type (double stranded DNA), the corresponding weight of insert constituting the predetermined moles ratio of vector to insert DNA (1:5) was calculated giving the appropriate volume of insert DNA via concentration of each insert, which was determined by NanoDrop prior to ligation. The amount of T4 Ligase and buffer for the ligation of the 3 variant were the same, using PCR H_2O to reach the total volume of 15 µL. The ligation reactions were conducted overnight at 4 °C. Quantitative composition of each ligation mix is shown in Table 4 in the result section. After ligation, transformation of the ligation products using chemically competent *E.coli* XL10 was carried out.

3.1.5. Sequencing of ligation product

The transformed cells were plated on nutrient agar containing kanamycin as selection factor, and only cells incorporated the ligated plasmid containing kanamycin resistance gene could grow after an overnight incubation at 37 °C. Freshly transformed colonies from each successful transformation of each variants were taken and cultured in 3 mL LB medium containing

kanamycin and put in inclined position for improved aeration. After successful overnight incubation at 37 °C, 150 rpm, plasmid minipreps of the liquid culture was carried out as previously described.

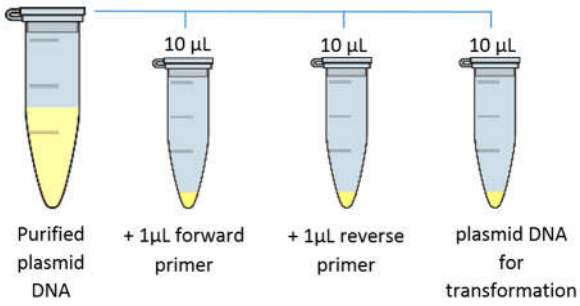

Figure 9. Schematic depiction of plasmid DNA preparation for sequencing and a subsequent transformation after positive confirmation of the correct ligation product containing pET-26b(+) and insert DNA.

The purified plasmid of each colony was aliquoted into 3 Eppendorf tubes. 1 µL of forward or 1 µL reverse pET-26b(+) primers was added to the first and second aliquot respectively, ready for shipping to LGC Genomic for Sequencing. The third aliquot was saved for a subsequent transformation after a confirmed successful ligation product of expression vector containing the gene of interest.

3.1.6. Culturing of confirm plasmid DNA

The plasmid DNA from the confirmed cultures with each containing expression vector, pET-26b(+), and *Hi*C gene was introduced to competent *E.coli* strain BL21-Gold(DE3) as expression host for periplasmic expression of recombinant protein. The transformed cells were plated on nutrient agar with kanamycin and incubated overnight at 37 °C.

3.2. Protein expression in shaker flasks

3.2.1. Analysis of recombinant protein

For the Expression of recombinant protein in laboratory scale using shaker flasks, the preculture was prepared from a single freshly transformed colony from the corresponding variant, cultured overnight at 37 °C, 150 rpm, in 25 mL LB medium containing kanamycin. An appropriate volume of preculture, depending on its optical density at a wavelength of 600 nm (OD_{600}), were taken as an inoculum for the main culture resembling a start OD_{600} of 0.1. The main culture in 200 mL LB medium were incubated at 37 °C, 150 rpm, and checked for its OD_{600} at regular interval reaching an OD_{600} value of ca. 0.8. Subsequently, the temperature was decreased to 20 °C at which the induction by IPTG and the expression of recombinant protein respectively were carried out. 0.05 mM IPTG were added into the culture, and probes of 1 mL culture were taken in 2 hours interval to visualize the induction of the culture throughout the 20 hours

fermentation. The probes were centrifuged yielding two fractions: the supernatant and the cell pellet.

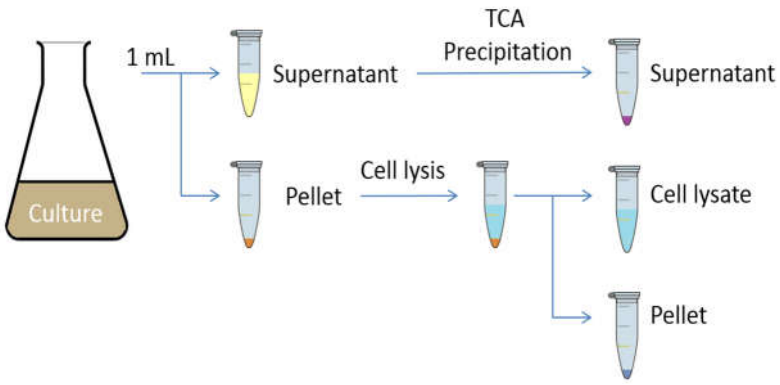

Figure 10. Working scheme for analysis of recombinant protein. The proteins in the supernatant of the culture are precipitated using Trichloroacetic acid (TCA). The pellet of the culture containing cells is lysed using celLytic *reagent, releasing soluble protein in the cell lysate fraction and insoluble protein in the pellet fraction.*

The cell pellet and the supernatant of each probes taken in 2 hours interval were treated with CelLytic™ B inducing cell lysis and with TCA precipitation method respectively (Figure 10). The resulting fractions: supernatant with TCA precipitation treatment, cell lysate and pellet were run through SDS PAGE for protein analysis. Protocols are to be found in the appendix section (Appendix 6.3, 6.4).

3.3. Protein expression in bioreactor

In order to increase the amount of expressed protein, fermentations in a larger bioreactor scale, were carried out. The fermentation were constituted by two distinct phase, an overnight batch phase, in which the nutrient is a limiting factor and will be used to its exhaustion by the culture growth resembling a start culture for the subsequent fed-batch phase. In the second phase, a regular amount of medium containing IPTG as inducing agent was fed into the system in a manner that the specific growth maintained at 0.1 h^{-1}, inducing the expression of the recombinant protein. The system was inoculated with the desired plasmid containing cells directly from the cryovial without preculture, and the incubation temperature were hold constantly at 37 °C throughout the first and the second phase of fermentation. Due to a sterile workflow, kanamycin was added in a very low amount, 350 µL per reactor to prevent plasmid loss. Air was used for the saturation of oxygen at 100%, and nitrogen on the other hand for the depletion at 0% in calibration of the sensor.

Parameter values like base weight, concentration of CO_2 and O_2 emitted due to respiration of the cells (off-CO_2 and off-O_2), pH, temperature and stirring velocity as well as dissolved O_2 were registered by the system software. Probes for determination of biomass, and for SDS PAGE analysis were taken every 2 hours in duplicate and triplicate respectively, after the probing timetable in Table 5 (in the result section). The predetermined value of the pH was 7,

monitored by pH meter and maintained by the addition of base (NH_4OH) compensating decrease of the pH caused by metabolism of the culture. As the culture grew, the stirring velocity incremented automatically compensating the increase intake of dissolved oxygen, and parallel to that the CO_2 emitted by the culture also rose. After the end of the fed-batch, the culture was harvested and proceeded to purification steps.

The detailed information of bioreactor parameter, calculated fermentation-lapse, synthetic media are available in Appendix 6.9 – 6.11.

3.3.1. Biomass analysis

A duplicate of 5 mL sample at each probing time point (exception: 10 mL sample for the 0^{th} hour) were taken for the determination of cell dry weight (CDW). These samples were centrifuged at 3000 g for 10 min yielding the biomass, which was then washed from the remaining growing medium by resuspension in 5-10 mL RO water followed by decanting the supernatant after a repeated centrifugation. In the meanwhile all samples of the time points were collected, and dried. The biomass were determined gravimetrically by drying the resuspended biomass at 105 °C for 24 h, and subsequently weighed. By subtracting the weight difference of beaker glasses with or without dried biomass, the biomass concentration in relation to its sample volume can be calculated (Table 5 in Result section). Optical density of samples at a wavelength of 600 nm was also measured.

3.3.2. Analysis of recombinant protein

1.5 mL sample were taken in triplicate according to the sampling timetable (Table 5). The cells were then separated from the supernatant by centrifugation at 7800 g, 4 °C for 20 min. The resulting fraction of cell pellet and supernatant were prepared and proceeded to SDS PAGE for the protein expression analysis.

For comparable result due to an increasing biomass in fed-batch culture, samples which were taken volume-wise were mathematically adapted to get a more comparable value of a cell dry weight (CDW) of 1 mg at each time point. Firstly the centrifuged cells of 1.5 mL sample were resuspended back into its initial volume with binding buffer. Using data of the cell dry weight determined previously by gravimetric method, the biomass in 1.5 mL was calculated (Table 5). The equivalent sample volume (Table 5) containing 1 mg biomass was then taken to proceed with the celLytic protocol and followed by SDS PAGE sample preparation protocol.

3.4. Protein purification

ÄKTA purification system based on affinity chromatography using immobilized nickel ions in columns as stationary phase (HisTrap 5 mL columns), was used to purify our His-tagged proteins. All three variants was purified from the cell lysate and prepared prior to ÄKTA purification as follows, the cells were separated from the supernatant by centrifugation at 4 °C, 6693 g for 30 min, the pellet was then resuspended in binding buffer with the ratio of 25 mL binding buffer per 5 g pellet. The suspension was sonicated at 60% amplitude for 45 s with 2 min break between each session for a total of 3 sonication-rounds. It was subsequently filtered through 0.22 μm filter to have a cell-free sample before being injected into the column.

The injected sterilized cell lysate undertook binding and eluting process during the purification steps. During the binding process the recombinant protein carrying 6xHis-tag was bound to the stationary phase, due to its affinity to the immobilized nickel ions. The unspecific bound proteins were eluted by directing 10% elution buffer into the column, leaving the recombinant protein retained in the column. In the elution process, an increasing gradient of elution buffer to 100%, containing 500 mM of imidazole which compete with the polyhistidine-tagged protein, elute the target protein into fractions, which automatically collected by the system sampler. SDS PAGE analysis of these fractions was carried out to reveal which fractions contain the protein of interest. These fractions were pooled together and concentrated by vivaspin with a molecular weight cut-off of 10 kDa at 4000 rpm, 4 °C for 30 min. The retained solution was resuspended and proceeded with desalting process by PD-10 desalting columns containing Sephadex G-25 as stationary phase. In this step the imidazole was removed from the enzyme solution and the buffer was changed towards 0.1 M Tris-HCl pH 7.

3.5. Activity and kinetic assay : *p*-NPA & *p*-NAA

In order to characterize the kinetic activity of the mutant enzymes on ester as well as on amide bond, protein concentration of purified enzymes is to be determined. The protein concentration of the three enzymes were determined by BIO-RAD protein assay (Appendix 6.6).

The activity assay on ester substrate was carried out in triplicate using *p*-NPA solution B after the workflow described in Appendix 6.7. The enzyme activity on particular substrate are depicted as a diagram of the measured absorbance against time.

For the kinetic assay on ester substrate, *p*-NPA with a range of concentration from 0.07 to 8.264 mM was used as substrate gradient. Blank reactions without enzyme replaced by the same

amount of buffer were also carried up. The same workflow and conditions were kept constant as used in activity assay described in Appendix 6.7.

Kinetic assay on amide substrate, was carried out on *p*-NAA. The concentration range used was from 0.010 to 2.044 mM, due to low solubility, for 1 h with 15 min interval time, at the same temperature and wavelength. Blank reactions without enzyme replaced by the same amount of buffer were also carried up. (Appendix 6.8)

The Michaelis-Menten parameters, K_M and k_{cat}, were determined from the data acquired by kinetic assay as follows: the triplicate of each absorbance reading within a substrate concentration of the same interval were averaged and substracted by the value of the blank of the corresponding interval of the same substrate concentration. These values were plotted against the time, forming the corresponding graphs, from which the trendline subsequently generated. The slope of trendline-equations, the so called absorbance, were used for the calculation of volumetric activity by using formula below. The determined specific activity and the corresponding substrate concentration were plotted in Sigma plot software (version 12.5) with a non- linear regression of the Michaelis-Menten equation delivering K_M value. For the determination of k_{cat}, the specific activity and substrate concentration were plotted, and the slope of the tangential trendline of the graph is the value of k_{cat}/K_M, and k_{cat} can be accordingly calculated.

$$Volumetric\ activity = UmL^{-1} = \frac{Abs.V_f}{\varepsilon.\ d.V_e}.d_f$$

$$Specific\ \ activity = Umg^{-1} = \frac{Volumetric\ Activity}{Enzyme\ concentration} = \frac{UmL^{-1}}{mgmL^{-1}}$$

Δ Abs : slope of the equation generated by putting the averaged value of triplicate against time.

ε : molar extinction coefficient of *p*-NP in certain conditions. ε for K_2PO_4 at pH 7, 50 mM: 11.86 M^{-1} cm^{-1}

d : pathlength of the light: 1 cm

V_f : final volume (20 µL enzyme + 200 µL substrate solution)

V_e : enzyme volume: 20 µL

d_f : dilution factor of enzyme solution used

3.6. Hydrolysis of PA 6.6

Nylon 6.6 film was cut in size of 2x2 cm. Hydrolysis of the cut pieces of film was performed at 2 different temperatures (37 °C and 50 °C). Prior to hydrolysis, the films undertook three washing steps, for 30 min each to remove any impurity, at respective temperature for each hydrolysis: Triton X100 (5 g L^{-1}), Na_2CO_3 (100 mg mL^{-1}), and MQ water were used as washing solutions. The washed films were air dried and ready to proceed with the hydrolysis. They were incubated in 10 mL of K_2PO_4 buffer containing 5 µM of Enzyme (WT, SM or DM) in 50 mL falcon conical centrifuge tube at the designated temperature, 37 °C or 50 °C, 150 rpm for 1 week. A blank without enzyme for each incubation temperature were also set up following the same preparation workflow as described above. After the incubation, the films were once again washed with the three mentioned solutions to remove adsorbed enzyme molecules and air dried to proceed with water contact angle analysis and the solution of the treatment were freeze dried for 3 days to proceed with gas chromatography and mass spectrometry analysis.

3.7. Water contact angle

The surface hydrophobicity of the enzymatic-treated and blank sample were measured via Water Contact Angle (WCA). After the consecutive washing steps, which follow the hydrolysis, removing proteins from the surface, as described above, polymer films were analyzed with a Drop shape analysis system using ddH_2O as test liquid with drop size of 2 µL, and deposition speed of 100 µL min^{-1}. WCA were measured via the static sessile drop method after 5 s. Data were obtained from the average of the measurements taken from at least 8 different points of the surface of each sample, delivering statistically reproducible data. The measurement were to be repeated to achieve a comparable water contact angle on both side of the water droplet (Pellis et al., 2015).

3.8. Gas Chromatography and Mass Spectrometry

The lyophilized solution of the enzyme treatment of the nylon 6.6 film containing a possible released hydrolyzed products were resuspended in ethylacetate. The amount of products was determined by GC analysis by using 7890A GC system (Agilent Technologies, USA) equipped with Mass Selective detector 5975C VL with triple-Axis detector. GC columns used were Agilent DB-17 ms.

4. RESULT AND DISCUSSION

4.1. Subcloning

The composition of the digestion mix followed the formulation stated in Table 3. The digestion of the plasmid DNA by the restriction enzyme *Nco*I and *Xho*I, which contained the gene of interest, yield sticky ends on both side of the genes, providing compatible ends for the expression vector pET-26b(+), which accordingly digested by the same restriction enzymes.

Table 3. Digestion composition. Concentration [ngμL^{-1}] of plasmid DNA after Plasmid Miniprep Purification System determined by NanoDrop prior to digestion, giving information of the volume of each plasmid DNA constituting end-mass of 0.5 - 1 μg to be used in digestion process. Restriction enzyme: XhoI and NcoI, 0.5 μL of each for every reaction (WT, SM, DM, and pET-26b(+)).

Concentration Determination

Concentration [ng/μL]			
WT	SM	DM	pET-26b(+)
91	86	90	64

Digestion

	Volume [μL]			
	WT	SM	DM	pET-26b(+)
Cutsmart buffer	2	2	2	2
Plasmid DNA	10	11	10	15
Rest.enzyme (*Nco*I+*Xho*I)	0.5 + 0.5	0.5 + 0.5	0.5 + 0.5	0.5 + 0.5
PCR H_2O	7	6	7	2
Total Vol.	20	20	20	20

The digested products were run in 0.8% agarose gel in order to separate the digested fractions of the plasmid and purify *Hi*C genes shown as a band at the size of about 0.57 kbp in Figure 11.

The digested expression vector was also run in agarose gel to remove the 62 bp of the multi cloning site forming the compatible sticky ends for the further cloning.

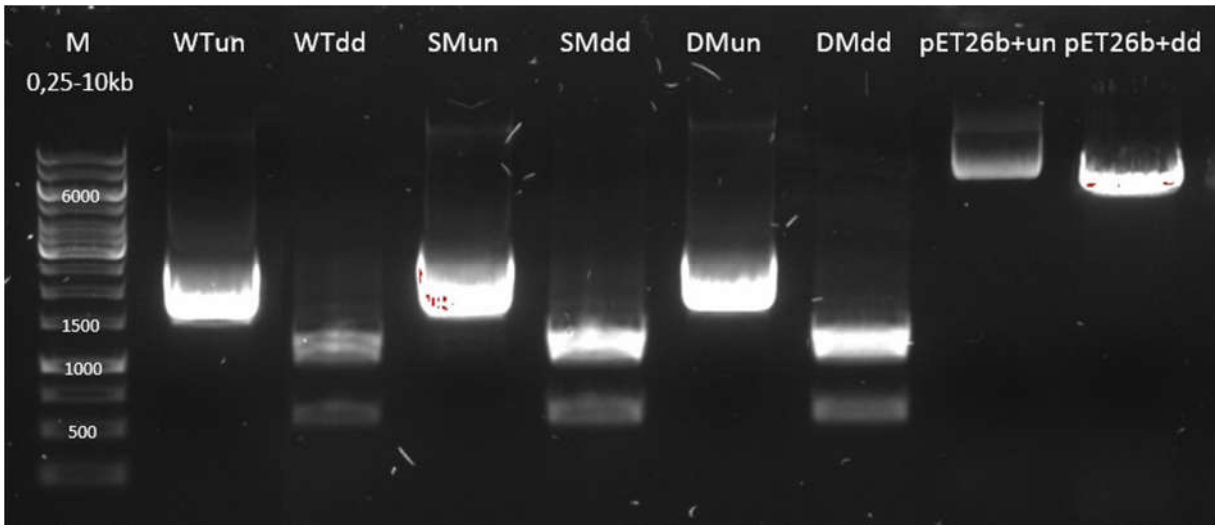

Figure 11. Agarose gel of undigested and double digested HiC genes and pET-26b(+) vector (restriction enzyme: XhoI and NcoI). pET-26b+dd well contained the double amount of plasmid DNA in comparison to pET-26b+un well perceived as a more intense band. WT: wild type, SM: single mutant, DM: double mutant, un: undigested, dd: double digested.

After obtaining both vector and insert DNA, the vector subsequently dephosphorylated by *Antartic* phosphatase removing the 5' phosphate group thus prohibiting self-ligation. Based on the previous ligation attempts yielding low to none ligation product by using “ready to use” Ligation mix (TAKARA, Japan) and T4 ligase under suggested manual by manufacturer, few parameters of the test setup were modified, comprising the approach of overnight incubation at lower temperature, at 4 °C, to preserve the overhangs. A concern of further phosphatase activity degrading the DNA vector was also taken into account by performing ligation with non-dephosphorylated vector DNA with intact 5' phosphate. The ligation formulation is listed in Table 4. After transformation of ligation product into *E.coli* XL10, colony growth on nutrient agar was observed from *E.coli* transformed by ligation product of the dephosphorylated vector incubated overnight at 4 °C.

Table 4. Ligation composition. Concentration [ng μL^{-1}] of inserts and peT-26b(+) digested by XhoI and NcoI determined by NanoDrop prior to Ligation, giving information of the volume of insert DNA needed to achieve a mole ratio of vector to insert of 1:5. Legend: total vol.: total volume.

Concentration Determination

Concentration [ng μL^{-1}]			
pET-26b(+)	WT	SM	DM
14	1.6	2.45	1.9

Ligation

	WT	SM	DM
	Volume [µL]		
Vector DNA	3	3	3
Insert DNA	12	8.5	11
T4 Ligase	3	3	3
Buffer	2	2	2
PCR H_2O	0	3.5	1
Total Vol.	15	15	15

From the grown colonies of each variant, different colonies were sampled for liquid culture. The purified plasmid from the culture of each variants were sequenced and the correct expression vector containing the gene of interest were transformed into *E.coli* BL21-Gold(DE3). The successful transformation indicated the incorporation of the plasmid DNA into the cells, displaying the kanamycin resistant trait of the grown colonies. Subcloning of the gene of interest (WT, SM, or DM) into the expression vector pET-26b(+) and its subsequent transformation into the designated expression host, *E.coli* BL21-Gold(DE3), was a success.

4.2. Shaker flask production scale

4.2.1. Growth curve

The growth of variants with single and double point mutation is moderately faster than the wild type by about ±0.1 on OD_{600} value. Interestingly the growth curve of the DM showed a slight

bending at OD_{600} reading at 120 min resembling an imminent reach of stationery phase plateau, while the WT and the SM still showed a steady gradient going upwards.

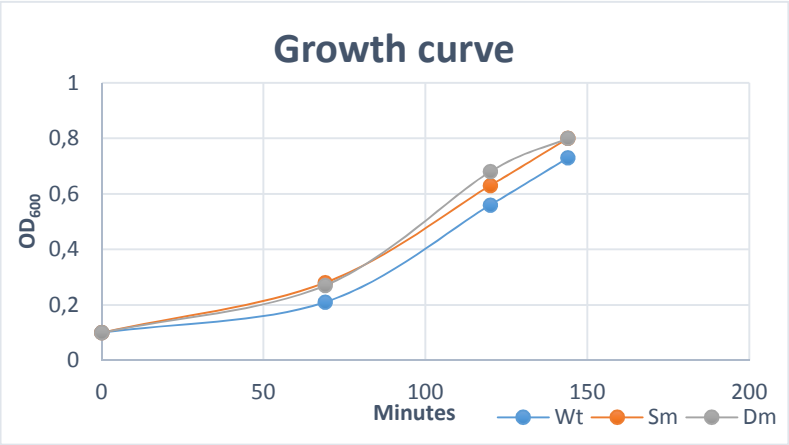

Figure 12. Growth curve of main culture starting from the inoculation of overnight preculture at OD_{600} of 0.1 reaching the OD_{600} of ±0.8 ready for IPTG induction at 20°C. Legend: WT: Wild type, SM: Single Mutant, DM: Double Mutant.

4.2.2. Analysis of recombinant protein

Under conditions of high level expression, the expressed protein may not be folded properly or become unstable resulting in insoluble accumulation of in the so-called inclusion bodies. This will be retrieved in the pellet-fraction of the cells, while the soluble protein will be found in the cell lysate fraction. The recombinant protein found in the supernatant fraction of the culture are supposed to be passively released due to lysis of the cells during fermentation.

Qualitative protein analysis by SDS PAGE referring to 1 mg biomass (described in the later analysis of bioreactor fermentation) incorporated only the fractions of a constant cell weight of 1 mg, which showed whether the production of recombinant protein increased or decreased with the time at a constant amount of biomass during the fermentation, and in which fractions the protein would be found for the later enzyme purification. In contrast to that, by analyzing the time points probes of the protein expression in shaker flask based on the volume (1 mL), the SDS PAGE gels of the fractions provide information of what might happened during the fermentation, and consequently the appropriate time of harvest yielding the maximum amount of recombinant protein in the fraction of interest. Due to lysis of the cells during fermentation, inclusion bodies and soluble protein will be released into the medium and change the composition of the fractions during the time of fermentation, as can be seen clearly in the WT (Figure 13) and further described below.

In case of WT, the inclusion bodies started to be formed from the 2th hour and built up during the fermentation time. While the production of soluble protein reached its peak at 8th hour before it started to decrease overtime. An increase of *Hi*C in supernatant was observed accordingly from the same time point (8th hour), giving indices of the passive release of soluble protein into the supernatant due to lysis of the cells. The same manner were also observed in the SM and DM, where the accumulation of inclusion bodies and the increase of *Hi*C in supernatant were evidenced, indicating a possible lysis of the cells thus releasing the soluble as well as the insoluble protein into the medium. However the SDS PAGE gel of the cell lysate of SM and DM did not fit the interpretation due to the qualitatively constant amount of enzyme in this fraction throughout the fermentation time, despite the increase of the cutinase band observed in the pellet and supernatant fractions. However in the later Fed-Batch bioreactor fermentation under optimal as well as controlled environment (temperature, pH and aeration) WT and DM also suffered under cell lysis starting from 8th h/10th h respectively, while SM grew in compliance with the theoretical growth curve of biomass based on specific growth of 0.1 h^{-1}. The enzyme expression using shaker flask did not yield enough enzyme for the research purposes. Attempts of stopping the fermentation earlier at the peak of enzyme expression at 8th h, especially of the WT, preventing product loss into the supernatant has been performed, but it did not make any substantial different of the concentration of enzyme purified.

Double band observed in the supernatant in all variant has been suspected to be led by possible protease activity present in the supernatant cleaving some part of the recombinant protein released into the supernatant, resulting slightly smaller molecule at almost the same size. Western blot revealed only one band, probably caused by C-terminally cleavage of the enzyme. Another thought was an inadequate denaturation agent used for SDS PAGE sample preparation by using Dithiotreitol (DTT) instead of the volatile β-Mercaptoethanol (β-ME). Taking into account that the chemical reduction of protein disulfide bonds is an equilibrium reaction, the disulfide bonds are constantly breaking and re-forming, by which β-ME is needed in large excess to drive the equilibrium reaction toward completion. Inadequate denaturation of protein leaving some disulfide bonds intact might cause different velocity of the Protein running in the gel. From this investigation, the intensity of the bands decrease with the increase of both denaturation agents, without showing any improvement of protein denaturation, which should result in the disappearance of double band. The maximum concentration to warrant a true result is 0.32 M for DTT and 0.8 M for β-ME. β-ME in concentration of 0.4 M (standard recipe – Appendix 6.5) was chosen as the concentration of denaturation agent used in SDS PAGE sample preparation.

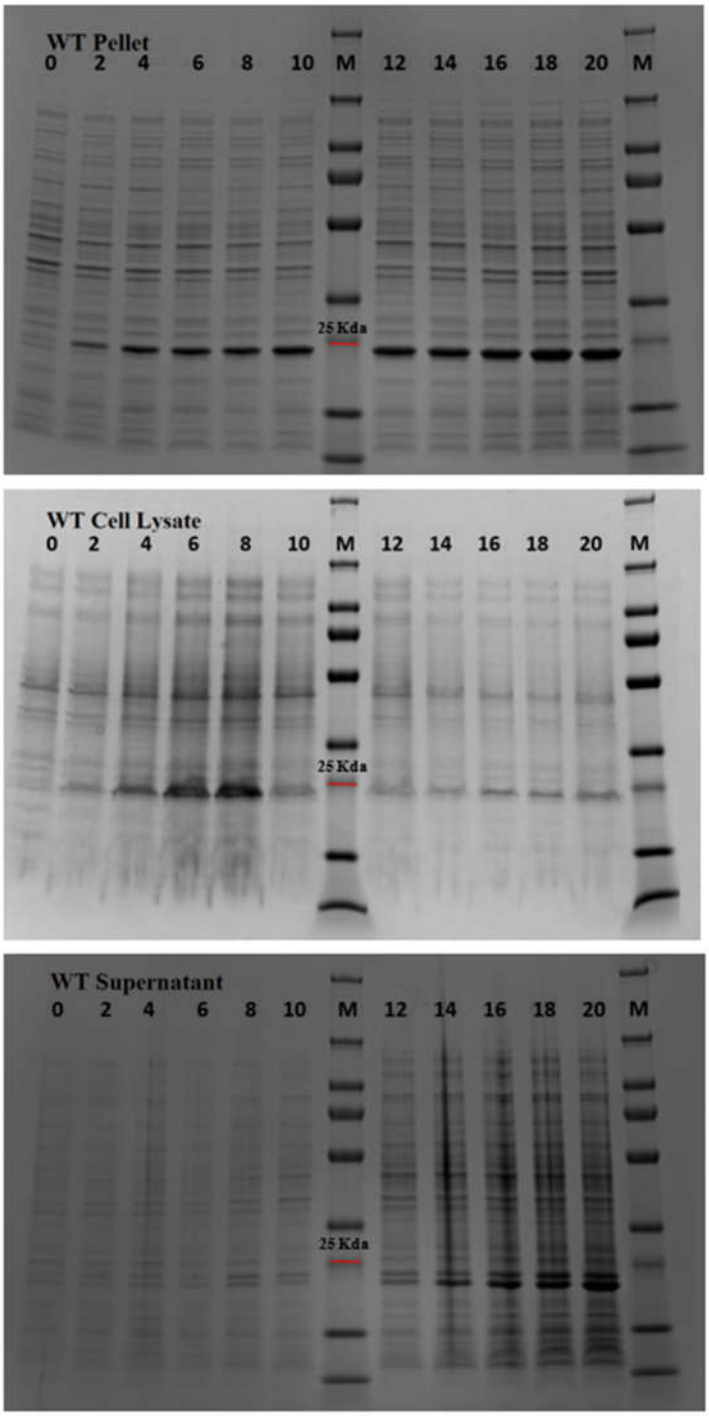

Figure 13. SDS PAGE Gel of treated pellet after cell lytic treatment- and supernatant after TCA precipitation protocol. Legend: Pellet: contains insoluble protein originating from the pellet of the culture, cell lysate: contains soluble protein originating from the pellet of the culture, Supernatant: precipitated protein originating from the supernatant of the culture. HiC cutinase size : ~23 kDa (the red line on the marker highlighting the molecule size 25 kDa), WT: wild type.

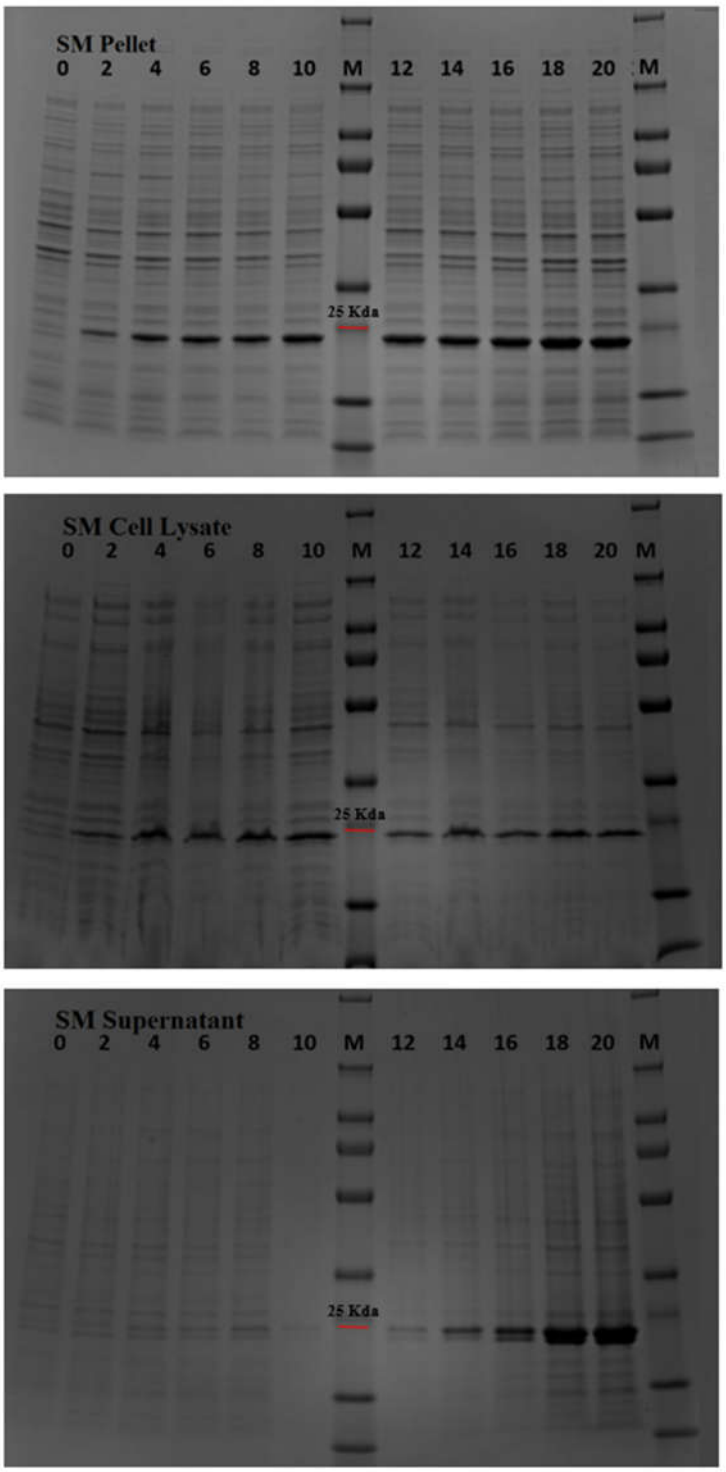

Figure 14. SDS PAGE Gel of treated pellet after cell lytic treatment- and supernatant after TCA precipitation protocol. Legend: Pellet: contains insoluble protein originating from the pellet of the culture, cell lysate: contains soluble protein originating from the pellet of the culture, Supernatant: precipitated protein originating from the supernatant of the culture. HiC cutinase size : ~23 kDa (the red line on the marker highlighting the molecule size 25 kDa), SM: single mutant.

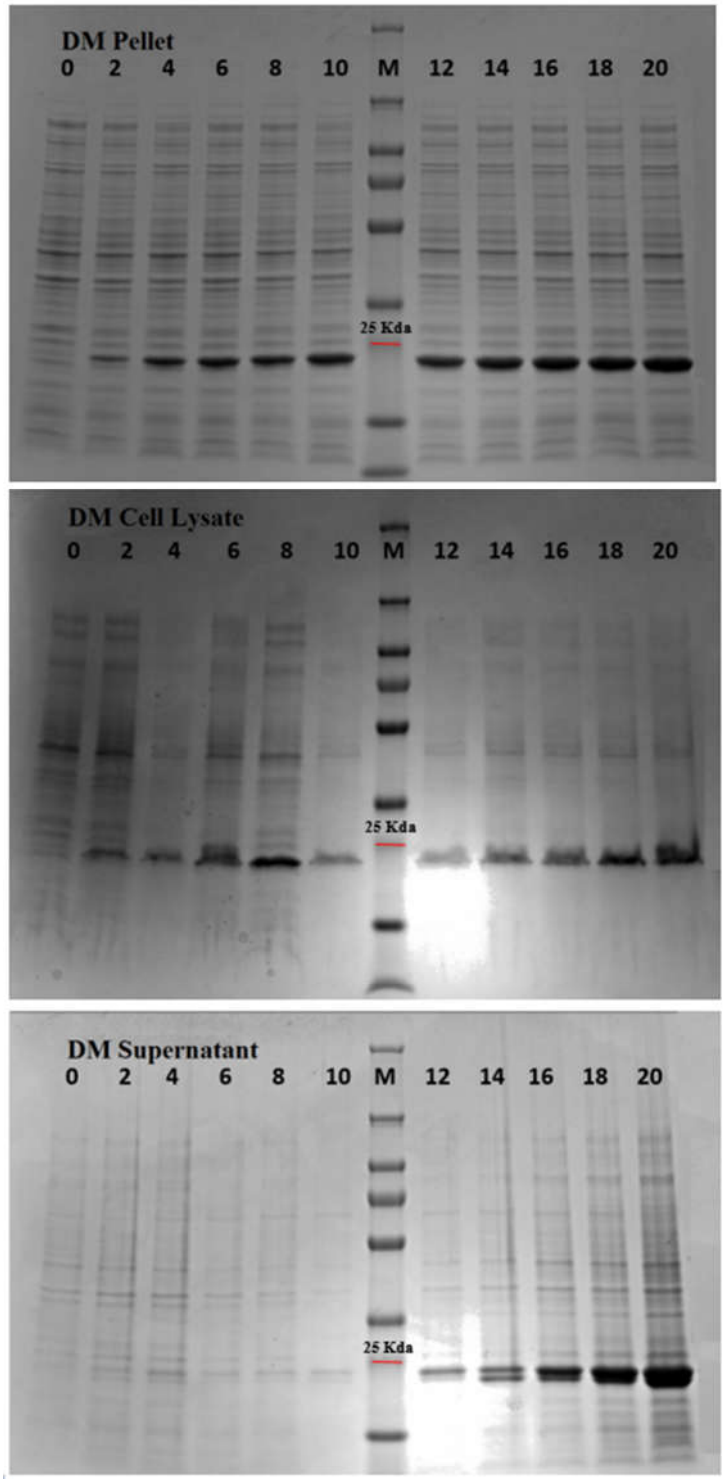

Figure 15. SDS PAGE Gel of treated pellet after cell lytic treatment- and supernatant after TCA precipitation protocol. Legend: Pellet: contains insoluble protein originating from the pellet of the culture, cell lysate: contains soluble protein originating from the pellet of the culture, Supernatant: precipitated protein originating from the supernatant of the culture. HiC cutinase size : ~23 kDa (the red line on the marker highlighting the molecule size 25 kDa), DM: double mutant.

4.3. Bioreactor production scale

4.3.1. Batch process

The fermentation lapse of the wild type (WT), Single Mutant (SM), Double Mutant (DM) in Batch processes prior to induction with IPTG was compared (Figure 16 - Figure 18). The logarithmic growth of the WT took place about 2 hours earlier than the mutants, which was implied by the plunging value of the dissolved oxygen level (pO_2) resulting in an increase of the stirrer speed maintaining the predetermined value of the dissolved oxygen level. The pH level went down for only a moderate amount (less than 0.2) observed in all three systems at the time point where the pO_2 started to plunge. As a response to the decrease of pH due to the catabolic activity leading to acid production, base was pumped in an automated manner accordingly to maintain the pH level at 7. In all systems the pH was maintained at 7 and the pH decrease stopped at the peak of cultures growth emphasized by the peak of pO_2 usage, which corresponds to the peak of stirrer-speed and the peak of the off-CO_2 emission (particularly observed in WT and DM). From this point the pH rose to about 7,8 without any base addition. Stressed or dying cells may be responsible for this further pH increase. The rough depiction of base usage in SM depicted in Figure 17 as a slope, was due to technical error causing skipped registration of the real time base usage during fermentation. The slope was reconstructed from the total amount of base used at the end of fermentation. The base usage of the WT and SM are comparable, whereas of the DM is about 30% lower. The off-CO_2 emitted by the cells through respiration of the WT is substantially less (about 50%) than of the DM despite the qualitatively comparable timespan of the peak. The off-CO_2 of SM was registered as a constant value of 0.1, while the off-O_2 decreased steadily through the batch process. However it worked normally in Fed-Batch process. Batch-End is indicated by the leveling of stirrer, pO_2- and off CO_2-value to a constant level.

4.3.2. Fed-Batch process

The Fed-Batch medium containing IPTG was fed into the system maintaining the specific growth at 0.1 h^{-1}. Independently on the initial value of the dissolved oxygen (pO_2) at the end of the Batch process, the pO_2 value decreased drastically in the first hour with the start of the Fed-Batch and followed by steady rise of the stirrer maintaining the dissolved oxygen at the predetermined value. In the same way the pH decreased in less than 4 h due to cell growth implied by the increasing value of off-CO_2 emission and responded by the increasing amount of base pumped into the system to maintain the pH at 7. The pH value was maintained in WT and DM, while it settled at a bit higher pH of 7,1 in SM, possibly due to calibration issues of pH meter. The rough depiction of base usage in SM depicted in Figure 20 as a slope, was due to technical error causing skipped registration of the real time base usage during fermentation. The slope was reconstructed from the amount of base used at 5 probing time points, which is manually noted in addition to computerized data log, constituting a fairly comparable trend with the course of pH usage of the WT and DM fermentation. The off-O_2 however stayed fairly on a constant level in WT and DM, while having a noticeable fluctuation in SM fermentation.

4.3.3. Fermentation lapse during Batch process prior to IPTG induction.

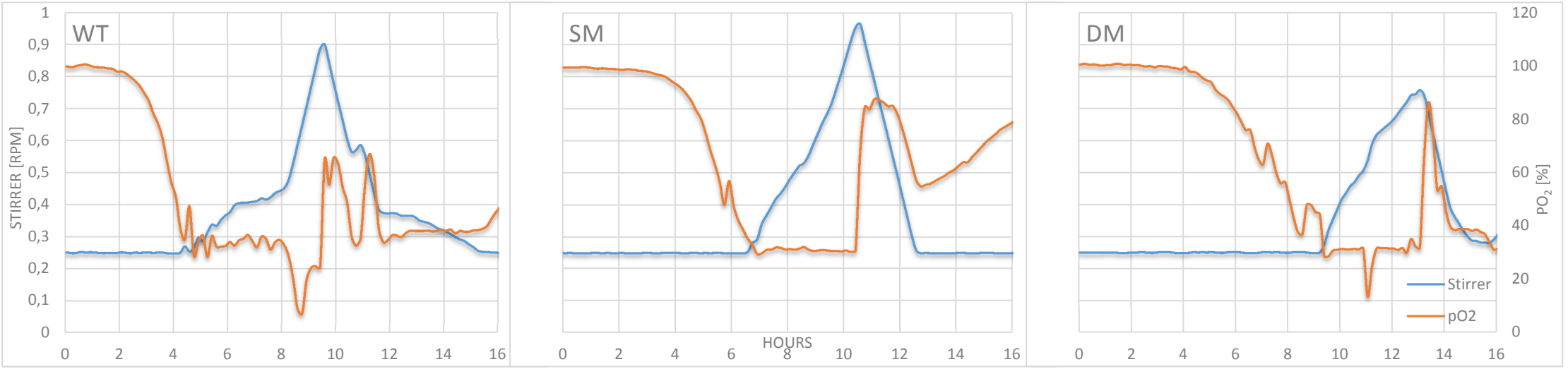

Figure 16. Dissolved oxygen (pO_2) to stirrer diagram in batch process. The logarithmic growth of the culture is implied by the dramatic drop of the dissolved oxygen level resulting in the increase of the stirrer speed maintaining the predetermined value of dissolved oxygen (100% saturation by air, 0% depletion by nitrogen). Batch-End is indicated by the leveling of stirrer and pO_2 value to a constant level.

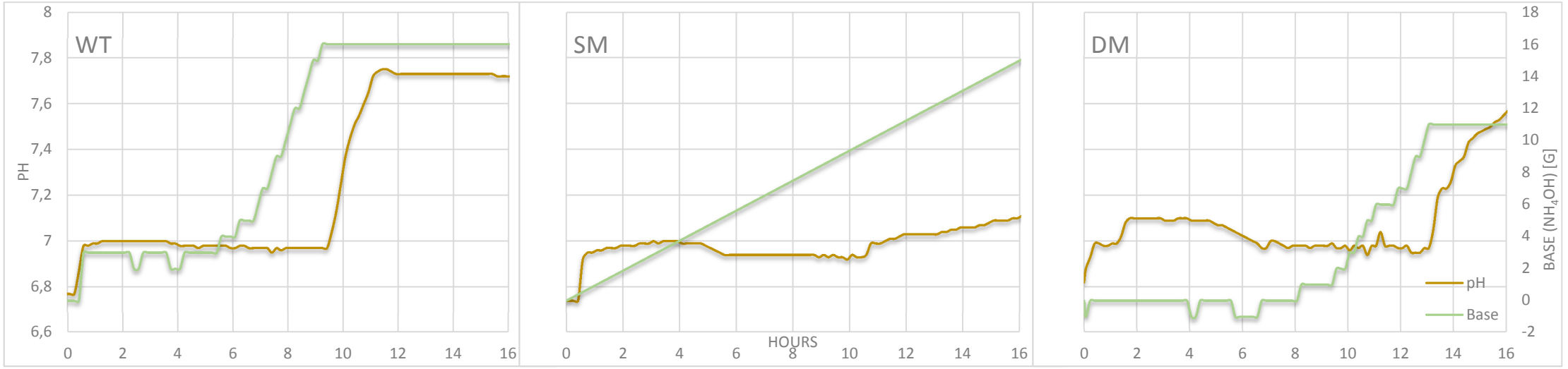

Figure 17. The pH diagram in batch process. The cell growth followed by secretion of acid due to catabolic activity reduces the pH resulting in the response of the base (NH4OH) addition into the system maintaining the predetermined pH-value of 7.

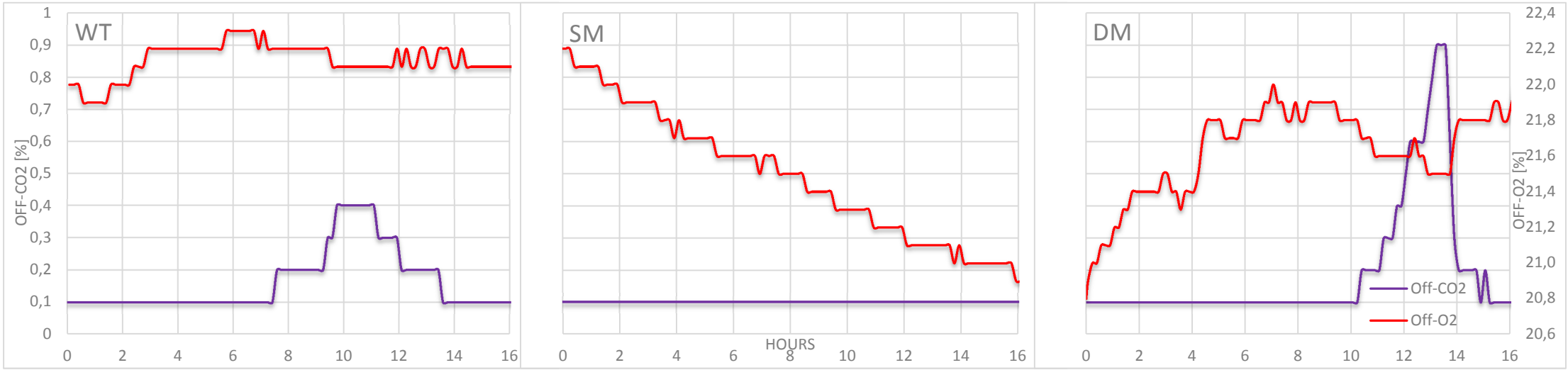

Figure 18. The off-CO_2 diagram in batch process. The Off-Gas of the system are registered in two component; off-CO_2 and off-O_2. The peak of off-CO_2 corresponds to the high degree of cell respiration taken place.

4.3.4. Fermentation lapse during Fed-Batch process after IPTG induction.

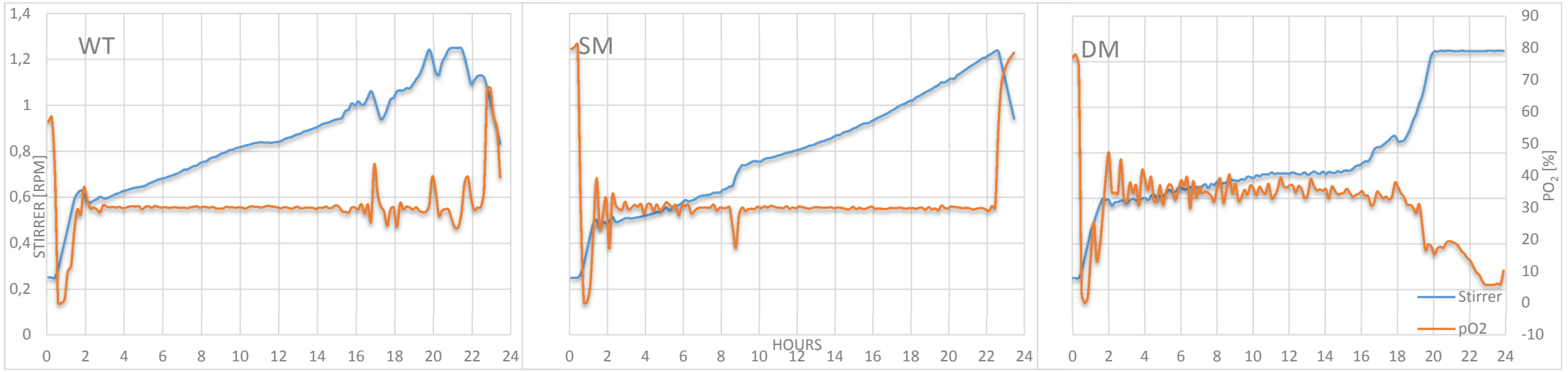

Figure 19. Dissolved oxygen (pO_2) to stirrer diagram in fed-batch process. The medium containing IPTG was fed into the system in a manner that the specific growth reach 0.1 h^{-1}, the dissolved oxygen (pO_2) decrease drastically in the first hour with the start of the Fed-Batch and followed by the continuous rise of the stirrer maintaining the dissolved oxygen at the predetermined value.

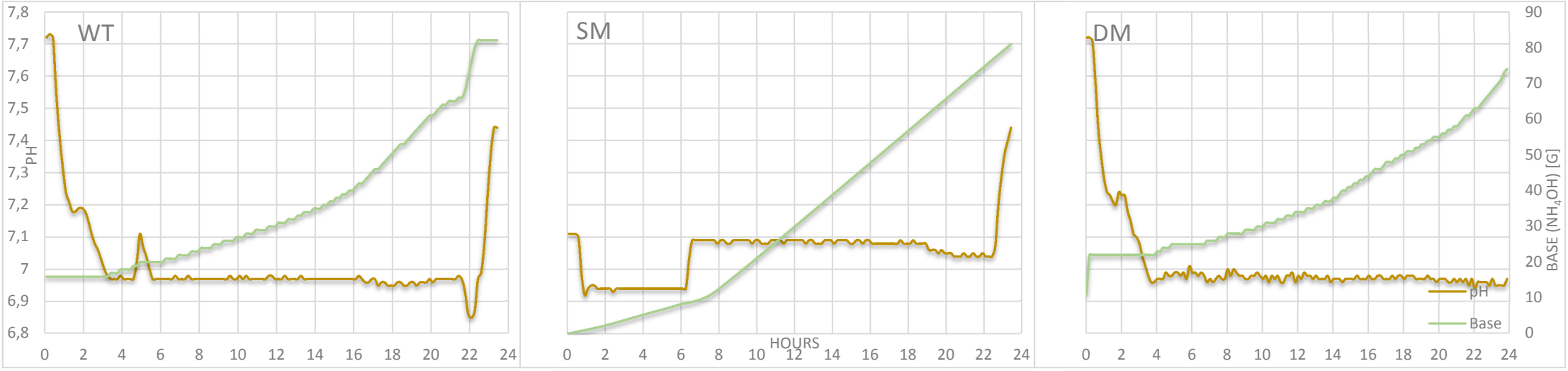

Figure 20. The pH diagram in fed-batch process. The pH decreased accordingly with the cell growth leading to acid production and responded by the increasing amount of base pumped into the system to maintain the given pH at 7.

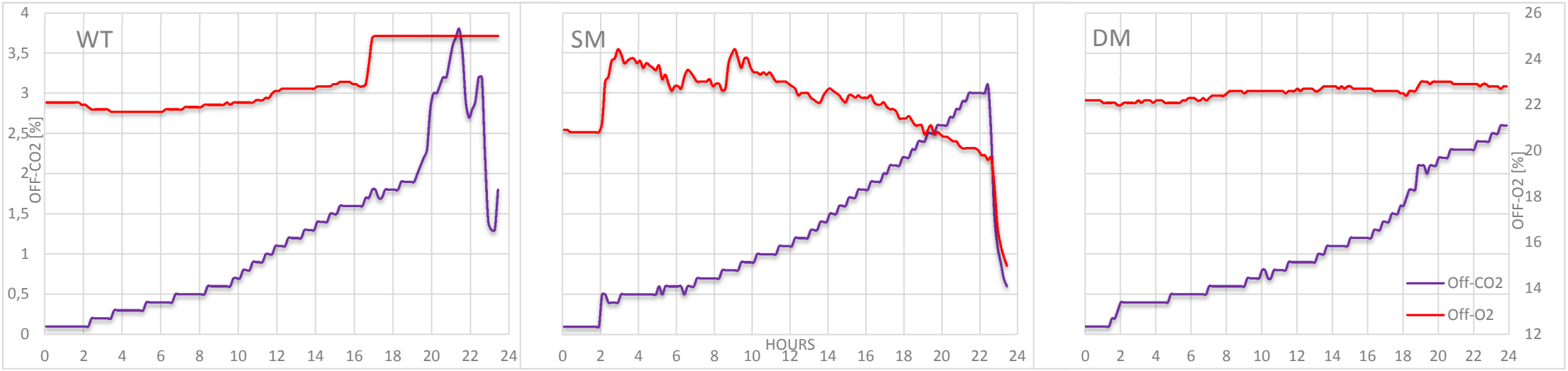

Figure 21. The off-CO_2 diagram in fed-batch process. The off-CO_2 produced by cell respiration increased accordingly with the cell growth. The off-O_2 however stayed fairly on a constant level with a noticeable fluctuation in SM system.

4.3.5. Analysis of recombinant protein

Samples for the determination of CDW were taken at the end of Batch-Process (B1 – Table 5), resembling the start biomass of the fed-Batch and consequently the induction of recombinant protein. CDW was determined gravimetrically and used to calculate the volume of the sample taken for SDS PAGE analysis (Sample volume of 1 mg CDW - Table 5).

Table 5. Measured values of CDW and OD_{600}, resuspension of cell pellet in 1.5 mL binding buffer, and calculated volume of sample for SDS PAGE preparation. B: Batch (the end of the batch process, which means the start of the fed-batch fermentation, corresponds with Time 0h). F: Fed batch. CDW is gravimetrically determined after an overnight drying step and calculated in proportion of its sample volume. Biomass in 1.5 mL time points sample was calculated from the determined CDW. Optical density at wavelength of 600nm was measured at each time points. Sample volume: sample volume taken from the resuspended 1.5 mL sample, used for SDS PAGE analysis in Figure 22 - Figure 24 constituting 1 mg CDW.

Strain	Code	Time	Cell dry weight (CDW) [g/L]	OD_{600}	Biomass in 1.5 mL [mg]	Sample Volume of 1 mg CDW [uL]
Wild Type	B1	0	4.82	14.4	7.23	207.5
(WT)	F2	2	5.74	18.7	8.61	174.2
	F3	4	6.54	19.75	9.81	152.9
	F4	6	7.71	25.5	11.56	129.7
	F5	8	8.94	29.85	13.41	111.9
	F6	23	12.61	38.6	18.91	79.3
Single Mutant	B1	0	5.77	17.2	8.65	173.3
(SM)	F2	2	6.59	20.25	9.88	151.7
	F3	4	7.62	23.27	11.43	131.2
	F4	6	8.99	25.6	13.48	111.2
	F5	8	10.36	29.5	15.54	96.5
	F6	23	23.35	74.4	35.02	42.8
Double Mutant	B1	0	4.32	18.2	6.48	231.5
(DM)	F2	2	4.91	18.15	7.36	203.7
	F3	4	6.24	20.5	9.36	160.3
	F4	6	7.59	24	11.38	131.8
	F5	8	9.04	28.15	13.56	110.6
	F6	24	14.67	49.05	22.00	68.2

In the SDS PAGE analysis, the band of *Hi*C with molecular size of 23 kDa was observed in the cell lysate of all Strains (Figure 23 - Figure 24), and very faint bands in pellet fraction of WT (Figure 23). On the other hand, the induced cutinase was also present in cell lysate fraction at time point B1. At this point, the culture was still in the batch phase prior to IPTG induction.

This could be explained by the presence of lactose as contamination in LB medium, previously reported about spontaneous induction prior to IPTG induction. The ingredient of the synthetic Batch medium GLU01 (Appendix 6.9.) are mainly salts, which buffer the acidity (KH_2PO_4, K_2HPO_4), biological buffering agent (Sodium citrate), divalent ionic salt (Mg^{2+} and Ca^{2+}) for high density culture, minerals, trace elements and nitrogen sources (ammonium chloride, diammonium sulfate), glucose and yeast extract boosting the growth of the culture. Despite of the lack of possible evidence of expression inducing substances, it is still not clear what caused the expression of recombinant protein in the batch phase, thus leaky expression may come into consideration. However in the purification, the expression of recombinant protein showed good yield.

A complete resuspension of the cell pellet in binding buffer, especially of time points containing high density of cells, was very challenging leaving a big clump of undissolved cells leading to incorrect result, e.g. WT at time point F5, and in DM at time point F6.

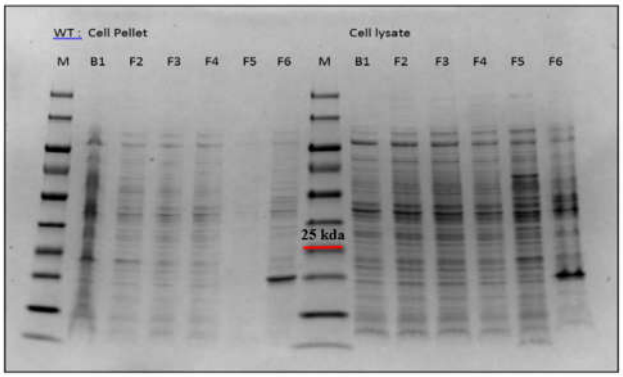

Figure 22. SDS PAGE Gel of Cell Pellet and Cell Lysate of WT with reference to 1mg biomass. HiC cutinase size: ~23 kDa (the red line on the marker is 25 kDa)

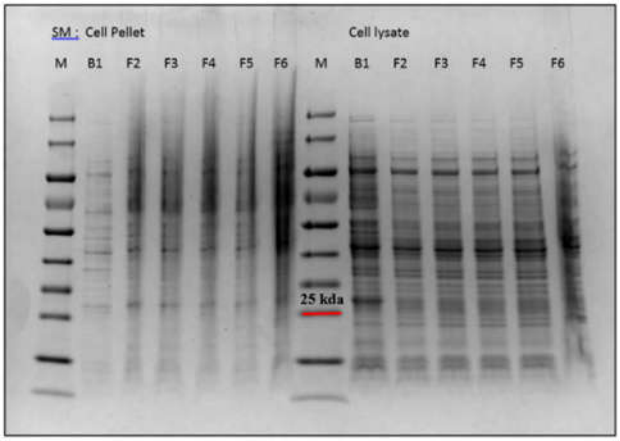

Figure 23. SDS PAGE Gel of Cell Pellet and Cell Lysate of SM with reference to 1mg biomass. HiC cutinase size: ~23 kDa (the red line on the marker is 25 kDa)

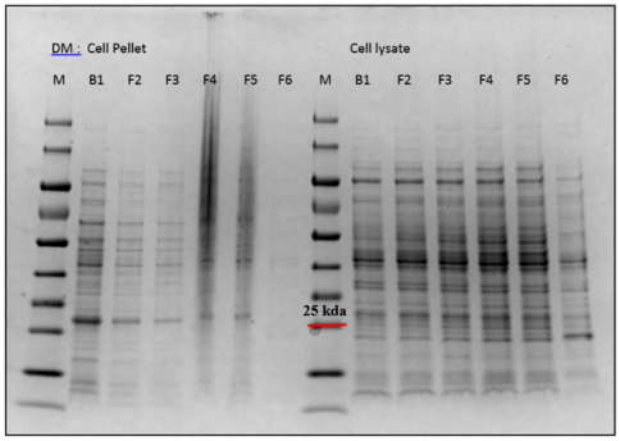

Figure 24. SDS PAGE Gel of Cell Pellet and Cell Lysate of DM with reference to 1mg biomass. HiC cutinase size: ~23 kDa (the red line on the marker is 25 kDa)

4.3.6. Purification

Purification of the recombinant enzyme was carried out by the ÄKTA system utilizing Fast Protein Liquid Chromatography (FPLC). After sample loading into the column, the unspecific bound proteins, depicted as the first peak in the graph, was eluted by 10% elution buffer, which represent the first step of the purification process. In the subsequent step, an increasing gradient

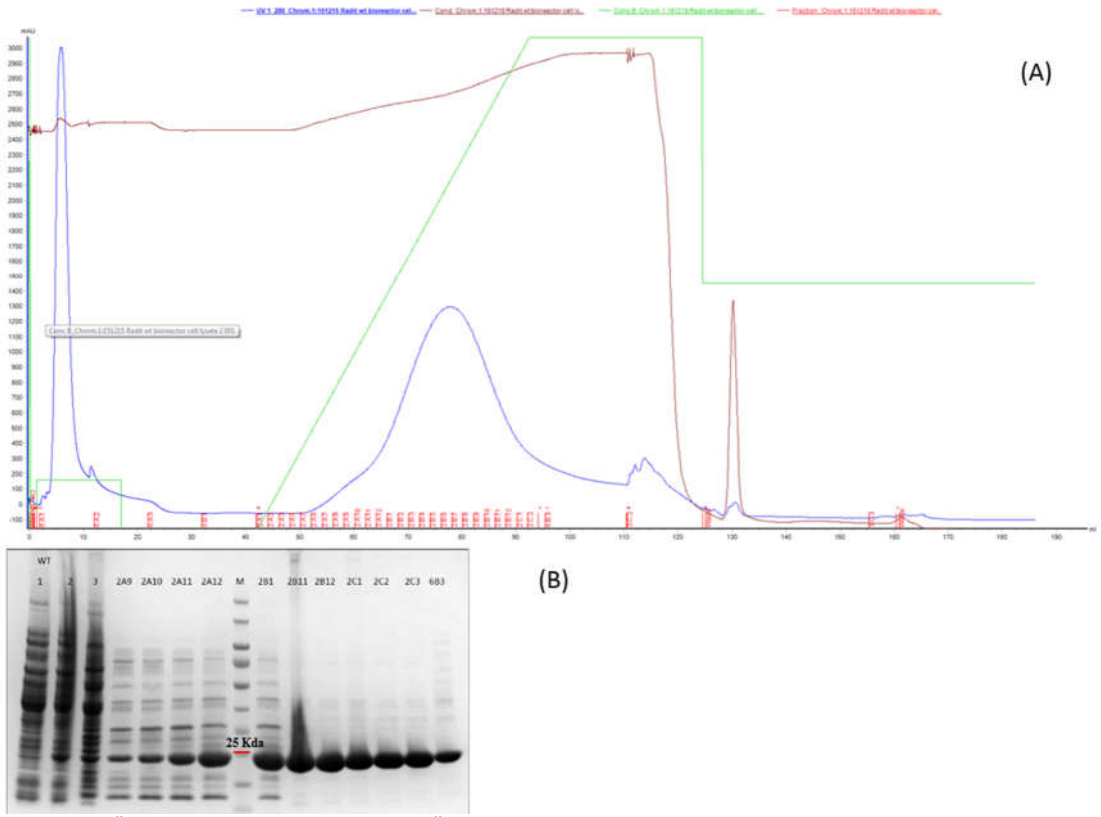

Figure 25. ÄKTA purification process WT. ÄKTA analysis diagram (A) and SDS PAGE (B) analysis of purified cutinase WT from 137 g pellet. SDS PAGE gel analysis was done to ensure purification and to visualize which fraction to be taken for further processing of the enzyme. The fractions 1: Cell lysate, 2: Flow-through from the column, 3: eluted fraction during 10% B.. The red line on the marker represents a band size of ~25 kDa.

of elution buffer to 100%, depicted as a green slope going upwards, elute gradually the specifically bound proteins, which constituted the second peak (Figure 25 - Figure 27). Although, some unspecific bound proteins other than the target protein were still present as shown in the SDS PAGE gel analysis (Figure 25 (B) lane 2A9 - 6B3). The confirmed fractions by SDS PAGE analysis containing the protein of interest were pooled together, concentrated, desalted and undertook buffer change towards 0.1 M Tris-HCl pH 7.

Protein concentration of 3 mg mL^{-1} of WT with total volume of 38 mL purified from 137 g biomass, representing 0.83 mg recombinant protein per gram biomass, were successfully obtained and proceeded for further characterization.

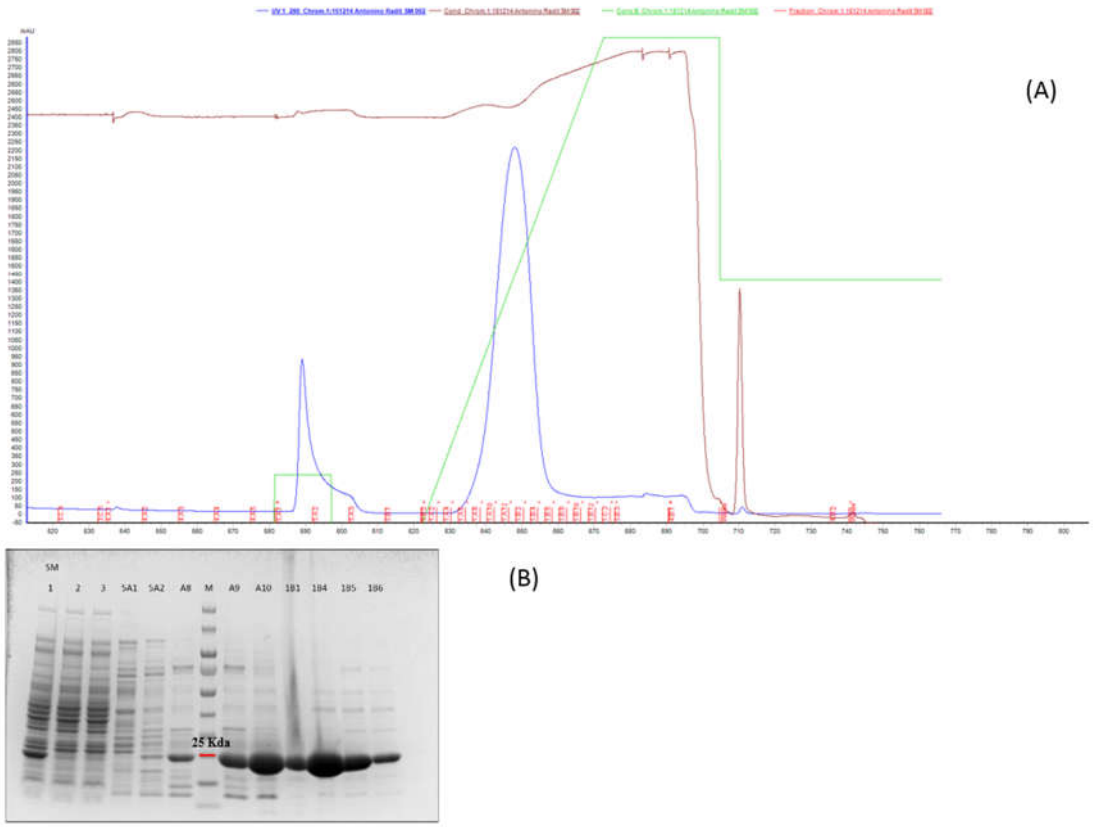

Figure 26. Äkta purification process SM. *ÄKTA analysis diagram (A) and SDS PAGE (B) analysis of purified cutinase SM from 129 g pellet. SDS PAGE gel analysis was done to ensure purification and to visualize which fraction to be taken for further processing of the enzyme. The fractions 1: Cell lysate, 2 & 3: eluted fraction during sample-loading into the column (the fraction at the middle and at the end).The red line on the marker represents a band size of ~25 kDa.*

In the case purification of SM, the sample of the fraction 1B1 (Figure 26), depicted as the peak during the elution in the second step, formed precipitate after heat treatment for SDS PAGE preparation, possibly caused by high concentration of protein in the fraction. Protein concentration of 12 mg mL^{-1} of SM with total volume of 13mL purified from 129 g biomass, representing 1.20 mg recombinant protein per gram biomass, were successfully obtained and proceeded for further characterization.

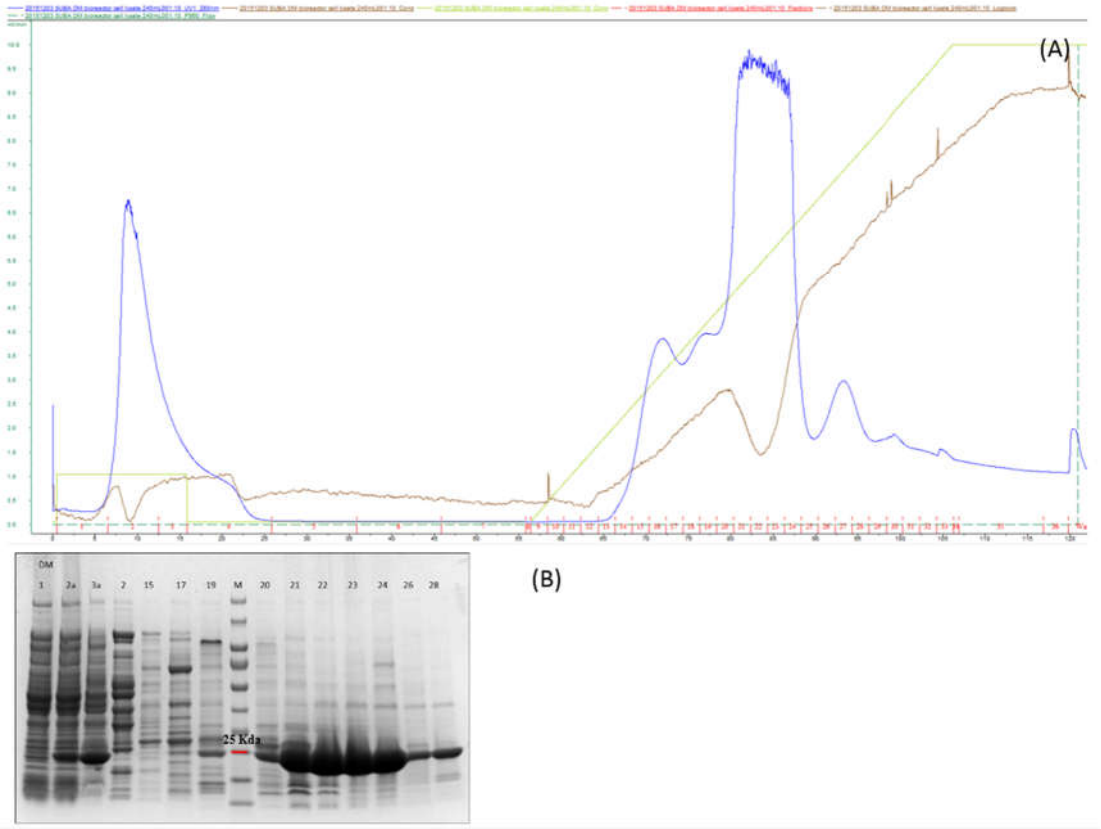

Figure 27. Äkta purification process DM. ÄKTA analysis diagram (A) and SDS PAGE (B) analysis of purified cutinase DM from 48 g pellet. SDS PAGE gel analysis was done to ensure purification and to visualize which fraction to be taken for further processing of the enzyme. The fractions 1: eluted fraction during sample-loading into the column, 2a & 3a: raw lysate filtered and unfiltered. The red line on the marker represents a band size of ~25 kDa.

Protein concentration of 6 mg mL^{-1} of DM with total volume of 14mL purified from 48 g biomass, representing 1.75 mg recombinant protein per gram biomass, were successfully obtained and proceed for further characterization.

Despite the benefit of protein expression in periplasmic space, in which fewer contaminating proteins are present, compared to cytoplasmic expression facilitating the purification, the selective disruption of periplasm were not used due to its feasibility in our circumstance. However the benefit of correct folding of the disulfide bonds owing the required machinery in periplasm should be attained.

4.3.7. Cell dry weight (CDW) comparison

The theoretical curve of cell dry weight was derived from known value of specific growth rate of *E.coli* strain used and absolute biomass at the start of the fed-batch (Figure 28 - Figure 30).

The experimentally determined biomass of the SM showed a very comparable trend to the theoretical one. However in the WT and DM fermentation, a substantial deviation from the theoretical curve is to be taken into consideration. The secretory production of target protein into the periplasm is physically limited by periplasmic volume and usually results in an increase of cellular stress and reduced cell growth (S. H. Yoon et al., 2010). Toxicity of recombinant protein could also lead to the loss of biomass.

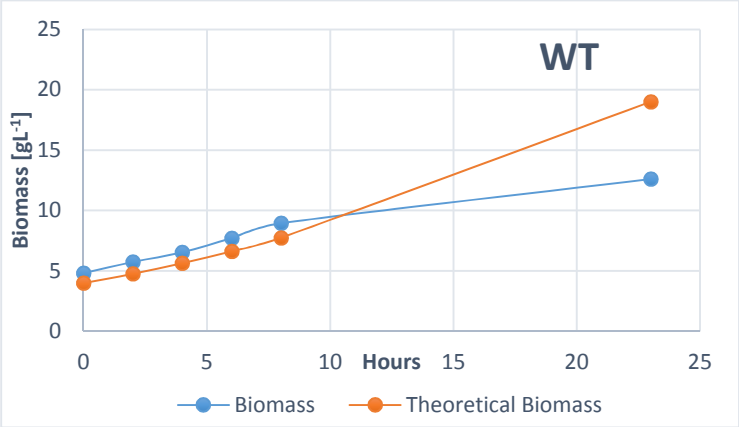

Figure 28. Comparison of calculated biomass with experimentally determined biomass growth of the WT.

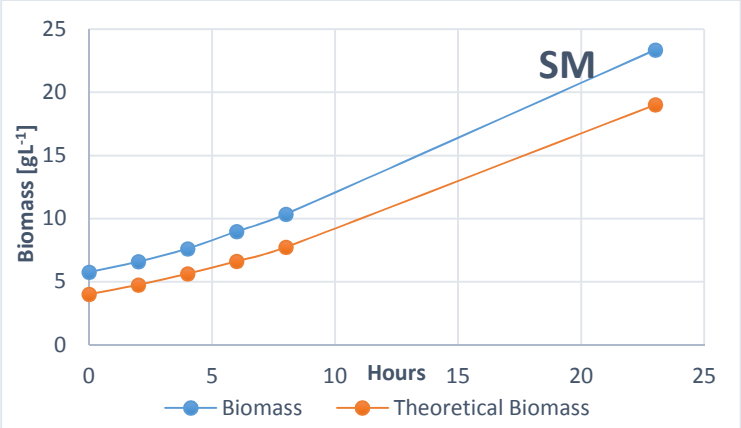

Figure 29. Comparison of calculated biomass with experimentally determined biomass growth of the SM.

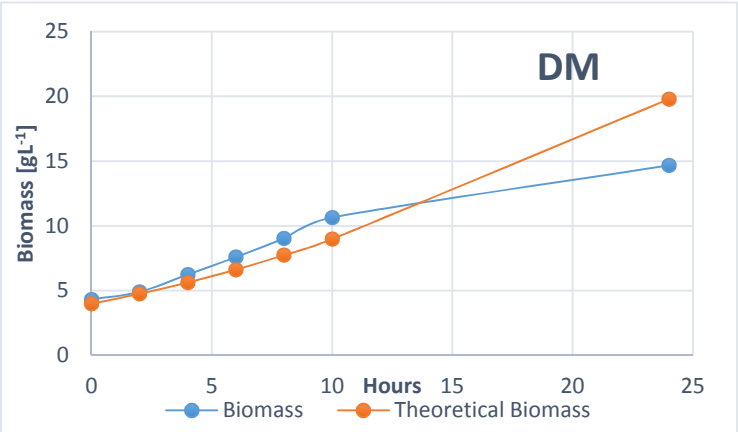

Figure 30. Comparison of calculated biomass with experimentally determined biomass growth of the DM

4.3.8. Activity and kinetic assay

Due to the unavailability of *p*-NPB (*p*-nitrophenyl butyrate) containing the preferred short chains (C4) carbon , *p*-NPA (*p*-nitrophenyl acetate) constituting two carbon atom less in the chain of the ester was used for the activity and kinetic assay of the enzyme on ester bonds. The enzyme was diluted accordingly for activity and kinetic assay respectively.

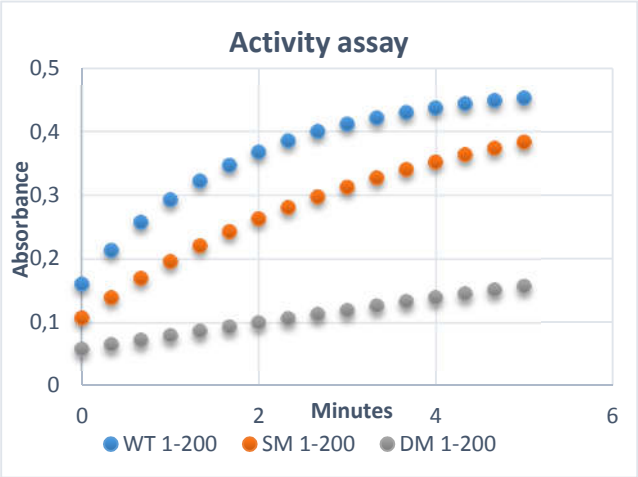

Figure 31. Activity assay of WT, SM, DM in 200 times dilution

Table 6. K_M and k_{cat}/k_M of WT, SM, DM enzymes on p-NPA

Substrate: *p*-NPA	K_M [µM]	k_{cat}/K_M [s^{-1} μM^{-1}]
WT	3.7277	89,617
SM	5.1526	10,994
DM	5.1956	4,6476

As expected the WT showed higher activity on hydrolyzing ester bonds compared to the mutants, represented by the reach of the lower K_M, having higher values than SM and DM. The lower K_M value of the WT translated to the lower substrate concentration required for effective catalysis to occur, which means higher activity on hydrolyzing ester bonds by the WT enzyme compared to the mutants. The shape of the curve also showed higher reactivity of the WT, changing into a form of a line towards the double mutant. The decrease of enzyme efficiency (k_{cat}/K_M) of the SM and accordingly of the DM towards ester were observed and were in compliance with the previous investigation by Syrén 2012 (Table 1).

In order to characterize the activity of the mutant enzymes on amide bond, *p*-NAA (p-nitrophenyl acetanilide) featuring an amide bond, and constituting the same number of carbon atoms as the ester substrate counterpart (*p*-NPA) for a better comparability, was used as a substrate for activity- and kinetic assay. Adaption and tailoring of working protocol of the substrate was attempted, yet it showed poor solubility building clump in the working solution K_2HPO_4, pH 7, thus no reliable determination of activity- and kinetic assay on amide bonds were possible.

4.3.9. Water contact angle (WCA)

The hydrolysis of amide bonds on the surface of polyamides resulting changes of surface properties, render the material less hydrophobic owing to the formation of hydrophilic groups (Silva, Araújo, Casal, Gübitz, & Cavaco-Paulo, 2007). The blank polymer without enzyme at 37 °C (data not shown), which underwent the same test parameter, had a WCA value of 43° which corresponds perfectly to WCA value of the WT treated film. The SM and the DM showed comparable WCA values to each other, displaying a slight higher WCA than the WT. Under consideration of their standard deviation, the value are qualitatively the same, which could be translated to very less to none activity of the enzyme at 37 °C.

The blank at 50 °C has a rather high standard deviation (data not shown) leaving a rather big margin of error in comparing the data, despite of a high resemblance with the WCA value of the WT. In the analysis the WCA value at 50 °C, the WT treated film will be used as a basis value in comparing the change in WCA value of the other mutants. The treatment by the variants of the enzyme with introduced amidase like properties should reduce the WCA of the polymer surface due to enzymatic activity on amide bonds reducing the hydrophobicity of the film.

However the measurement data set of SM and DM at 50 °C did not show a distinct decrease of WCA compared to the WT under the consideration of their overlapping standard deviation.

Attention have to be paid in conducting the measurement of WCA. The measurement with drop analyzer is a delicate process, requiring multiple attempts to achieve comparable angle of both side of the drop in limited surface area of the films, compromising the reproducibility of the measurements by wetting the surface area for the next droplets.

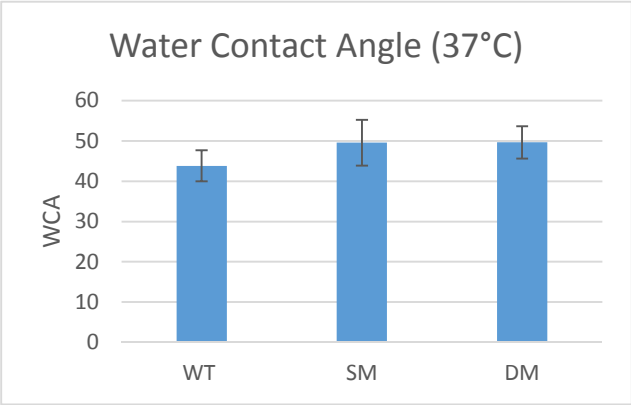

Figure 32. Water contact angle of treated PA 6.6 of film size of 2x2 cm, at 37 °C, 150 rpm, for 1 week with 0.5 µM of WT, SM, and DM enzyme in 10 mL K_2HPO_4.

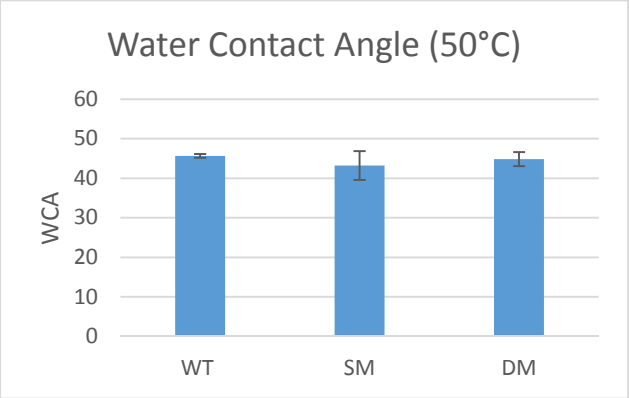

Figure 33. Water contact angle of treated PA 6.6 of film size of 2x2 cm, at 50 °C, 150 rpm, for 1 week with 0.5 µM of WT, SM, and DM enzyme in 10 mL K_2HPO_4.

4.3.10. Gas Chromatography and Mass Spectrometry (GC/MS)

Higher degree of abundance on overall peaks registered at 50 °C than at 37 °C are shown (Figure 34). Peaks at elution time of 28 min are the potential resemblance of the released hydrolysis product, where there is an overlapping of peaks at the same elution time of all three variants indicating the same registered substance we expected to have in our enzyme hydrolysis comparison. The different peak intensity could be translated to different amount of hydrolysis product, where the WT should have the lowest activity on amide substrate, while SM and DM featuring mutation that possibly accept the hydrogen atom donated by the reacting nitrogen of the amide substrate should show greater activity thus releasing greater hydrolysis product registering greater peaks in the diagram. However the abundance on the peaks at 28 min does not vary significantly between the hydrolysis at 37 °C and 50 °C. The abundance of DM remained at about the same level at both incubation temperature at 150.000 as well as of the WT at 100.000. The double mutation of DM variant at position 64 and 167 (L64H, I167Q) provided two possible hydrogen acceptor, which might have facilitated a fully developed hydrogen bond in the ES complex in the TS, that reflected in its higher peak intensity by the increased specificity on amide substrate (Syrén & Hult, 2011). An interesting distinction was on the SM treated sample, which showed a lower peak at 50 °C than at 37 °C. Based upon the knowledge of the preliminary work of Syrén et al. 2012, the single mutation (SM) at position 167 (the I167Q mutant) showed a fifty times higher relative reaction specificity on amide to ester substrate. The hydrolysis product of SM at 37 °C inarguably shows a higher peak than the WT variant as seen in Figure 34. However this trend does not apply for the incubation at elevated temperature (50 °C), which should contribute to higher mobility of amorphous phase resulting in better hydrolysis of the polymer.

Apart of the encouraging standpoint, the result presented here is limited and we are still unable to assure whether the peaks at 28 min are the peaks of the possible released hydrolysis product due to some deviation on theoretical level described above, while the exact released product(s) is or are still remained theoretical as well, thus requiring further establishment of the detection method. Furthermore the T_m determination of *Hi*C in the CHES buffer (Baker et al. 2012) suggests a decent temperature margin for higher incubation temperature at about 60 °C, which still lies below the T_m of *Hi*C representing conducive working temperature. Incubation attempts at more elevated temperature might facilitate higher degree of hydrolysis, thus yielding distinctive peaks to be compared to the result of lower incubation temperatures.

Another alternative method to determine the released hydrolysis product, is by quantifying the primary amines released by hydrolysis, which react with the sodium salt of 2,4,6-trinitrobenzenesulfonic acid (TNBS) into hexamethylenediamine described by Morcol et al. (1997) and used in the work by Silva et al. (2004) for the same purpose of this work, with a preliminary elimination step of protein by trichloroacetic acid before the amine quantification.

In addition, the formed amino groups at the surface of the polyamide film resulting from the enzymatic hydrolysis, could also be detected by wool reactive dye staining of α-bromoacrylamide dye reactive group (Lewis, D.M 1992), which specifically designed to react with the primary amino groups.

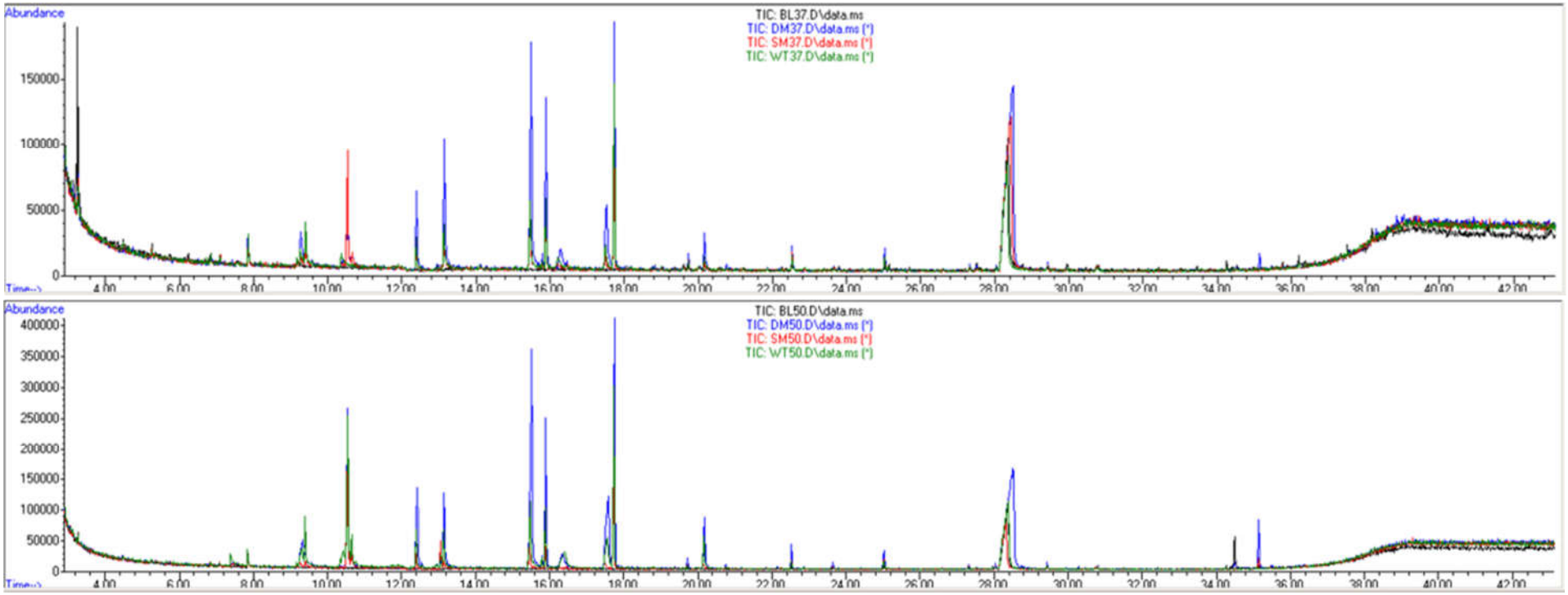

Figure 34. Gas Chromatography and Mass Spectrometry analysis of the remaining enzyme treatment solution from PA 6.6 hydrolysis

.

5. CONCLUSION AND PERSPECTIVES

The main goal of this master thesis was to express *Humicola insolens* cutinase (*Hi*C) in its wild type form (WT), with single mutation (SM), and double mutation (DM). Being an esterolytic enzyme, *Hi*C showed interestingly the same α/β hydrolase fold and the Ser/His/Asp catalytic triad as found prolyl oligopeptidase (Syrén, 2013). The introduction of enzyme assisted hydrogen bond by point mutation(s) resembled the spatial arrangement of substrate assisted hydrogen bond of the prolyl oligopeptidase in transition state, which facilitate the prerequisite nitrogen inversion in hydrolysis of amide bond (Syrén, 2013). The subsequent preliminary investigation of expressed enzymes took place by means of hydrolysis of soluble ester and amide substrate, determination of water contact angle of treated PA6.6 film, and analysis of the released hydrolysis products of PA6.6 film in the remaining treatment solution by gas chromatography (GC) and mass spectrometry (MS). The cutinase with a single mutation (SM) at position 167 (I167Q) has been shown in the work by Syrén et al., (2012) to have an enhanced relative reaction specificity on amide to ester substrate by about 50 times compared to the WT cutinase. The point mutation L64H was combined with the point mutation I167Q thus creating a double mutant enzyme (DM). Both mutant enzymes were expressed in parallel to the wild type enzyme (WT) to compare their activity on compounds featuring amide bonds.

In the first step, the subcloning of each *Hi*C gene (WT, SM, DM) into the expression vector pET-26b(+) was carried out. The *Hi*C gene in its parent vector and the pET-26b(+) vector were digested by *Nco*I and *Xho*I forming compatible ends for each other, while preserving pelB leader for periplasmic expression of soluble protein and His-tag for purification based on affinity chromatography. The overnight incubation at low temperature (4°C) showed a significant increase of the ligation yield by T4 DNA Ligase compared to the working parameters suggested by the manufacturer. Successful ligation of all three variants was confirmed by sequencing, and the subsequent transformation into the expression host BL21-Gold(DE3) was successfully carried out.

The production of recombinant proteins were carried out in shaker flasks and due to the limited amount of purified recombinant protein expressed, a bigger scale of fermentation in bioreactor was conducted. In the analysis of SDS PAGE of the cell fractions originated from shaker flask production scale, an accumulation of inclusion bodies (IB) was observed in all three variants increasing with the fermentation time. The production peak of soluble protein in cell lysate fraction of the WT was found to be in the 8th hour of the fermentation time and from this time point afterwards significant decrease of band intensity was observed, while on the other hand

the amount of soluble protein in the supernatant fraction increased. This indicated passive release of soluble protein due to lysis of the cells. The same trend of increasing IB and soluble protein in the supernatant fraction was also observed in the SM and DM, however no significant decrease of the amount of soluble protein in cell lysate fraction was detected, discouraging the interpretation of the release of soluble protein into the medium due to lysis of the cells. Early harvest at the peak of protein production in cell lysate of all variant at 8^{th} hour of fermentation time was attempted, yielding no significant gain of soluble recombinant protein compared to the harvest at 20^{th} hour.

In the bioreactor fermentation, WT and DM also suffered under biomass loss starting from $8^{th}/10^{th}$ hour respectively despite an optimal controlled environment (temperature, pH and aeration), while SM grew in compliance with the theoretical growth curve of biomass based on specific growth of 0.1 h^{-1}. The secretory production of target protein into the periplasm is physically limited by periplasmic volume and usually results in an increase of cellular burden and reduced cell growth (S. H. Yoon et al., 2010). Toxicity of recombinant protein could also lead to the loss of biomass. The amount of recombinant protein per biomass produced by WT, SM, and DM were as follows: 0.83 mg g^{-1}, 1.20 mg g^{-1}, 1.75 mg g^{-1}.

The activity assay on *p*-NPA (*p*-nitrophenyl acetate) showed a decrease of ester substrate specificity of the mutant enzymes (SM, DM) featuring hydrogen acceptor which facilitate amide bond hydrolysis compared to the WT. The kinetic assay on *p*-NPA provided us with the information of the K_M value of the three enzyme, WT: 3.7277 µM, SM : 5.1526 µM DM: 5.1956 µM. The lower K_M value of the WT translated to the lower substrate concentration required for effective catalysis to occur, which means higher activity on hydrolyzing ester bonds by the WT enzyme compared to the mutants. Due to the different substrate used for determination of enzyme efficiency (k_{cat}/K_M) in this work, a comparison with the k_{cat}/K_M value on *p*-NPB of the previously investigated SM in the work by Syrén et al., (2012) would be less comparable. However we can agree with the decrease of k_{cat}/K_M value of the SM and accordingly of the DM towards ester. The k_{cat}/K_M value of the three enzymes are as follow WT: 89,617 s^{-1} μM^{-1}, SM: 10,994 s^{-1} μM^{-1}, DM: 4,6476 s^{-1} μM^{-1}.

The characterization of mutant enzymes on amide substrate, *p*-NAA (p-nitrophenyl acetanilide), did not produce a reliable result, thus further adaption and tailoring of working protocol are needed.

It has been shown by Heumann et al. (2006a) that there was no correlation between cutinase activity on *p*-NP esters and their activity for the hydrolysis of PET fibers. The hydrolysis of PA

6.6 film was conducted despite the lack of knowledge of hydrolysis activity on soluble amide substrate. The hydrolysis of PA 6.6 took place for 7 days at 2 different incubation temperatures, 37 °C and 50 °C in K_2HPO_4 buffer at pH 7. The water contact angle (WCA) of treated films were measured and the remaining treatment solutions were further processed for GC/MS analysis. The WCA of SM and DM at 37 °C as well as at 50 °C did not show any significant decrease of hydrophobicity to WT under consideration of their standard deviation. In the analysis by GC/MS, the overlapping of peaks of the samples from the hydrolysis with the three variants at the same elution time (at 28 min), indicating the same registered substance of different intensity, represented a potential resemblance of the released hydrolysis product. Despite the greater intensity of overall peaks at 50 °C, the intensity of the suspected peaks of all three variant at 28 min remained qualitatively comparable in both incubation temperatures, which was in agreement with the WCA results of no significant hydrolysis activity at the corresponding temperature. However the results presented in this work are still limited by means of characterizing and exploring the full potential of the mutant enzymes. Thus further investigation assuring the validity of the suspected peaks at 28 min of the potential released hydrolysis product is required. The reported temperature stability of *Hi*C could potentially facilitate a higher incubation temperature at about 60 °C, which still lies below the T_m of *Hi*C (T_m of *Hi*C at pH 8.0, and pH 5.0 in CHES buffer is 62.7 °C, and 64.3 °C respectively (Baker et al., 2012)) representing conducive working temperature for hydrolysis of PA 6.6 close to its T_g (55°C). Incubation attempts at elevated temperature should contribute to higher mobility of amorphous phase resulting in better hydrolysis of the polymer, thus yielding distinctive peaks for a better comparability of amide bond hydrolysis activity of the three enzymes.

Determination of the released primary amine with TNBS method and determination of the formed amino groups on the PA 6.6 surface by reactive dye might represent an alternative methods for quantitative or qualitative determination of amide bond hydrolysis activity in the further study.

In conclusion, the periplasmic expression of *Hi*C with pET system successfully yielded a moderate amount of soluble recombinant protein enabled by high density culture under a high degree of process control in semi-batch bioreactor fermentation. The thermostability of *Hi*C, particularly the SM, which previously investigated by Syrén et al., 2012, displaying up to fifty times increase of reaction specificity for amide bond hydrolysis compared to the WT enzyme, has the potential to work at the glass transition temperature (T_g) of PA 6.6 (at 55°C), which has been shown to be advantageous for hydrolysis of amorphous phase. The capability of the DM

is yet to be uncovered, thus further investigations i.e. characterization with soluble substrate, the appropriate concentration of enzymes being used, higher hydrolysis temperature, are necessary.

6. APPENDIX

6.1. Compentent cells for calcium chloride transformation

1. Preparation of preculture: inoculate 10 mL of LB broth with a single colony from a freshly streaked plate or with 200 µL of an *E.coli* stock culture kept at -80 °C in an Erlenmeyer flask. Incubate at 37 °C at 150 rpm overnight.
2. Preparation of culture: inoculate 100mL of LB broth preheated at 37 °C with cells from the preculture in order to obtain an OD_{600} of 0.1.
3. Incubate at 37 °C at 150 rpm until the preculture reached an OD_{600} of ± 0.8.
4. Put the cells on ice for 15 min. For all subsequent steps, keep the cells as close to 0 °C as possible (in an ice bath) and chill all containers in ice before adding cells.
5. To harvest, transfer the cells to a cold centrifuge bottle and centrifuge the cells at 4500 rpm for 10 min at 4 °C.
6. Carefully pour off and discard the supernatant. The supernatant must be sterilized before it is discarded in the sink. Collect it in the Erlenmeyer in which the culture has been incubated.
7. Resuspend the cell pellet in 32 mL of cold RF-1 [100 mM KCl, 50mM $MnCL{\cdot}4H_2O$, 30 mM CH_3COOK, 10 mM $CaCl_2{\cdot}2H_2O$, 15%(w/v) glycerol, adjust the pH to 5.8 with 200 mM CH_3COOH and filter with 0.2 µm filter] and mix carefully. Transfer the suspension in a 50 mL falcon tube.
8. Put the cells on ice for 15 min.
9. Centrifuge the cells at 4500 rpm for 10 min at 4 °C
10. Remove the supernatant carefully with a pipette. The supernatant must be sterilized before it is discarded in the sink. Collect it in the Eylenmeyer in which the culture has been incubated.
11. Resuspend the cell pellet in 8mL of cold RF-2 [10 mM MOPS, 10 mM KCl, 50 mM $CaCl_2{\cdot}2H_2O$, 15% glycerol, adjust pH to 6.8 with 1M NaOH and filter with a 0.22 µm filter] and mix carefully.
12. Put the cells on ice for 15 min.
13. Aliquot 100 µL of the suspension in cold 1.5mL sterilized tubes and put the tubes in dry ice.
14. Store the tubes in -80 °C freezer until required for use.

6.2. Transformation

1. Resuspend the Lyophilized plasmid with 50 µL sterilized milli-Q water.
2. Pipette 10 µL of the resuspended solution from step 1 / ligation product into 100 µL of the competent cells and mix carefully with the aid of the pipette.
3. Incubate the tube for 20 min on ice, and mix carefully every 5 min by inverting the tube.
4. After 20 min on ice, put the tube into a heating block (previously set to 42°C) for 45 seconds and then incubate it on ice for a further 2 min.
5. Add 900 µL of LB-broth (preheated at 42°C) to the cell sample and incubate the tube at 37 °C at 150 rpm for an hour.
6. Take 100 µL of the sample from the last step and plate it in nutrient agar medium containing kanamycin (first dilution).
7. Centrifuge the rest at 10000 rpm for 3 min and remove 800 µL of the supernatant.
8. Resuspend the pellet in the remaining supernatant and plate it (second dilution).
9. Incubate the plates at 37 °C overnight.

6.3. Cell lytic

Stock solution : Cell lytic B 10x Sigma Aldrich.

Working Solution : Cell lytic B 1x (diluted in binding buffer).

Lysis protocol:

1. Resuspend the pellet of the culture in 200 µL cell lytic 1x.
2. Incubate at 26 °C for 5-10 min at 600 rpm.
3. Centrifuge the tube at 4°C, 14.000 rpm for 5 min.
4. Separate the supernatant from the pellet into a new microtube.
5. For SDS PAGE, add 2x Laemmli sample buffer:
   For cell lysate : 20 µL probe + 20 µL sample buffer.
   For pellet : pellet + 100 µL sample buffer.
6. Boil sample for 10 min at 95 °C in the heat block before loading into polyacrylamide gel.

6.4. TCA protein precipitation

(originally from Luis Sanchez)

Revised : October 10, 2001

Author : clw

Stock solution : 100% (w/v) Trichloroacetic adic (TCA).

Recipe: dissolve 500 g TCA (as shipped) into 350 mL dH_2O, store at RT.

Precipitation protocol:

1. Add 1 volume of TCA stock to 4 volumes of protein sample. i.e. in 1.5 mL tube with maximum vol., add 250 µL TCA to 1.0 mL sample.
2. Incubate 10 min at 4°C.
3. Spin tube in microcentrifuge at 14.000 rpm, for 5 min.
4. Remove supernatant, leaving protein pellet intact. Pellet should be formed whitish, fluffy precipitation.
5. Wash pellet with 200 µL cold acetone.
6. Spin tune in microfuge at 14.000 rpm, for 5 min.
7. Repeat steps 4-6 for a total of 2 acetone washes.
8. Dry pellet by placing tube in heat block at 95 °C for 5-10 min to drive off acetone.
9. For SDS PAGE, add 2x or 4x Laemmli sample buffer and boil sample for 10 min at 95°C heat block before loading sample onto polyacrylamide gel.

6.5. SDS PAGE

Laemmli sample buffer

2X Laemmli sample buffer: 16 ml

10.4	ml	dH2O
1.2	ml	0.5M Tris pH 6.8
1.9	ml	Glycerol
1.0	ml	20% SDS
0.5	ml	β-mercaptoethanol
1	%	Bromophenol blue

Solution Composition	Composition
Staining solution	0.125% Coomassie Brilliant blue R250, 30% ethanol, 10% acetic acid.
Destaining solution	30% ethanol, 10% acetic acid.
Reservoir Buffer	3 gL^{-1} Tris base, 14.4 gL^{-1} glycine, 20 % SDS in H_2O.

6.6. BIORAD protein assay: determination of protein concentration

1. Prepare the following BSA (bovine serum albumin) -standards for absorption to concentration value calibration : 1 mg mL^{-1}, 0.5 mg mL^{-1}, 0.25 mg mL^{-1}, 0.2 mg mL^{-1}, 0.125 mg mL^{-1}, 0.1 mg mL^{-1}, 0.0625 mgmL^{-1}, 0.05 mgmL^{-1}, 0.03125 mgmL^{-1}, 0.025 mg mL^{-1}.
2. Add 10 µL of the prepared BSA standard and the sample, whose concentration to be determined into the wells of a 96-well micro-titer plate (in triplicate).
3. Add 200 µL of 1x Bio-Rad reaction solution in each well.
4. Incubate the plate for 5 min at 400 rpm at room temperature.
5. The measurement of the absorption carried out by TECAN plate reader at the wavelength of 595 nm.
6. The concentration and the absorption of the BSA standard are to be put against each other forming a calibration line, whose equation will be used to calculate the concentration of the samples according to its measured absorption value. R^2 should has a value as close to 1 as possible to have a representative regression line of the data.

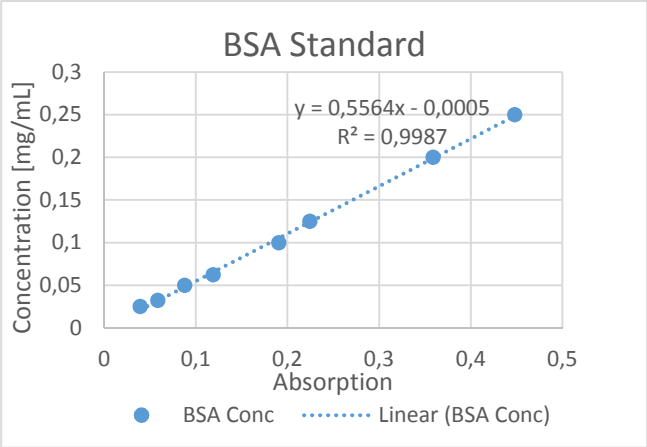

Figure 35. Calibration curve of protein concentration assay

6.7. Activity and kinetic assay of carboylesterases on p-NPA

Solution A: dissolve 18 mg p-NPA in 1 mL DMSO (100 mM).

Solution B: add 40 µL Solution A with 1 mL buffer (100 mM K_2HPO_4, pH 7).

Acitvity assay:

Put 20 µL of the enzyme into the well of 96-well plate, and add subsequently 200 µL of solution B shortly before the measurement begins (in triplicate). The measurement is carried out by TECAN plate reader at 25 °C for 5 min with 14s interval time and reading wavelength of 405 nm.

Kinetic assay:

The following concentration gradient of ester substrate, p-NPA, consisting of buffer (K_2HPO_4, pH 7), DMSO and solution A/B is to be prepared. 200 µL of each gradient solution is added into 20 µL enzyme in a 96-well plate (in triplicate), and subsequently read by TECAN plate reader at 25°C for 5 min with 14 s interval time and reading wavelength of 405nm.

mM pNPA	Buffer [mL]	DMSO [mL]	Solution A [mL]
8.264	9.000	0.000	1.000
6.734	9.000	0.200	0.800
5.145	9.000	0.400	0.600
3.497	9.000	0.600	0.400
mM pNPA	**Buffer [mL]**	**DMSO [mL]**	**Solution B [mL]**
1.748	4.200	0.800	5.000
0.583	7.336	0.997	1.668
0.233	8.700	1.000	0.700
0.070	8.800	1.000	0.200

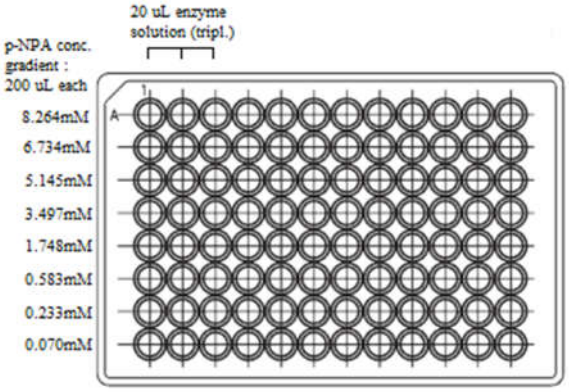

Figure 36. Illustration of workflow for kinetic assay.

6.8. Activity and kinetic assay of carboylesterases on p-NAA

Solution A: dissolve 18.16 mg p-NAA in 1 mL DMSO (100 mM).

Solution B: add 23 µL Solution A with 1 mL buffer (100mM K_2HPO_4, pH 7).

Acitvity assay:

Put 20 µL of the enzyme into the well of 96-well plate, and add subsequently 200 µL of solution B shortly before the measurement begins (in triplicate). The measurement is carried out by TECAN plate reader at 25 °C for 5 min with 14 s interval time and reading wavelength of 405 nm.

Kinetic assay:

The following concentration gradient of amide substrate, p-NAA, consisting of buffer (100 mM K_2HPO_4, pH 7), DMSO and solution B is to be prepared. 200 µL of each gradient solution is added into 20 µL enzyme in a 96-well plate (in triplicate), and subsequently read by TECAN plate reader at 25 °C for 1 h with 15 min interval time and reading wavelength of 405 nm.

mM pNAA	Buffer [mL]	DMSO [µL]	Solution B [mL]
2.044	0	0	10
1.504	2.6	54	7.4
1.001	5	104	4.9
0.493	7.4	155	2.4
0.246	8.6	180	1.2
0.100	9.3	194	0.49
0.061	9.5	200	0.3
0.010	9.7	204	0.05

6.9. Batchmedia for bioreactor fermentation

Synthetic Batchmedia GLU01 for *E.coli* fermentations

Total volume:	4 kg
date of manufacture:	09.12.2015
Application:	FH 361 (WT), FH 362 (SM)
End weight:	4000.25

Step	Component	formula	company	product-number	Lot-number	amount	Tara ± 2.5%	307.00 g weighted
add	RO-Water	H_2O	(-)	(-)	(-)	2000 g	± 50.0 g	2014.69 g
dissolved	Potassium dihydrogen phosphate	KH_2PO_4	Roth	PO18.5	094207333	12.00 g	± 0.30 g	12.02 g
dissolved	Dipotassium phosphate	K_2HPO_4	Merck	1.05101.9029	A675001539	18.32 g	± 0.46 g	18.32 g
dissolved	Glucose monohydrate	$C_6H_{12}O_6 \cdot H_2O$	Agrana	Dextrodyn 20.200	2214.022	52.80 g	± 1.32 g	52.80 g
dissolved	Yeast extract	(-)	SIGMA	Y1625-2506	1001268021	2.40 g	± 0.06 g	2.42 g
dissolved	Sodium citrate dihydrate	$Na_3C_6H_5O_7 \cdot 2H_2O$	Neuber	447200	SZ20507018	1.53 g	± 0.04 g	1.54 g
dissolved	Magnesium sulfate heptahydrate	$MgSO_4 \cdot 7H_2O$	Roth	PO27.3	094211069	1.60 g	± 0.04 g	1.62 g
dissolved	Calcium chloride dihydrate	$CaCl_2 \cdot 2H_2O$	Merck	1.42000.5000	K92676300035	0.32 g	± 0.01 g	0.32 g
dissolved	Trace Element Solution for *E.coli*	(-)	Maria.C	(-)	07/2013	0.800 mL	± 0.02 g	0.8 mL
dissolved	Ammonium chloride	NH_4Cl	Neuber	449641	52300	10.00 g	± 0.25 g	10.14 g
dissolved	Diammonium sulfate	$(NH_4)_2SO_4$	Neuber	461966	4325A	8.40 g	± 0.21 g	8.48 g
dissolved	RO-Water	H_2O	(-)	(-)	(-)	ad 4000.0 g	± 100.00 g	4000.25 g

Synthetic Batchmedia GLU01 for *E.coli* fermentations

Total volume:	2 kg
date of manufacture:	27.11.2015
Application:	FH 360 (DM)
End weight:	2000.24 g

Step	Component	formula	company	product-number	Lot-number	amount	Tara ± 2.5%	318.28 g weighted
add	RO-Water	H_2O	(-)	(-)	(-)	1000 g	± 25.0 g	1004.30 g
dissolved	Potassium dihydrogen phosphate	KH_2PO_4	Roth	PO18.5	94207333	6.00 g	± 0.15 g	6.20 g
dissolved	Dipotassium phosphate	K_2HPO_4	Merck	1.05101.9029	A675001539	9.16 g	± 0.23 g	9.15 g
dissolved	Glucose monohydrate	$C_6H_{12}O_6 \cdot H_2O$	Agrana	Dextrodyn 20.200	2214.022	26.40 g	± 0.66 g	26.46 g
dissolved	Yeast extract	(-)	SIGMA	Y1625-2506	1001268021	1.20 g	± 0.03 g	1.20 g
dissolved	Sodium citrate dihydrate	$Na_3C_6H_5O_7 \cdot 2H_2O$	Neuber	447200	SZ20507018	1.53 g	± 0.04 g	1.54 g
dissolved	Magnesium sulfate heptahydrate	$MgSO_4 \cdot 7H_2O$	Roth	PO27.3	094211069	0.80 g	± 0.02 g	0.80 g
dissolved	Calcium chloride dihydrate	$CaCl_2 \cdot 2H_2O$	Merck	1.42000.5000	K92676300035	0.16 g	± 0.00 g	0.20 g
dissolved	Trace Element Solution for *E.coli*	(-)	Maria.C	(-)	07/2013	0.400 mL	± 0.01 g	0.4 mL
dissolved	Ammonium chloride	NH_4Cl	Neuber	449641	52300	5.00 g	± 0.13 g	5.02 g
dissolved	Diammonium sulfate	$(NH_4)_2SO_4$	Neuber	461966	4325A	4.20 g	± 0.11 g	4.25 g
dissolved	RO-Water	H_2O	(-)	(-)	(-)	ad 2000.0 g	± 50.00 g	2000.24 g

6.10. Fed-batch media for bioreactor fermentation

Synthetic Fed-Batchmedia GLU01 for *E.coli* fermentations

Total volume:	4 kg
date of manufacture:	09.12.2015
Application:	FH 361 (WT), FH 362 (SM)
End weight:	4012.51

Step	Component	formula	company	product-number	Lot-number	amount	Tara ± 2.5%	311.92 g weighted
add	RO-Water	H_2O	(-)	(-)	(-)	2000 g	± 50.0 g	2012.08 g
dissolved	Potassium dihydrogen phosphate	KH_2PO_4	Roth	PO18.5	94207333	12.00 g	± 0.30 g	12.01 g
dissolved	Dipotassium phosphate	K_2HPO_4	Merck	1.05101.9029	A675001539	18.32 g	± 0.46 g	18.56 g
dissolved	Glucose monohydrate	$C_6H_{12}O_6 \cdot H_2O$	Agrana	Dextrodyn 20.200	2214.022	435.60 g	± 10.89 g	435.67 g
dissolved	Sodium citrate dihydrate	$Na_3C_6H_5O_7 \cdot 2H_2O$	Neuber	447200	SZ20507018	25.26 g	± 0.63 g	25.40 g
dissolved	Magnesium sulfate heptahydrate	$MgSO_4 \cdot 7H_2O$	Roth	PO27.3	094211069	13.20 g	± 0.33 g	13.26 g
dissolved	Calcium chloride dihydrate	$CaCl_2 \cdot 2H_2O$	Merck	1.42000.5000	K92676300035	2.64 g	± 0.07 g	2.66 g
dissolved	Trace Element Solution for *E.coli*	(-)	Maria.C	(-)	07/2013	6.6 mL	± 0.17 g	6.6 mL
dissolved	IPTG	$C_9H_{18}O_5S$	Clontech	8070-x	1187	0.015572 g	± 0.0004 g	0.0155 g
dissolved	RO-Water	H_2O	(-)	(-)	(-)	ad 4000.0 g	± 100.00 g	4012.51 g

Synthetic Fed-Batchmedia GLU01 for *E.coli* fermentation

Total volume:	3 kg
date of manufacture:	27.11.2015
Application:	FH 360 (DM)
End weight:	3000.13

Step	Component	formula	company	product-number	Lot-number	amount	Tara ± 2.5%	309.89 weighted
add	RO-Water	H_2O	(-)	(-)	(-)	1500 g	± 37.5 g	1501.56 g
dissolved	Potassium dihydrogen phosphate	KH_2PO_4	Roth	PO18.5	94207333	9.00 g	± 0.23 g	9.05 g
dissolved	Dipotassium phosphate	K_2HPO_4	Merck	1.05101.9029	A675001539	13.74 g	± 0.34 g	13.70 g
dissolved	Glucose monohydrate	$C_6H_{12}O_6 \cdot H_2O$	Agrana	Dextrodyn 20.200	2214.022	329.97 g	± 8.25 g	330.35 g
dissolved	Sodium citrate dihydrate	$Na_3C_6H_5O_7 \cdot 2H_2O$	Neuber	447200	SZ20507018	18.95 g	± 0.47 g	19.00 g
dissolved	Magnesium sulfate heptahydrate	$MgSO_4 \cdot 7H_2O$	Roth	PO27.3	094211069	9.90 g	± 0.25 g	9.90 g
dissolved	Calcium chloride dihydrate	$CaCl_2 \cdot 2H_2O$	Merck	1.42000.5000	K92676300035	1.98 g	± 0.05 g	1.97 g
dissolved	Trace Element Solution for *E.coli*	(-)	Maria.C	(-)	07/2013	5 mL	± 0.12 g	5 mL
dissolved	IPTG	$C_9H_{18}O_5S$	Clontech	8070-x	1187	0.011679 g	± 0.0003 g	0.0120 g
dissolved	RO-Water	H_2O	(-)	(-)	(-)	ad 3000.0 g	± 75.00 g	3000.13 g

6.11. Fermentation sheets

Fermentation: FH361 / Cutinase
09.12.015

FH CAMPUS WIEN
Fachbereich Bioengineering

Host:	*E. coli*	
Strain:	BL21 (DE3) + (pET26b+ with WT gene)	
Product:	cutinase	
Strategy:	Batch + exponential Fed Batch with μ = 0.1 [h^{-1}]	
Start OD600:	0,05	
	Miniforst#1	
pH:	7	
temperature:	37°C during batch phase, 37°C during Fed Batch phase	
stirrer speed:	min: 400 rpm, max: 1200rpm	
Aeration:	only Air (min: 30 L/h, max: 200 L/h)	
DO-cascade (DASGIP):	Stirrer: (X1=0, Y1=400rpm, X2=40, Y2=1200rpm)	
	Gasflow: (X1=40, Y1=30 L/h, X2=80, Y2=200L/h)	
	XO_2: (X1=0, Y1=21%, X2=100, Y2=21%)	
antifoam:	5% Glanapon 2000 (w/w) (fatty acid esters + alkylene oxide polymers)	
base:	25% Ammonia (NH_3)	
Batch media:	Semi synthetic Batchmedia GLU01 for E. coli fermentations	c(C-Source): 12 g/kg
Fed Batch media:	Synthetic Fed-Batchmedia GLU01 for E. coli fermentations	c(C-Source): 99 g/kg
Comments:	Induction: IPTG only direct into the feed bottle	

Samples:

	type	number	amount [mL]	comment
■	Cells-Pellet	3x	1,50	
■	supernatant	3x	1,50	
■	cell dry weight	2x	5,00	(2x10ml for batch-end sample)

Calculations:

Volume batch	1,75	L
Biomass concentration	4	g L-1
absolute biomass batch	7	g
specific growth rate	0,1	h-1
generations	3,3	
fedbatch duration	22,9	h-1
final biomass total	68,94	g
new biomass	61,9	g
final biomass concentration	18,8	g L-1
max. volume	3,673	L
Feed Volume	1,923	L
Yield (x/s)	0,33	g g-1
Fedbatch: C_Glucose	99,0	g kg-1
Fedbatch: C_Glucose * H_2O	108,90	g kg-1

Induction:

M(IPTG):	238,3	g/mol
IPTG needed:	0,5	µmol / g CDW
	3,0	kg feed prepared
	98,018	g theoretical CDW with FB
	49,0089568	µmol IPTG
	0,0000490	mol IPTG
add	0,011679	g IPTG into feed

Feed and sample plan:

sample	t [h]	time	generation	biomass [g]	Δglucose [g]	flowrate [kg h-1]	flowrate [g h-1]	Σ feed [kg]	reactor volume [kg]	CDW [g/L]
•	0	08:20	0,00	7,0					1,750	4,0
	1	09:20	0,14	7,7	2,2	0,023	22,533	0,023	1,773	4,4
•	2	10:20	0,29	8,5	2,5	0,025	24,902	0,047	1,797	4,8
	3	11:20	0,43	9,4	2,7	0,028	27,521	0,075	1,825	5,2
•	4	12:20	0,58	10,4	3,0	0,030	30,416	0,105	1,855	5,6
	5	13:20	0,72	11,5	3,3	0,034	33,615	0,139	1,889	6,1
•	6	14:20	0,87	12,8	3,7	0,037	37,150	0,176	1,926	6,6
	7	15:20	1,01	14,1	4,1	0,041	41,057	0,217	1,967	7,2
•	8	16:20	1,15	15,6	4,5	0,045	45,375	0,263	2,013	7,7
	9	17:20	1,30	17,2	5,0	0,050	50,147	0,313	2,063	8,3
	10	18:20	1,44	19,0	5,5	0,055	55,421	0,368	2,118	9,0
	11	19:20	1,59	21,0	6,1	0,061	61,250	0,429	2,179	9,8
	12	20:20	1,73	23,2	6,7	0,068	67,691	0,497	2,247	10,8
	13	21:20	1,88	25,7	7,4	0,075	74,811	0,572	2,322	11,1
	14	22:20	2,02	28,4	8,2	0,083	82,678	0,655	2,405	11,8
	15	23:20	2,16	31,4	9,0	0,091	91,374	0,746	2,496	12,6
	16	00:20	2,31	34,7	10,0	0,101	100,984	0,847	2,597	13,4
	17	01:20	2,45	38,3	11,0	0,112	111,604	0,959	2,709	14,1
	18	02:20	2,60	42,3	12,2	0,123	123,342	1,082	2,832	15,0
	19	03:20	2,74	46,8	13,5	0,136	136,314	1,218	2,968	15,8
	20	04:20	2,89	51,7	14,9	0,151	150,650	1,369	3,119	16,6
	21	05:20	3,03	57,2	16,5	0,166	166,494	1,535	3,285	17,4
	22	06:20	3,17	63,2	18,2	0,184	184,004	1,719	3,469	18,2
•	23	07:20	3,32	69,8	20,1	0,203	203,356	1,923	3,673	19,0

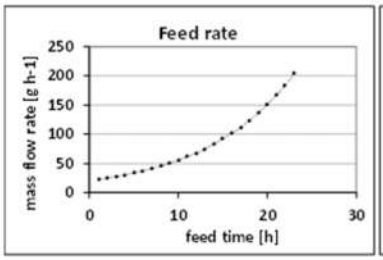

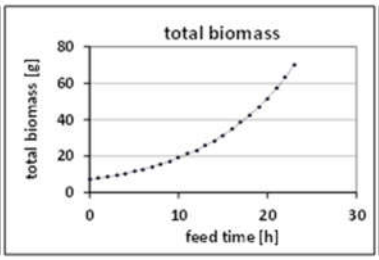

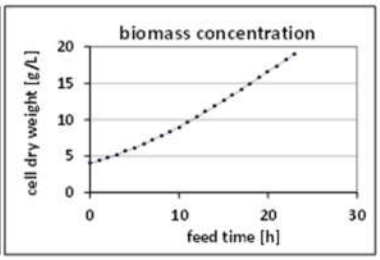

Fermentation: FH361 / Cutinase

09.12.015

FH CAMPUS WIEN
Fachbereich Bioengineering

Host:	*E. coli*	
Strain:	BL21 (DE3) + (pET26b+ with SM gene)	
Product:	cutinase	
Strategy:	Batch + exponential Fed Batch with μ = 0.1 [h^{-1}]	
Start OD600:	0,05	
	Minifors#1	
pH:	7	
temperature:	37°C during batch phase, 37°C during Fed Batch phase	
stirrer speed:	min: 400 rpm, max: 1200rpm	
Aeration:	only Air (min: 30 L/h, max: 200 L/h)	
DO-cascade (DASGIP):	Stirrer: (X1=0, Y1=400rpm, X2=40, Y2=1200rpm)	
	Gasflow: (X1=40, Y1=30 L/h, X2=80, Y2=200L/h)	
	XO_2: (X1=0, Y1=21%, X2=100, Y2=21%)	
antifoam:	5% Glanapon 2000 (w/w) (fatty acid esters + alkylene oxide polymers)	
base:	25% Ammonia (NH_3)	
Batch media:	Semi synthetic Batchmedia GLU01 for E. coli fermentations	c(C-Source): 12 g/kg
Fed Batch media:	Synthetic Fed-Batchmedia GLU01 for E. coli fermentations	c(C-Source): 99 g/kg
Comments:	Induction: IPTG only direct into the feed bottle	

Samples:

	type	number	amount [mL]	comment
☑	Cells-Pellet	3x	1,50	
☑	supernatant	3x	1,50	
☑	cell dry weight	2x	5,00	(2x10ml for batch-end sample)

Calculations:

Volume batch	1,75	L
Biomass concentration	4	g L-1
absolute biomass batch	7	g
specific growth rate	0,1	h-1
generations	3,3	
fedbatch duration	22,9	h-1
final biomass total	68,94	g
new biomass	61,9	g
final biomass concentration	18,8	g L-1
max. volume	3,673	L
feed Volume	1,923	L
Yield (x/s)	0,33	g g-1
Fedbatch: C_Glucose	99,0	g kg-1
Fedbatch: C_Glucose *H_2O	108,90	g kg-1

Induction:

M(IPTG):	238,3	g/mol
IPTG needed:	0,5	µmol / g CDW
	3,0	kg feed prepared
	98,018	g theoretical CDW with FB
	49,0089568	µmol IPTG
	0,0000490	mol IPTG
add	0,011679	g IPTG into feed

Feed and sample plan:

sample	t [h]	time	generation	biomass [g]	Δglucose [g]	flowrate [kg h-1]	flowrate [g h-1]	Σ feed [kg]	reactor volume [kg]	CDW [g/l]
•	0	08:20	0,00	7,0					1,750	4,0
	1	09:20	0,14	7,7	2,2	0,023	22,533	0,023	1,773	4,4
•	2	10:20	0,29	8,5	2,5	0,025	24,902	0,047	1,797	4,8
	3	11:20	0,43	9,4	2,7	0,028	27,521	0,075	1,825	5,2
•	4	12:20	0,58	10,4	3,0	0,030	30,416	0,105	1,855	5,6
	5	13:20	0,72	11,5	3,3	0,034	33,615	0,139	1,889	6,1
•	6	14:20	0,87	12,8	3,7	0,037	37,150	0,176	1,926	6,6
	7	15:20	1,01	14,1	4,1	0,041	41,057	0,217	1,967	7,2
•	8	16:20	1,15	15,6	4,5	0,045	45,375	0,263	2,013	7,7
	9	17:20	1,30	17,2	5,0	0,050	50,147	0,313	2,063	8,3
	10	18:20	1,44	19,0	5,5	0,055	55,421	0,368	2,118	9,0
	11	19:20	1,59	21,0	6,1	0,061	61,250	0,429	2,179	9,8
	12	20:20	1,73	23,2	6,7	0,068	67,691	0,497	2,247	10,3
	13	21:20	1,88	25,7	7,4	0,075	74,811	0,572	2,322	11,1
	14	22:20	2,02	28,4	8,2	0,083	82,678	0,655	2,405	11,8
	15	23:20	2,16	31,4	9,0	0,091	91,374	0,746	2,496	12,6
	16	00:20	2,31	34,7	10,0	0,101	100,984	0,847	2,597	13,4
	17	01:20	2,45	38,3	11,0	0,112	111,604	0,959	2,709	14,1
	18	02:20	2,60	42,3	12,2	0,123	123,342	1,082	2,832	15,0
	19	03:20	2,74	46,8	13,5	0,136	136,314	1,218	2,968	15,8
	20	04:20	2,89	51,7	14,9	0,151	150,650	1,369	3,119	16,6
	21	05:20	3,03	57,2	16,5	0,166	166,494	1,535	3,285	17,4
	22	06:20	3,17	63,2	18,2	0,184	184,004	1,719	3,469	18,2
•	23	07:20	3,32	69,8	20,1	0,203	203,356	1,923	3,673	19,0

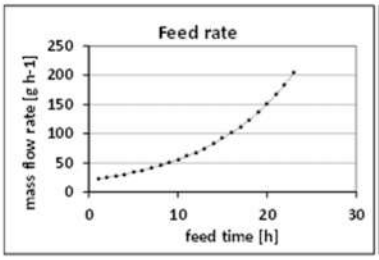

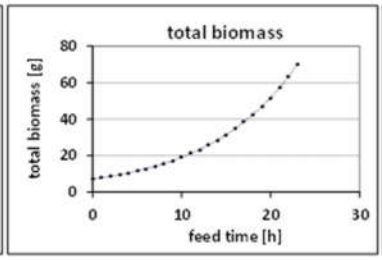

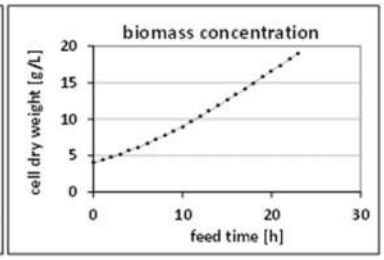

Fermentation: FH360 / Cutinase

30.11.015

FH CAMPUS WIEN
Fachbereich Bioengineering

Host:	*E. coli*	
Strain:	BL21 (DE3) + (pET26b+ with DM gene)	
Product:	cutinase	
Strategy:	Batch + exponential Fed Batch with $\mu = 0.1$ [h^{-1}]	
Start OD600:	0,05	
	Minifors#1	
pH:	7	
temperature:	37°C during batch phase, 37°C during Fed Batch phase	
stirrer speed:	min: 400 rpm, max: 1200rpm	
Aeration:	only Air (min: 30 L/h, max: 200 L/h)	
DO-cascade (DASGIP):	Stirrer: (X1=0, Y1=400rpm, X2=40, Y2=1200rpm)	
	Gasflow: (X1=40, Y1=30 L/h, X2=80, Y2=200L/h)	
	XO_2: (X1=0, Y1=21%, X2=100, Y2=21%)	
antifoam:	5% Glanapon 2000 (w/w) (fatty acid esters + alkylene oxide polymers)	
base:	25% Ammonia (NH_3)	
Batch media:	Semi synthetic Batchmedia GLU01 for E. coli fermentations	c(C-Source): 12 g/kg
Fed Batch media:	Synthetic Fed-Batchmedia GLU01 for E. coli fermentations	c(C-Source): 99 g/kg
Comments:	Induction: IPTG only direct into the feed bottle	

Samples:

	type	number	amount [mL]	comment
☐	Cells-Pellet	3x	1,50	
☐	supernatant	3x	1,50	
☐	cell dry weight	2x	5,00	(2x10ml for batch-end sample)

Calculations:

Volume batch	1,75	L
Biomass concentration	4	g L-1
absolute biomass batch	7	g
specific growth rate	0,1	h-1
generations	3,46	
fedbatch duration	24,0	h-1
final biomass total	77,03	g
new biomass	70,0	g
final biomass concentration	19,8	g L-1
max. volume	3,897	L
Feed Volume	2,147	L
Yield (x/s)	0,33	g g-1
Fedbatch: C_Glucose	99,0	g kg-1
Fedbatch: C_Glucose * H_2O	108,90	g kg-1

Induction:

M(IPTG):	238,3	g/mol
IPTG needed:	0,5	µmol / g CDW
	3,0	kg feed prepared
	98,018	g theoretical CDW with FB
	49,0089568	µmol IPTG
	0,0000490	mol IPTG
add	0,011679	g IPTG into feed

Feed and sample plan:

sample	t [h]	time	generation	biomass [g]	Δglucose [g]	flowrate [kg h-1]	flowrate [g h-1]	Σ feed [kg]	reactor volume [kg]	CDW [g/L]
•	0	08:13	0,00	7,0					1,750	4,0
	1	09:13	0,14	7,7	2,2	0,023	22,533	0,023	1,773	4,4
•	2	10:13	0,29	8,5	2,5	0,025	24,902	0,047	1,797	4,8
	3	11:13	0,43	9,4	2,7	0,028	27,521	0,075	1,825	5,2
•	4	12:13	0,58	10,4	3,0	0,030	30,416	0,105	1,855	5,6
	5	13:13	0,72	11,5	3,3	0,034	33,615	0,139	1,889	6,1
•	6	14:13	0,87	12,8	3,7	0,037	37,150	0,176	1,926	6,6
	7	15:13	1,01	14,1	4,1	0,041	41,057	0,217	1,967	7,2
•	8	16:13	1,15	15,6	4,5	0,045	45,375	0,263	2,013	7,7
	9	17:13	1,30	17,2	5,0	0,050	50,147	0,313	2,063	8,3
•	10	18:13	1,44	19,0	5,5	0,055	55,421	0,368	2,118	9,0
	11	19:13	1,59	21,0	6,1	0,061	61,250	0,429	2,179	9,8
	12	20:13	1,73	23,2	6,7	0,068	67,691	0,497	2,247	10,3
	13	21:13	1,88	25,7	7,4	0,075	74,811	0,572	2,322	11,1
	14	22:13	2,02	28,4	8,2	0,083	82,678	0,655	2,405	11,8
	15	23:13	2,16	31,4	9,0	0,091	91,374	0,746	2,496	12,6
	16	00:13	2,31	34,7	10,0	0,101	100,984	0,847	2,597	13,4
	17	01:13	2,45	38,3	11,0	0,112	111,604	0,959	2,709	14,1
	18	02:13	2,60	42,3	12,2	0,123	123,342	1,082	2,832	15,0
	19	03:13	2,74	46,8	13,5	0,136	136,314	1,218	2,968	15,8
	20	04:13	2,89	51,7	14,9	0,151	150,650	1,369	3,119	16,6
	21	05:13	3,05	57,2	16,5	0,166	166,494	1,535	3,285	17,4
	22	06:13	3,17	63,2	18,2	0,184	184,004	1,719	3,469	18,2
	23	07:13	3,32	69,8	20,1	0,203	203,356	1,923	3,673	19,0
•	24	08:13	3,46	77,2	22,3	0,225	224,743	2,147	3,897	19,8

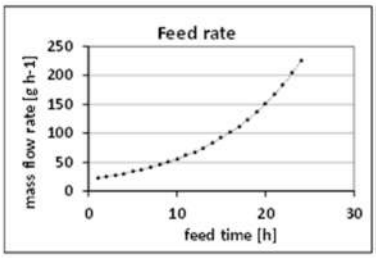

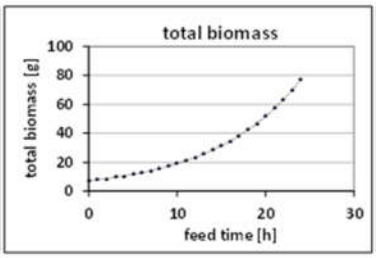

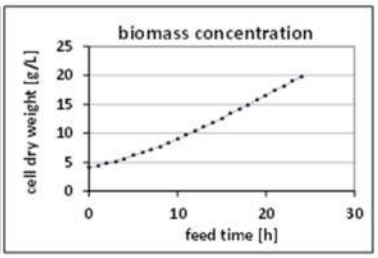

7. Reference

Abrahmsen, L., Tom, J., Burnier, J., Butcher, K. A., Kossiakoff, A., & Wells, J. A. (1991). Engineering subtilisin and its substrates for efficient ligation of peptide bonds in aqueous solution. *Biochemistry*, *30*(17), 4151–4159. http://doi.org/10.1021/bi00231a007

Araújo, R., Silva, C., O'Neill, A., Micaelo, N., Guebitz, G., Soares, C. M., … Cavaco-Paulo, A. (2007). Tailoring cutinase activity towards polyethylene terephthalate and polyamide 6,6 fibers. *Journal of Biotechnology*, *128*(4), 849–857. http://doi.org/10.1016/j.jbiotec.2006.12.028

Baker, P. J., Poultney, C., Liu, Z., Gross, R., & Montclare, J. K. (2012). Identification and comparison of cutinases for synthetic polyester degradation. *Applied Microbiology and Biotechnology*, *93*(1), 229–240. http://doi.org/10.1007/s00253-011-3402-4

Baptista, R. P., Santos, A. M., Fedorov, A., Martinho, J. M. G., Pichot, C., Elaïssari, A., … Taipa, M. A. (2003). Activity, conformation and dynamics of cutinase adsorbed on poly(methyl methacrylate) latex particles. *Journal of Biotechnology*, *102*(3), 241–249.

Battistel, E., Morra, M., & Marinetti, M. (2001). Enzymatic surface modification of acrylonitrile fibers. *Applied Surface Science*, *177*(1), 32–41.

Bentley, W. E., Mirjalili, N., Andersen, D. C., Davis, R. H., & Kompala, D. S. (1990). Plasmid-encoded protein: the principal factor in the "metabolic burden" associated with recombinant bacteria. *Biotechnology and Bioengineering*, *35*(7), 668–681.

Berkmen, M. (2012). Production of disulfide-bonded proteins in Escherichia coli. *Protein Expression and Purification*, *82*(1), 240–251.

Berkmen, M., Boyd, D., & Beckwith, J. (2005). The nonconsecutive disulfide bond of Escherichia coli phytase (AppA) renders it dependent on the protein-disulfide isomerase, DsbC. *The Journal of Biological Chemistry*, *280*(12), 11387–11394. http://doi.org/10.1074/jbc.M411774200

Bizzozero, S. A., & Dutler, H. (1981). Stereochemical aspects of peptide hydrolysis catalyzed by serine proteases of the chymotrypsin type. *Bioorganic Chemistry*, *10*(1), 46–62.

Bonneau, P. R., Graycar, T. P., Estell, D. A., & Jones, J. B. (1991). Alteration of the specificity of subtilisin BPN' by site-directed mutagenesis in its S1 and S1' binding sites. *Journal of the American Chemical Society*, *113*(3), 1026–1030. http://doi.org/10.1021/ja00003a043

Brady, L., Brzozowski, A. M., Derewenda, Z. S., Dodson, E., Dodson, G., Tolley, S., … Menge, U. (1990). A serine protease triad forms the catalytic centre of a triacylglycerol lipase. *Nature*, *343*(6260), 767–770. http://doi.org/10.1038/343767a0

Burkinshaw, S. M. (1995). Chemical principles of synthetic fibre dyeing. *Blackie, London*.

Cammenberg, M., Hult, K., & Park, S. (2006). Molecular Basis for the Enhanced Lipase-Catalyzed N-Acylation of 1-Phenylethanamine with Methoxyacetate. *ChemBioChem*, *7*(11), 1745–1749.

Carvalho, C. M., Aires-Barros, M. R., & Cabral, J. M. (1999). Cutinase: from molecular level to bioprocess development. *Biotechnology and Bioengineering*, *66*(1), 17–34.

Choi, J. H., Keum, K. C., & Lee, S. Y. (2006). Production of recombinant proteins by high cell density culture of Escherichia coli. *Chemical Engineering Science*, *61*(3), 876–885.

Choi, J. H., & Lee, S. Y. (2004). Secretory and extracellular production of recombinant proteins using Escherichia coli. *Applied Microbiology and Biotechnology*, *64*(5), 625–635.

Chung, B. H., Sohn, M.-J., Oh, S.-W., Park, U.-S., Poo, H., Kim, B. S., … Lee, Y. I. (1998). Overproduction of human granulocyte-colony stimulating factor fused to the PelB signal peptide in Escherichia coli. *Journal of Fermentation and Bioengineering*, *85*(4), 443–446.

de Barros, D. P. C., Fonseca, L. P., Fernandes, P., Cabral, J. M. S., & Mojovic, L. (2009). Biosynthesis of ethyl caproate and other short ethyl esters catalyzed by cutinase in organic solvent. *Journal of Molecular Catalysis B: Enzymatic*, *60*(3–4), 178–185. http://doi.org/10.1016/j.molcatb.2009.05.004

Del Solar, G., & Espinosa, M. (2000). Plasmid copy number control: an ever-growing story. *Molecular Microbiology*, *37*(3), 492–500.

Deslongchamps, P. (1975). Stereoelectronic control in the cleavage of tetrahedral intermediates in the hydrolysis of esters and amides. *Tetrahedron*, *31*(20), 2463–2490.

Duarte, D. R., Castillo, E., Bárzana, E., & López-Munguía, A. (2000). Capsaicin hydrolysis by Candida antarctica lipase. *Biotechnology Letters*, *22*(22), 1811–1814.

Eberl, A., Heumann, S., Kotek, R., Kaufmann, F., Mitsche, S., Cavaco-Paulo, A., & Gübitz, G. M. (2008). Enzymatic hydrolysis of PTT polymers and oligomers. *Journal of Biotechnology*, *135*(1), 45–51. http://doi.org/10.1016/j.jbiotec.2008.02.015

Egmond, M. R., & de Vlieg, J. (2000). Fusarium solani pisi cutinase. *Biochimie*, *82*(11), 1015–1021.

Fan, C.-Y., & KÃ¶ller, W. (1998). Diversity of cutinases from plant pathogenic fungi: differential and sequential expression of cutinolytic esterases by *Alternaria brassicicola*. *FEMS Microbiology Letters*, *158*(1), 33–38. http://doi.org/10.1111/j.1574-6968.1998.tb12796.x

Ferenci, T., & Silhavy, T. J. (1987). Sequence information required for protein translocation from the cytoplasm. *Journal of Bacteriology*, *169*(12), 5339.

Fischer-Colbrie, G., Heumann, S., & Guebitz, G. (Eds.). (2006a). *Enzyme for molymer surface modification. Modified fibers with medical and specialty applications; ; Edwards, J. V., Buschle-Diller, G., Goheen, S. C., Eds.* (Vol. 8). Dordrecht: Springer.

Fischer-Colbrie, G., Heumann, S., & Guebitz, G. (2006b). Enzymes for polymer surface modification. In *Modified fibers with medical and specialty applications* (pp. 181–189). Springer. Retrieved from http://link.springer.com/chapter/10.1007/1-4020-3794-5_11

Flipsen, J. A. C., Appel, A. C. M., van der Hijden, H. T. W. M., & Verrips, C. T. (1998). Mechanism of removal of immobilized triacylglycerol by lipolytic enzymes in a sequential laundry wash process. *Enzyme and Microbial Technology*, *23*(3–4), 274–280. http://doi.org/10.1016/S0141-0229(98)00050-7

Francetic, O., Belin, D., Badaut, C., & Pugsley, A. P. (2000). Expression of the endogenous type II secretion pathway in Escherichia coli leads to chitinase secretion. *The EMBO Journal*, *19*(24), 6697–6703. http://doi.org/10.1093/emboj/19.24.6697

Fresht, A. (1999). *Structure and mechanism in protein science: a guide to enzyme catalysis and protein folding*. WH Freeman and Co., New York.

Fülöp, V., Szeltner, Z., Renner, V., & Polgár, L. (2001). Structures of Prolyl Oligopeptidase Substrate/Inhibitor Complexes USE OF INHIBITOR BINDING FOR TITRATION OF THE CATALYTIC HISTIDINE RESIDUE. *Journal of Biological Chemistry*, *276*(2), 1262–1266.

Gonçalves, A. P., Cabral, J. M., & Aires-Barros, M. R. (1996). Immobilization of a recombinant cutinase by entrapment and by covalent binding. Kinetic and stability studies. *Applied Biochemistry and Biotechnology*, *60*(3), 217–228.

Gorenstein, D. G. (1987). Stereoelectronic effects in biomolecules. *Chemical Reviews*, *87*(5), 1047–1077.

Gottesman, S. (1996). Proteases and their targets in Escherichia coli. *Annual Review of Genetics*, *30*, 465–506. http://doi.org/10.1146/annurev.genet.30.1.465

Grodberg, J., & Dunn, J. J. (1988). ompT encodes the Escherichia coli outer membrane protease that cleaves T7 RNA polymerase during purification. *Journal of Bacteriology*, *170*(3), 1245–1253.

Gusakov, A. V., Sinitsyn, A. P., Berlin, A. G., Markov, A. V., & Ankudimova, N. V. (2000). Surface hydrophobic amino acid residues in cellulase molecules as a structural factor responsible for their high denim-washing performance. *Enzyme and Microbial Technology*, *27*(9), 664–671.

Gustafsson, C., Govindarajan, S., & Minshull, J. (2004). Codon bias and heterologous protein expression. *Trends in Biotechnology*, *22*(7), 346–353.

Hankin, L., & Kolattukudy, P. E. (1971). Utilization of cutin by a pseudomonad isolated from soil. *Plant and Soil*, *34*(1), 525–529.

Hedstrom, L. (2002). Serine protease mechanism and specificity. *Chemical Reviews*, *102*(12), 4501–4524.

Heinen, W., & Vries, H. de. (1966). Stages during the breakdown of plant cutin by soil microorganisms. *Archives of Microbiology*, *54*(4), 331–338.

Henderson, R. (1970). Structure of crystalline α-chymotrypsin: IV. The structure of indoleacryloyl-α-chymotrypsin and its relevance to the hydrolytic mechanism of the enzyme. *Journal of Molecular Biology*, *54*(2), 341–354.

Henke, E., & Bornscheuer, U. T. (2003). Fluorophoric assay for the high-throughput determination of amidase activity. *Analytical Chemistry*, *75*(2), 255–260.

Heredia, A. (2003). Biophysical and biochemical characteristics of cutin, a plant barrier biopolymer. *Biochimica et Biophysica Acta (BBA)-General Subjects*, *1620*(1), 1–7.

Herrero Acero, E., Ribitsch, D., Steinkellner, G., Gruber, K., Greimel, K., Eiteljoerg, I., … others. (2011). Enzymatic surface hydrolysis of PET: Effect of structural diversity on kinetic properties of cutinases from Thermobifida. *Macromolecules*, *44*(12), 4632–4640.

Hsiung, H. M., & Becker, G. W. (1988). Secretion and folding of human growth hormone in Escherichia coli. *Biotechnology and Genetic Engineering Reviews*, *6*(1), 43–66.

Jaeger, K.-E., Dijkstra, B. W., & Reetz, M. T. (1999). Bacterial Biocatalysts: Molecular Biology, Three-Dimensional Structures, and Biotechnological Applications of Lipases. *Annual Review of Microbiology*, *53*(1), 315–351. http://doi.org/10.1146/annurev.micro.53.1.315

Jelsch, C., Longhi, S., & Cambillau, C. (1998). Packing forces in nine crystal forms of cutinase. *Proteins*, *31*(3), 320–333.

Jeong, K. J., & Lee, S. Y. (2000). Secretory production of human leptin in Escherichia coli. *Biotechnology and Bioengineering*, *67*(4), 398–407.

Kadokura, H., Tian, H., Zander, T., Bardwell, J. C. A., & Beckwith, J. (2004). Snapshots of DsbA in action: detection of proteins in the process of oxidative folding. *Science (New York, N.Y.)*, *303*(5657), 534–537. http://doi.org/10.1126/science.1091724

Kane, J. F., & Hartley, D. L. (1988). Formation of recombinant protein inclusion bodies in Escherichia coli. *Trends in Biotechnology*, *6*(5), 95–101. http://doi.org/10.1016/0167-7799(88)90065-0

Kazlauskas, R. J., & Bornscheuer, U. T. (1998). Biotransformations with Lipases. In H.-J. Rehm & G. Reed (Eds.), *Biotechnology* (pp. 36–191). Wiley-VCH Verlag GmbH. Retrieved from http://onlinelibrary.wiley.com/doi/10.1002/9783527620906.ch3/summary

Kellis, J., Estell, D., & Cascão-Pereira, L. (2012). *Conference Book, EMBO conference catalytic mechanism by biological systems* (Vol. 7–10 October 2012).

Kellis Jr, J. T., Poulose, A. J., & Yoon, M.-Y. (2001). *Enzymatic modification of the surface of a polyester fiber or article*. Google Patents. Retrieved from https://www.google.com/patents/US6254645

Knogge, W. (1996). Fungal infection of plants. *The Plant Cell*, *8*(10), 1711.

Kold, D., Dauter, Z., Laustsen, A. K., Brzozowski, A. M., Turkenburg, J. P., Nielsen, A. D., … Wimmer, R. (2014). Thermodynamic and structural investigation of the specific SDS binding of Humicola insolens cutinase. *Protein Science: A Publication of the Protein Society*, *23*(8), 1023–1035. http://doi.org/10.1002/pro.2489

Koschorreck, K., Liu, D., Kazenwadel, C., Schmid, R. D., & Hauer, B. (2010). Heterologous expression, characterization and site-directed mutagenesis of cutinase CUTAB1 from Alternaria brassicicola. *Applied Microbiology and Biotechnology*, *87*(3), 991–997. http://doi.org/10.1007/s00253-010-2533-3

Lauwereys, M., De Geus, P., De Meutter, J., Stanssens, P., & Matthyssens, G. (1991). Cloning, expression and characterization of cutinase, a fungal lipolytic enzyme. *Lipases: Structure, Mechanism and Genetic Engineering*, *16*, 243–251.

Lei, S.-P., Lin, H. C., Wang, S.-S., Callaway, J., & Wilcox, G. (1987). Characterization of the Erwinia carotovora pelB gene and its product pectate lyase. *Journal of Bacteriology*, *169*(9), 4379–4383.

Leliaert, F., Verbruggen, H., & Zechman, F. W. (2011). Into the deep: new discoveries at the base of the green plant phylogeny. *Bioessays*, *33*(9), 683–692.

Lithwick, G., & Margalit, H. (2003). Hierarchy of sequence-dependent features associated with prokaryotic translation. *Genome Research*, *13*(12), 2665–2673.

Liu, B., Schofield, C. J., & Wilmouth, R. C. (2006). Structural analyses on intermediates in serine protease catalysis. *Journal of Biological Chemistry*, *281*(33), 24024–24035.

Liu, Z., Gosser, Y., Baker, P. J., Ravee, Y., Lu, Z., Alemu, G., … others. (2009). Structural and functional studies of Aspergillus oryzae cutinase: enhanced thermostability and hydrolytic activity of

synthetic ester and polyester degradation. *Journal of the American Chemical Society*, *131*(43), 15711–15716.

Longhi, S., & Cambillau, C. (1999). Structure-activity of cutinase, a small lipolytic enzyme. *Biochimica et Biophysica Acta (BBA)-Molecular and Cell Biology of Lipids*, *1441*(2), 185–196.

Longhi, S., Knoops-Mouthuy, E., Cambillau, C., Mannesse, M., Verheij, H. M., De Haas, G. H., & Egmond, M. (1997). Crystal structure of cutinase covalently inhibited by a triglyceride analogue. *Protein Science*, *6*(2), 275–286.

Lucic, M. R., Forbes, B. E., Grosvenor, S. E., Carr, J. M., Wallace, J. C., & Forsberg, G. (1998). Secretion in Escherichia coli and phage-display of recombinant insulin-like growth factor binding protein-2. *Journal of Biotechnology*, *61*(2), 95–108.

Maeda, H., Yamagata, Y., Abe, K., Hasegawa, F., Machida, M., Ishioka, R., … Nakajima, T. (2005). Purification and characterization of a biodegradable plastic-degrading enzyme from Aspergillus oryzae. *Applied Microbiology and Biotechnology*, *67*(6), 778–788. http://doi.org/10.1007/s00253-004-1853-6

Makrides, S. C. (1996). Strategies for achieving high-level expression of genes in Escherichia coli. *Microbiological Reviews*, *60*(3), 512–538.

Mannesse, M. L., Cox, R. C., Koops, B. C., Verheij, H. M., de Haas, G. H., Egmond, M. R., … de Vlieg, J. (1995). Cutinase from Fusarium solani pisi hydrolyzing triglyceride analogs. Effect of acyl chain length and position in the substrate molecule on activity and enantioselectivity. *Biochemistry*, *34*(19), 6400–6407.

Martinez, C., De Geus, P., Lauwereys, M., Matthyssens, G., & Cambillau, C. (1992). Fusarium solani cutinase is a lipolytic enzyme with a catalytic serine accessible to solvent. *Nature*, *356*(6370), 615–618.

Martinez, C., de Geus, P., Stanssens, P., Lauwereys, M., & Cambillau, C. (1993). Engineering cysteine mutants to obtain crystallographic phases with a cutinase from Fusarium solani pisi. *Protein Engineering*, *6*(2), 157–165.

Melo, E. P., Airesbarros, M. R., & Cabral, J. M. S. (1995). Triglyceride hydrolysis and stability of a recombinant cutinase fromFusarium solani in AOT-iso-octane reversed micelles. *Applied Biochemistry and Biotechnology*, *50*(1), 45–56.

Murphy, C. A., Cameron, J. A., Huang, S. J., & Vinopal, R. T. (1996). Fusarium polycaprolactone depolymerase is cutinase. *Applied and Environmental Microbiology*, *62*(2), 456–460.

Nakagawa, Y., Hasegawa, A., Hiratake, J., & Sakata, K. (2007). Engineering of Pseudomonas aeruginosa lipase by directed evolution for enhanced amidase activity: mechanistic implication for amide hydrolysis by serine hydrolases. *Protein Engineering Design and Selection*, *20*(7), 339–346.

Nyon, M. P., Rice, D. W., Berrisford, J. M., Hounslow, A. M., Moir, A. J., Huang, H., … Craven, C. J. (2009). Catalysis by Glomerella cingulata cutinase requires conformational cycling between the active and inactive states of its catalytic triad. *Journal of Molecular Biology*, *385*(1), 226–235.

Nyon, M. P., Rice, D. W., Berrisford, J. M., Huang, H., Moir, A. J., Craven, C. J., … Farah Diba, A. B. (2008). Crystallization and preliminary X-ray analysis of recombinant Glomerella cingulata cutinase. *Acta Crystallographica Section F: Structural Biology and Crystallization Communications*, *64*(6), 504–508.

Okkels, J. S., Svendsen, A., Borch, K., Thellersen, M., Patkar, S. A., Petersen, D. A., … Kretzschmar, T. (1997). New lipolytic enzyme with high capacity to remove lard in one wash cycle. *US Patent*, 97–5735.

Ollis, D. L., Cheah, E., Cygler, M., Dijkstra, B., Frolow, F., Franken, S. M., … Schrag, J. (1992). The alpha/beta hydrolase fold. *Protein Engineering*, *5*(3), 197–211.

Palmer, R. J. (2002). Polyamides, Plastics. In *Encyclopedia of Polymer Science and Technology*. John Wiley & Sons, Inc. Retrieved from http://onlinelibrary.wiley.com/doi/10.1002/0471440264.pst251/abstract

Parvinzadeh, M., Assefipour, R., & Kiumarsi, A. (2009). Biohydrolysis of nylon 6, 6 fiber with different proteolytic enzymes. *Polymer Degradation and Stability*, *94*(8), 1197–1205.

Pellis, A., Acero, E. H., Weber, H., Obersriebnig, M., Breinbauer, R., Srebotnik, E., & Guebitz, G. M. (2015). Biocatalyzed approach for the surface functionalization of poly(L-lactic acid) films using hydrolytic enzymes. *Biotechnology Journal*, *10*(11), 1739–1749. http://doi.org/10.1002/biot.201500074

Pio, T. F., & Macedo, G. A. (2009). Cutinases: properties and industrial applications. *Advances in Applied Microbiology*, *66*, 77–95. http://doi.org/10.1016/S0065-2164(08)00804-6

Pritchard, M. P., Ossetian, R., Li, D. N., Henderson, C. J., Burchell, B., Wolf, C. R., & Friedberg, T. (1997). A General Strategy for the Expression of Recombinant Human Cytochrome P450s inEscherichia coliUsing Bacterial Signal Peptides: Expression of CYP3A4, CYP2A6, and CYP2E1. *Archives of Biochemistry and Biophysics*, *345*(2), 342–354.

Pugsley, A. P. (1993). The complete general secretory pathway in gram-negative bacteria. *Microbiological Reviews*, *57*(1), 50–108.

Puigbò, P., Guzmán, E., Romeu, A., & Garcia-Vallvé, S. (2007). OPTIMIZER: a web server for optimizing the codon usage of DNA sequences. *Nucleic Acids Research*, *35*(suppl 2), W126–W131.

Purdy, R. E., & Kolattukudy, P. E. (1973). Depolymerization of a hydroxy fatty acid biopolymer, cutin, by an extracellular enzyme from Fusarium solani f. pisi: isolation and some properties of the enzyme. *Archives of Biochemistry and Biophysics*, *159*(1), 61–69.

Purdy, R. E., & Kolattukudy, P. E. (1975). Hydrolysis of plant cuticle by plant pathogens. Properties of cutinase I, cutinase II, and a nonspecific esterase isolated from Fusarium solani pisi. *Biochemistry*, *14*(13), 2832–2840.

Richter, F., Blomberg, R., Khare, S. D., Kiss, G., Kuzin, A. P., Smith, A. J., … others. (2012). Computational design of catalytic dyads and oxyanion holes for ester hydrolysis. *Journal of the American Chemical Society*, *134*(39), 16197–16206.

Ronkvist, Å. M., Lu, W., Feder, D., & Gross, R. A. (2009). Cutinase-Catalyzed Deacetylation of Poly(vinyl acetate). *Macromolecules*, *42*(16), 6086–6097. http://doi.org/10.1021/ma900530j

Ronkvist, Å. M., Xie, W., Lu, W., & Gross, R. A. (2009). Cutinase-Catalyzed Hydrolysis of Poly(ethylene terephthalate). *Macromolecules*, *42*(14), 5128–5138. http://doi.org/10.1021/ma9005318

Rosano, G. L., & Ceccarelli, E. A. (2014). Recombinant protein expression in Escherichia coli: advances and challenges. *Recombinant Protein Expression in Microbial Systems*, 7.

Samuels, L., Kunst, L., & Jetter, R. (2008). Sealing plant surfaces: cuticular wax formation by epidermal cells. *Plant Biology*, *59*(1), 683.

Scheidle, M., Dittrich, B., Klinger, J., Ikeda, H., Klee, D., & Büchs, J. (2011). Controlling pH in shake flasks using polymer-based controlled-release discs with pre-determined release kinetics. *BMC Biotechnology*, *11*, 25. http://doi.org/10.1186/1472-6750-11-25

Sezonov, G., Joseleau-Petit, D., & D'Ari, R. (2007). Escherichia coli physiology in Luria-Bertani broth. *Journal of Bacteriology*, *189*(23), 8746–8749.

Shashidhara, K. S., & Gaikwad, S. M. (2010). Conformational and functional transitions in class II alpha-mannosidase from Aspergillus fischeri. *Journal of Fluorescence*, *20*(4), 827–836. http://doi.org/10.1007/s10895-010-0625-1

Shishiyama, J., Araki, F., & Akai, S. (1970). Studies on cutin-esterase II. Characteristics of cutin-esterase from Botrytis cinerea and its activity on tomato-cutin. *Plant and Cell Physiology*, *11*(6), 937–945.

Silva, C., Araújo, R., Casal, M., Gübitz, G. M., & Cavaco-Paulo, A. (2007). Influence of mechanical agitation on cutinases and protease activity towards polyamide substrates. *Enzyme and Microbial Technology*, *40*(7), 1678–1685.

Silva, C., & Cavaco-Paulo, A. (2004). Monitoring biotransformations in polyamide fibres. *Biocatalysis and Biotransformation*, *22*(5–6), 357–360.

Silva, C., Matama, T., & Cavaco-Paulo, A. (2010). Biotransformation of synthetic fibers. *Encyclopedia of Industrial Biotechnology: Bioprocess, Bioseparation, and Cell Technology*.

Studier, F. W. (2005). Protein production by auto-induction in high density shaking cultures. *Protein Expression and Purification*, *41*(1), 207–234.

Studier, F. W., & Moffatt, B. A. (1986). Use of bacteriophage T7 RNA polymerase to direct selective high-level expression of cloned genes. *Journal of Molecular Biology*, *189*(1), 113–130.

Studier, F. W., Rosenberg, A. H., Dunn, J. J., & Dubendorff, J. W. (1990). [6] Use of T7 RNA polymerase to direct expression of cloned genes. *Methods in Enzymology*, *185*, 60–89.

Syrén, P.-O. (2013). The solution of nitrogen inversion in amidases. *FEBS Journal*, *280*(13), 3069–3083.

Syrén, P.-O., Hendil-Forssell, P., Aumailley, L., Besenmatter, W., Gounine, F., Svendsen, A., … Hult, K. (2012). Esterases with an Introduced Amidase-Like Hydrogen Bond in the Transition State Have Increased Amidase Specificity. *ChemBioChem*, *13*(5), 645–648.

Syrén, P.-O., & Hult, K. (2011). Amidases have a hydrogen bond that facilitates nitrogen inversion, but esterases have not. *ChemCatChem*, *3*(5), 853–860.

Unilever. (1994). Eukaryotic cutinase variant with increased lipolytic activity. U.S.

Vertommen, M., Nierstrasz, V. A., Van der Veer, M., & Warmoeskerken, M. (2005). Enzymatic surface modification of poly (ethylene terephthalate). *Journal of Biotechnology*, *120*(4), 376–386.

Vidinha, P., Augusto, V., Almeida, M., Fonseca, I., Fidalgo, A., Ilharco, L., … Barreiros, S. (2006). Sol-gel encapsulation: an efficient and versatile immobilization technique for cutinase in non-aqueous media. *Journal of Biotechnology*, *121*(1), 23–33. http://doi.org/10.1016/j.jbiotec.2005.06.018

Vidinha, P., Harper, N., Micaelo, N. M., Lourenco, N. M. T., Gomes da Silva, M. D. R., Cabral, J. M. S., … Barreiros, S. (2004). Effect of immobilization support, water activity, and enzyme ionization state on cutinase activity and enantioselectivity in organic media. *Biotechnology and Bioengineering*, *85*(4), 442–449. http://doi.org/10.1002/bit.10780

Waters, E. R. (2003). Molecular adaptation and the origin of land plants. *Molecular Phylogenetics and Evolution*, *29*(3), 456–463.

Weuster-Botz, D., Altenbach-Rehm, J., & Arnold, M. (2001). Parallel substrate feeding and pH-control in shaking-flasks. *Biochemical Engineering Journal*, *7*(2), 163–170. http://doi.org/10.1016/S1369-703X(00)00117-0

Williams, J. A. (2002). Keys to bioreactor selections. *Chemical Engineering Progress*, *98*(3), 34–41.

Winkler, F. K., D'Arcy, A., & Hunziker, W. (1990). Structure of human pancreatic lipase. *Nature*, *343*(6260), 771–774. http://doi.org/10.1038/343771a0

Wong, W.-K. R., Ali, A. B., & Ma, M. C. (2003). Cloning, expression, and characterization of diuretic hormone Manduca diuresin from Manduca sexta in Escherichia coli. *Protein Expression and Purification*, *29*(1), 51–57.

Yoon, M.-Y., Kellis, J., & Poulose, A. J. (2002). Enzymatic Modification of Polyester. *AATCC Review*, *2*(6). Retrieved from http://search.ebscohost.com/login.aspx?direct=true&profile=ehost&scope=site&authtype=crawler&jrnl=15328813&AN=31880222&h=sFThvmPnfEQ6niAKxgjIyordmMvl3sszeERMIMTw0AAYc4QzAbE4UQqS2oYWCDxM4uSlPjgK3MBiBmO0A3fLBg%3D%3D&crl=c

Yoon, S. H., Kim, S. K., & Kim, J. F. (2010). Secretory production of recombinant proteins in Escherichia coli. *Recent Patents on Biotechnology*, *4*(1), 23–29.

Zerner, B., Bond, R. P., & Bender, M. L. (1964). Kinetic evidence for the formation of acyl-enzyme intermediates in the α-chymotrypsin-catalyzed hydrolyses of specific substrates. *Journal of the American Chemical Society*, *86*(18), 3674–3679.

Zhang, T., Bertelsen, E., & Alber, T. (1994). Entropic effects of disulphide bonds on protein stability. *Nature Structural & Molecular Biology*, *1*(7), 434–438. http://doi.org/10.1038/nsb0794-434